THE PRODUCTION OF GALLIUM-67

BY PROTON INDUCED NUCLEAR REACTIONS

ON A TANDEM ^{nat}Ge / ^{nat}Zn TARGET

A thesis submitted to the

UNIVERSITY OF CAPE TOWN

in fulfilment of the requirements for the degree of

MASTER OF SCIENCE

by

CLIVE NAIDOO

Supervisor: Prof G. E. Jackson

Co-Supervisor: Dr T. N. van der Walt

September 1998

ACKNOWLEDGEMENTS

I would like to extend my sincere thanks and appreciation to:

My co-supervisor, Dr Nico van der Walt, Head of the Radioisotope Production Group, NAC, who originally proposed the ion exchange chromatographic separation for the Ge / Zn target and for his enthusiastic and continued contributions throughout the duration of this project. His encouraging and thorough approach has been immensely inspiring to me.

My supervisor, Prof Graham Jackson, for his enthusiastic interest and sound guidance which contributed to the completion of this thesis.

Dr Meiring Nortier who originally proposed the Ge / Zn target system, and Mr Stuart Dolley who performed the initial separation studies.

Mr Thierry Van Elst and Mr Michael Penny who built the hot cell facilities and the electronic control panel, respectively, and for those people who contributed in one way or another to the completion of this thesis.

My wife, Krishnee, for her love, support and encouragement during the course of this project.

Further I would like to declare that without the guidance and strength of the Lord, none of this work would have been possible.

ABSTRACT

Gallium-67 with a half life of 78.3 h and γ-rays with energies of 93, 185 and 300 keV is a cyclotron-produced radioisotope for which considerable demand exists. The isotope is usually supplied in a citrate solution which is widely used to detect malignant tumours and inflammatory lesions.

Presently the production route of ^{67}Ga at the National Accelerator Centre uses the proton bombardment of ^{nat}Zn targets which utilises 15-20 hours of cyclotron beam time per routine production. In an effort to save on expensive beam time, a study was undertaken to use a tandem ^{nat}Ge / ^{nat}Zn target to produce the same amount of ^{67}Ga activity, but using less than half of the beam time (7-8 hours). The purification method to separate the gallium radioisotopes from the tandem ^{nat}Ge / ^{nat}Zn target, with an organic polymer resin containing no ion exchange groups is presented here.

Values for distribution coefficients for Ga(III) on various types of Amberchrom resins and at different HCl concentrations, and values for distribution coefficients for Ga(III) (0.01-1.00 mmole / g resin) and contaminant elements (0.01-1.00 mmole / g resin) such as Ge(IV), Zn(II), Al(III), Fe(III), Fe(II), Ti(III) and Cu(II) on the Amberchrom CG-71cd resin, in 7 M HCl and 6 M HCl-0.5 M HF mixtures are also presented.

A quantitative separation of synthetic mixtures using Ga(III) {10 μg and 100 μg} as the principal element with 100 μg of the other element {Ge(IV), Zn(II), Al(III), Fe(II), Co(II), Ni(II), Cu(II), Cd(II) and In(III)} were also performed.

Elution curves of Ga(III)-Zn(II), Ga(III)-Cu(II), Ga(III)-Ti(III) and Ga(III)-Fe(II) on the Amberchrom CG-71cd resin in 7 M HCl together with elution curves of Ga(III)-Ge(IV), Ga(III)-Ti(III) and Ga(III)-Al(III) in 6 M HCl-0.5 M HF mixtures were determined to obtain an optimal chemical separation procedure to produce a carrier-free ^{67}Ga radioisotope that is within the specifications of the US Pharmacopoeia and British Pharmacopoeia.

CONTENTS

LIST OF FIGURES

LIST OF FIGURES (continued)

LIST OF TABLES

DEFINITION OF TERMS AND CONCEPTS

Activity

The rate of radioactive transformations (radioactive decays) in a given source or sample (i.e. the intensity of the radioactive source or sample).

Bombardment of target

Particles such as protons, deuterons, ^{3}He and α- particles that are accelerated by a cyclotron and directed on target material such as Ge or Zn.

Calibration

The reference time used by the radiopharmacist to indicate when the isotope may be injected into a patient.

Carrier-free radioisotope

This refers to a radioisotope produced to have a very high specific activity. Carrier-free strictly implies the absence of other isotopes of the same element as that of the desired radioisotope. In practice, the term is also used when only very low levels of the other isotopes of the same element are present in the final product.

Cyclotron

A highly sophisticated machine used for the acceleration of charged particles such as protons, deuterons, ^{3}He and α- particles.

Electronvolt (eV)

This is the energy an electron would gain when accelerated across a potential difference of one Volt. The units electronvolt (eV), kilo-electron volt (keV) and Mega-electronvolt (MeV) are more convenient than the S.I. unit, Joule.

EOB

End of bombardment: is normally used as a reference for the calculation of yields for the production of a specific radioisotope with cyclotrons.

Ge (Li)-detector

Germanium-lithium detector used for the observation of γ-rays.

Ge (Li)-γ spectrometer

Ge (Li) detector coupled to a multi-channel analyser for the determination of energy spectra.

Half-life

The average time interval required for one-half of any quantity of identical radioactive atoms to undergo radioactive decay (i.e. the time interval required for the activity of a source of any single radioactive substance to decrease to one-half). The half-lives of the known radioisotopes vary from less than a millionth of a second to more than a billion years.

Hot

In the radioactive sense of the word, it means highly radioactive and consequently posing a radiation hazard to personnel.

Isotope

One of two or more atomic species of an element having identical number of protons in the nucleus, but different number of neutrons. Thus, while chemically indistinguishable, they differ in mass and radioactive behaviour.

mCi / μAh

Millicurie per micro-ampere-hour. The activity of a radioactive source or sample is conveniently expressed in millicuries (1 millicurie = 3.7 X 10^7 radioactive transformations or decays per second). Radioisotope production yield is specified in units of mCi / μAh where μAh is the unit used for the accumulated charge received by the target during bombardment with a charged-particle beam.

Radiochemical purity

The amount of radioisotope found in a known chemical form.

Radioisotopic purity

The ratio of the activity of the desired radioisotope in relation to the presence of other radioisotopes of the same element.

Radionuclidic purity

The ratio of the activity of the desired radioisotope in relation to the total activity present in the sample.

Radiopharmaceutical

Medicine that contains one or more radioactive isotopes.

1 INTRODUCTION

1.1 NAC FACILITY BACKGROUND AND LAYOUT

The National Accelerator Centre (NAC) in Faure is a multidisciplinary scientific research laboratory, established in 1977 under the control of the Council for Scientific and Industrial Research. Since 1988 it has been one of several National Facilities administered by the Foundation for Research Development (FRD), and provides facilities for:

- training of students in basic and applied research using accelerated particle beams
- particle radiotherapy for the treatment of cancer
- the supply of accelerator-produced radioisotopes for diagnostic nuclear medicine and research.

The NAC is organised so as to bring together people working in medical, biological and physical sciences who are interested in the use of accelerated particle beams, by providing opportunities for research and postgraduate training in these separate disciplines, and also by stimulating mutual interest in the interdisciplinary areas.

The accelerators operated by the NAC are a 6 MV Van de Graaff accelerator, an 8 MeV injector cyclotron which provides light ions for a 200 MeV cyclotron, a second injector cyclotron which provides heavy ions and polarised ions for the 200 MeV machine, and the 200 MeV Separated-Sector Cyclotron itself.

The Van der Graaff accelerator is a high-precision, variable-energy machine, capable of accelerating light ions to energies of between 0.5 and 20 MeV with an energy spread of less than one part in 10 000. The accelerator can also produce pulsed beams of particles with 0.2-nanosecond pulses every 500 nanoseconds, which makes it particularly useful for research with neutrons. The NAC's Van der Graaff accelerator is used almost exclusively for materials research and for solid-state physics. This work is done in close collaboration with South African universities and technikons, as well as with overseas laboratories.

The Separated-Sector Cyclotron at the NAC is a variable-energy machine capable of accelerating protons to a maximum energy of 200 MeV. This gives the protons sufficient velocity to travel a distance equivalent to four times around the earth in only one second. Protons of 200 MeV can just pass through the human body, making them especially suitable for cancer therapy.

Two small conventional cyclotrons, designed and constructed by the NAC, are used as injectors (pre-accelerators) for the much larger Separated-Sector Cyclotron. The first injector uses an internal ion source to produce the intense beams of light ions required for radiotherapy and radioisotope production. The second is designed both for heavy ions, such as those of carbon, argon, and krypton, and for polarised proton and deuteron beams, and has therefore been provided with two external ion sources. It also provides an alternative source of protons for therapy.

The Separated-Sector Cyclotron has a diameter of 13.2 metres and a height of 7 metres. The four sector magnets together weigh 1400 tons, and are positioned to an accuracy of one-tenth of a millimetre. The cyclotron is housed in a vault surrounded by concrete walls more than 4 metres thick to provide shielding against neutrons. The entire facility contains over 30 000 cubic metres of concrete in the form of floor slabs, shielding walls or removable shielding roof beams. The accelerated particle beams are guided to specific areas within the shielded building for radiotherapy, radioisotope production or for basic research in a number of disciplines, including nuclear physics and radiobiology. The pathway of the accelerated particle beam from the separated sector cyclotron facility is shown in Figure 1.1.

Radiotherapy facilities are provided by the NAC at the Medical Radiation Group, together with a 30-bed Faure Hospital. The facilities at the NAC are specifically designed to provide beams of high energy protons and neutrons for radiotherapy and for related radiobiological experiments. Neutrons are potentially more effective in controlling certain types of tumour than the radiation from linear accelerators which are routinely used in radiotherapy. Protons have the advantage that much more of the dose delivered can be accurately localised within the tumour volume, which minimises damage to surrounding healthy tissue. Since 1989, cancer patients have regularly received treatment with neutron therapy, while the first facilities for proton therapy were commissioned in 1993. For proton therapy a computerized system has been developed which uses video cameras to locate the patient automatically, and then precisely positions the patient for therapy by using a motor driven treatment couch.

Figure 1.1 Separated-Sector Cyclotron accelerated particle beam pathway.

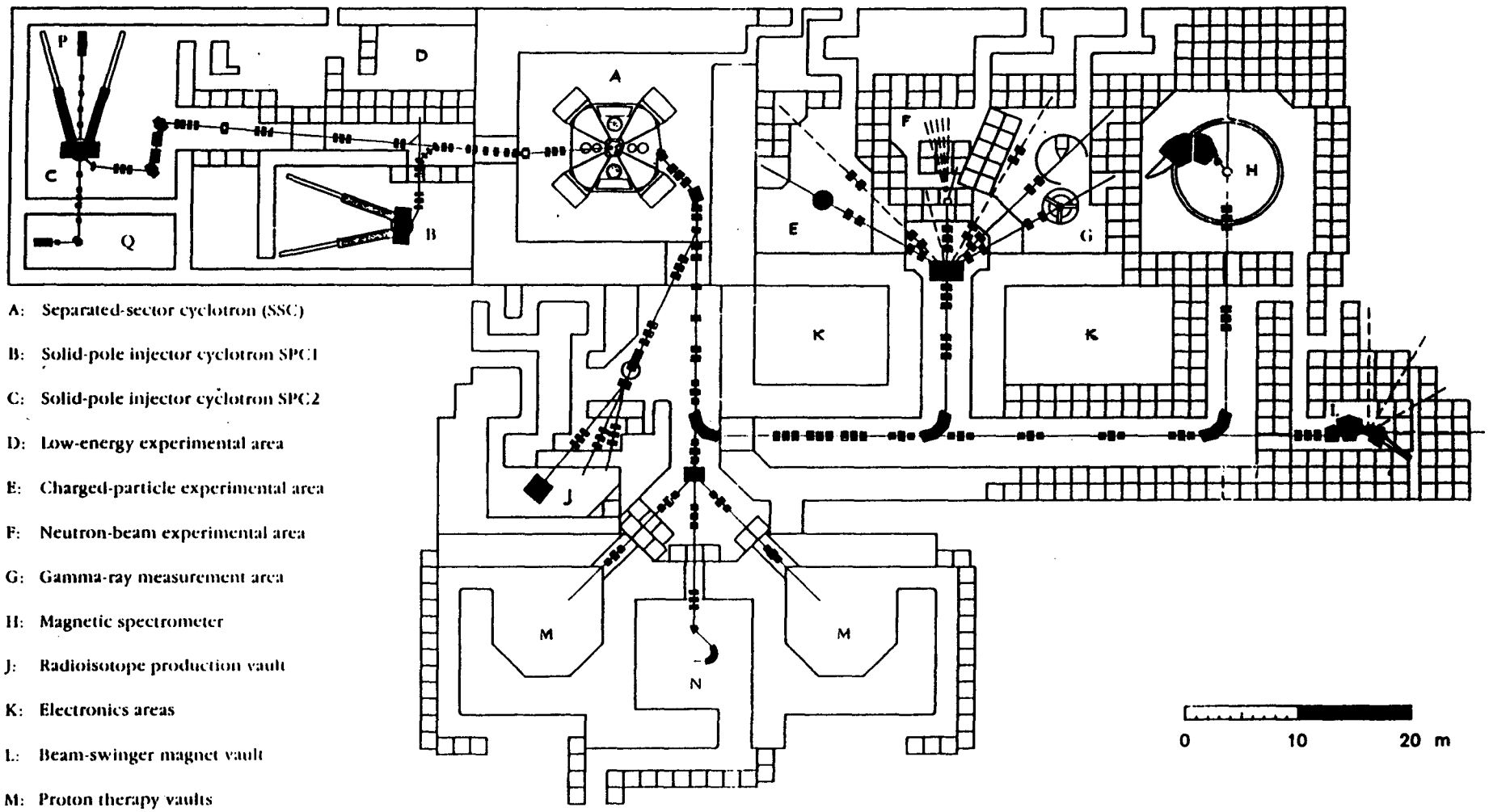

A: Separated-sector cyclotron (SSC)

B: Solid-pole injector cyclotron SPC1

C: Solid-pole injector cyclotron SPC2

D: Low-energy experimental area

E: Charged-particle experimental area

F: Neutron-beam experimental area

G: Gamma-ray measurement area

H: Magnetic spectrometer

J: Radioisotope production vault

K: Electronics areas

L: Beam-swinger magnet vault

M: Proton therapy vaults

N: Isocentric neutron therapy vault

P: Polarized-ion source (basement)

Q: ECR ion source (basement)

Radioisotopes have been manufactured in South Africa since 1965. This started at the old CSIR cyclotron in Pretoria, and since its closure in 1988 the radioisotope production programme has been continued with the Separated-Sector Cyclotron, supported by a strong research and development programme. The high energy of the Separated-Sector Cyclotron and its superior facilities make it possible to produce a wide variety of short-lived isotopes, such as ^{18}F, $^{81}Rb/^{81m}Kr$, ^{67}Ga, ^{111}In, ^{123}I, ^{201}Tl, as well as radioactively labelled compounds for medical purposes. In addition long-lived radioisotopes such as ^{22}Na, ^{55}Fe and ^{139}Ce are manufactured for non-medical use, and are also exported.

1.2 RADIOISOTOPE PRODUCTION FACILITY LAY-OUT

The main function of the NAC's Radioisotope Production Group, at present is to produce various radioisotopes and to deliver them in the required activity to the hospitals in South Africa. In order to obtain a perspective of the production procedures, a brief explanation of the facility lay-out and production sequence is given.

- The first step in the production of a specific radioisotope is the preparation of the target material (solid, liquid or gaseous) into a form suitable for bombardment with the proton beam. Solid targets of various materials are prepared by one or more of the following processes: cutting, machining, cold or hot sintering. Because of the heating of targets under irradiation, all targets have to be water-cooled, and therefore all water soluble or highly corrosive target materials have to be

encapsulated. Solid targets or target capsules are mounted in standardized target holders, while liquids and gases have to be contained in special target holders with high integrity, since leakage can cause serious contamination problems.

- Since radioisotope production targets become highly radioactive when irradiated; they are a radiation health hazard to personnel and therefore have to be handled remotely. For this purpose target holders are transported by means of a remotely-controlled target transport system. The transport system comprises a microcomputer control system, motorized trolleys and transportation rails connecting the target bombardment station (in the irradiation vault) to the hot-cell complex, parking loop and target storage area.

- The target bombardment station is a complex micro-computer controlled system which consists of three rotary target magazines behind one another, mounted inside a cylindrical radiation shield. Each magazine has a capacity to load five target holders and a maximum of three targets can be bombarded in tandem. A pneumatic robot arm facilitates transfer between the transport trolleys and the target magazines, and a pneumatic pusher arm connects the targets to the beamline. Cooling water to the target holders is also provided via the pusher arm. The various targets are bombarded for different time periods, varying from approximately 20 minutes up to a few months.

- After bombardment, the target holders are transported to one of the reception hot-cells, where the target material is removed from them.

- The chemical separation of the desired radioisotopes is performed in the chemical processing hot-cells. These hot-cells are lead shielded chambers where "hot" chemistry is performed under negative pressure atmospheric conditions.

- After separation, the radioisotopes are transported to the dispensing laboratory where the pharmacist performs the dispensing in aseptic conditions and performs the quality control, i.e. checks the chemical purity, radionuclidic purity, etc. of the final product.

- After dispensing, the vials containing the radioisotopes are sealed and then packed into lead pots and tins, and thereafter into boxes, before being dispatched to the various local hospitals or Cape Town International airport, for transport to remote hospitals. Figure 1.2 shows the schematic lay-out of the NAC's radioisotope production facility (Stevens, 1992).

1.3 RADIOISOTOPE PRODUCTION BACKGROUND

Cyclotron produced radioisotopes have become increasingly popular in research, medical and industrial fields despite their relatively high cost when compared to reactor produced radioisotopes. The two production methods are used to create two fundamentally different classes of radionuclides. Cyclotron produced radioisotopes are generally neutron deficient whilst reactor produced radioisotopes are neutron rich. The main advantage derived from cyclotron produced radioisotopes is that they usually have a high specific activity. Additionally it is more difficult to

Figure 1.2 **Schematic lay-out of NAC's radioisotope production facility (Stevens, 1992).**

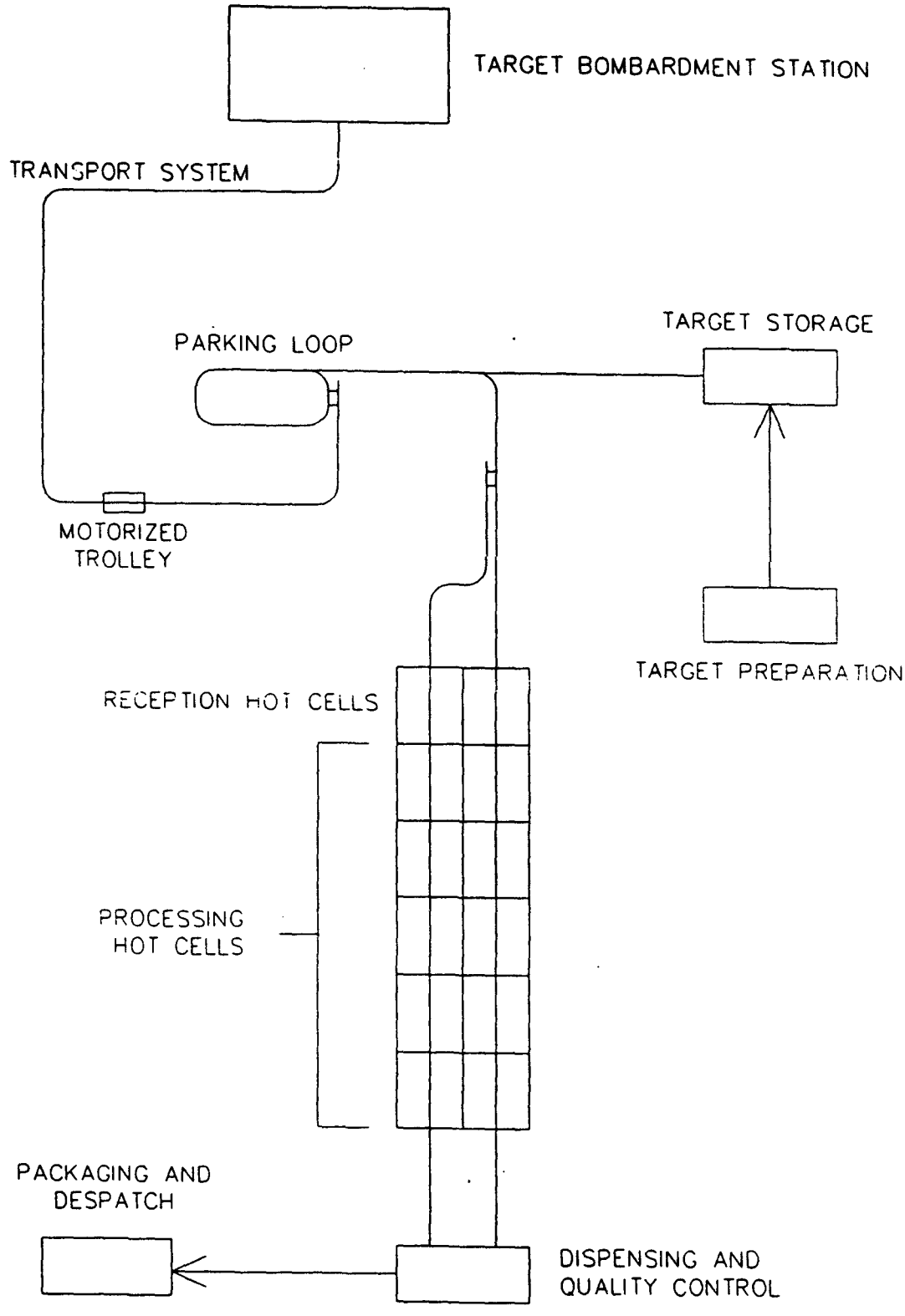

produce several isotopes, with convenient half-lives and decay characteristics, by neutron bombardment as compared to cyclotron irradiation.

The cyclotron invented by Lawrence (1934) can, from the chemist's point of view, be considered as a source of reagents, namely energetic protons, deuterons, helium(III) and alpha particles, which are used to induce nuclear reactions and form the required product. In short it realizes the eternal dream of the ancient alchemist: the transmutation of one element into another.

For the production of radiopharmaceuticals the following points play a very important role:

- The production method must be economically viable.
- The product must have a high specific activity.
- The chemical separation must be simple and easy to carry out in a hot-cell, with a minimum radiation exposure to the operator.
- The radiopharmaceutical must comply with specifications and be registered with the South African Medical Control Board.

A carrier-free radioisotope is usually characterized by: a high specific activity, a high radionuclidic purity (free from other radioisotopes), a high radiochemical purity (free from other chemical form, example $^{123}I^-$ must be free of $^{123}IO_3^-$), a high chemical purity (the presence of non-active material). Radionuclidic purity is normally determined by a high resolution gamma ray spectrometer while radiochemical purity is determined by paper, gel or thin layer chromatography. The chemical purity is normally

determined by flame atomic absorption spectrometry, electrothermal atomisation spectrometry, induced coupled plasma emission spectrometry, or colorimetric spectrophotometry.

Chemistry is therefore one of the most important disciplines in the preparation, separation and quality control of a carrier-free radioisotope and other radiopharmaceuticals.

The NAC utilises a proton beam of 66 MeV for the production of a number of radioisotopes for radiopharmaceutical and other applications. A radioisotope is produced by selecting an appropriate target material, and a small disc of this material is then bombarded with the proton beam. The resulting nuclear reaction that takes place in the target produces a new element - the radioisotope. This radioisotope then has to be chemically separated from the target material, and purified from all contaminants and then sterilised before it can be used as a medicine.

The chemical separation of a radioisotope from the target material is complicated by the very small amount (10^{-9}-10^{-12} g) of radioisotope formed compared to the amount (1–10 g) of non-radioactive target material present, but also by the presence of other radioisotopes produced by side reactions, and chemical impurities originally present in the target material. To isolate the required radioisotope a variety of chemical techniques such as precipitation, co-precipitation, gel filtration, solvent extraction, distillation, electrodeposition and ion exchange chromatography have been used.

The method that will be used in this study will involve ion exchange chromatography because of the simplicity and effectivity of the separation procedure and because in most separations, specialised pieces of equipment (such as centrifuges, mechanical shakers etc.) can be replaced by a single resin column. This technique works well within the confines of a hot cell and minimises the radiation exposure to the operator.

To plan an ion exchange separation the following points had to be taken into account. Since the specific radioisotope to be prepared is normally in picogram to nanogram in mass as compared to the gram amounts of the target material, a big separation factor, α^{A}_{B}, is needed to separate a radioisotope, A, from the target material, B, or vice versa. In general the radioisotope must have a large distribution coefficient ($D > 500$) and the target material a small distribution coefficient ($D < 10$). Initially the separation factor must be larger than 50. The resin column must have good kinetics, so that equilibrium is reached as quickly as possible as the ions move down the resin column, to obtain a sharp separation. A relatively small resin column is always preferred to a large column, since smaller elution volumes are required to elute the sorbed elements. This also leads to a short chemical separation process, which is often an important factor in the final product yield which is dependent on the half-life of the specific radioisotope. Less radioactive waste solutions are also generated which usually have to be stored before being released into strictly controlled on site waste dams.

Ion exchangers are divided mainly into three categories: cation exchangers (e.g. Dowex 50 and Bio-Rad AG 50-), anion exchangers (e.g. Dowex 1, Bio-Rad AG 1- etc.) and chelating ion exchangers (e.g. Chelex 100 and Purolite 940). There are

various other types also available such as those containing no ion exchange groups (e.g. Amberlite XAD-7) (Samuelson, 1956, Reiman and Walton, 1970, and Van der Walt, 1993).

The type of resin to be used depends on the charge of the radioisotope and the target material, i.e. positive or negative, and oxidation number of the isotope. If the radioisotope is for example a cation, or a cationic species is formed by complex formation, then a cation exchanger is often the chosen resin column, and if the target material is anionic or an anionic species is formed by complex formation, then an anion exchanger is often the chosen resin column to retain the radioisotope. At the same time a medium that will promote the adsorption of the required radioisotope cation and elute the target material anion needs to be determined.

The radioisotope and target material are normally not always of opposite charge. At times both can be cationic or anionic in nature and a separation with a cation exchanger or an anion exchanger can be devised with the aid of the distribution coefficients in an appropriate solution/resin system. Here the ion size, charge and valency of the element will play an important role. The element is more strongly adsorbed with increasing ion charge (eg. $M^{+} < M^{2+} < M^{3+}$ etc.). The other factor is the type or nature of the eluting solution (concentration, mixture of acid and organic solution etc.). For example when increasing the hydrochloric acid concentration, some of the transition metals will form a chlorine complex with different number of chlorine ligands.

Distribution coefficients of many elements on anion exchangers and cation exchangers in different media have been reported. The distribution coefficient determines to a great extent the cationic and anionic nature of the ions or complex ions.

The increase in crosslinkage of a resin normally results in an increase in the distribution coefficient of the element. For example with crosslinkages (2% and 4%), the element is not strongly retained and is easily eluted. Van der Walt, (1988) had shown this influence of crosslinkage on the distribution coefficients of a few selected elements on the anion exchangers (AG 1-X2, -X4, -X8 and -X10). Strelow et al., (1971) had shown the same effect on the cation exchangers (AG 50W-X2, -X4, -X8, -X12 and -X16).

For some elements that are strongly retained on the resin, the particle size of the resin plays an important role. Resin with small particle size (200 - 400 mesh) often showed less tailing, however Van der Walt et al., (1985) and Strelow, (1980) showed that sharp separations were also possible with a 2% and 4% crosslinkaged resin with a particle size (100-200 mesh).

The resin has reducing qualities and can reduce Fe(III), Ti(IV), V(V) and Cr(VI) to Fe(II), Ti(III), V(IV) and Cr(III) if the necessary stabilizer forms a complex with the element or in the absence of an oxidant. A more detailed explanation of the ion exchange behaviour of various metals on various ion exchange resins will be discussed in sections 2, 3 and 4.

Different ion exchange chromatographic separations are therefore possible with the aid and knowledge of the above factors. A chemical process to produce the radioisotope of interest can therefore be devised in the same way to separate the radioisotope from the cyclotron target material and other radioisotopes to produce a carrier-free final product.

1.4 MOTIVATION

Cyclotron produced radioisotopes which have to be in a specific chemical form or incorporated in an organic compound, are often used as tracers to monitor various body functions. Highly sophisticated equipment such as gamma-cameras and positron tomographs are then used to detect gamma rays and form images showing the tracer locations. This is one of the techniques used in diagnosing and localizing malignant tumours. The high purity radioisotopes which are produced at the NAC on a weekly basis satisfy South Africa's entire demand for certain important medical radioisotopes and radiopharmaceuticals. More than 1000 consignments are supplied to about forty provincial hospitals, private nuclear medicine practises and research institutions throughout the country and are used in nearly 10 000 patients per year. In addition, a number of other radiopharmaceutical products are under development and are available on request from the NAC for patient use, on prescription, and / or clinical trials, evaluations, etc. All these radioisotopes cannot be produced anywhere else in South Africa, cannot be imported cost-effectively from abroad because of their short half-lives and in most instances, cannot be replaced satisfactorily with other (reactor-produced or imported) radioisotopes (Higashi et al., 1972).

The cyclotron-produced ^{67}Ga which decays to the stable ^{67}Zn by 100% electron capture, is extensively used in nuclear medicine (Green and Welch, 1989). Its useful photon radiation energy is the 184.6 keV γ-rays. When injected as ^{67}Ga-citrate into the blood, it binds to plasma transferrin and is subsequently transported to the tumour tissue. Although the ^{67}Ga-citrate is not a tumour specific agent as stated by Vallabhajosula et al., (1981), radiogallium is known to concentrate in many types of tumours as well as non-malignant lesions, especially inflammatory ones. A variety of neoplasma accumulates ^{67}Ga in both primary and secondary sites including primarily Hodgkins disease, reticulum cell sarcoma, lymphoblastoma, myeloblastomas associated with myeloblastic leukemia, squamous cell carcinoma of the lung, poorly differentiated adenocarcinoma and hepatoma. Accumulation of ^{67}Ga in non-neoplastic lesions include sarcoidosis, active abscesses, fungal and bacterial infections of the lung, soft tissue and others (Van Rijk, 1986).

As a result, this radioisotope has gained widespread application as a diagnostic tool in nuclear medicine over the last two decades, and because ^{67}Ga is as good as other radiopharmaceuticals and is readily available, it has become one of the most widely used cyclotron produced pharmaceuticals. The usefulness of ^{67}Ga for the localization of a variety of malignant human tumours is extensively published as stated by Taylor and McCready, (1986) and Van Rijk (1986).

Previously the production route of ^{67}Ga at the NAC used the proton bombardment of ^{nat}Zn targets which utilised 15-20 hours of cyclotron beam time per routine production. Since the proton beam produced by the cyclotron is very expensive,

every successful effort to shorten the bombardment time of the target will save a lot of money. A study was undertaken to use for the first time a tandem ^{nat}Ge / ^{nat}Zn target, that produced the same amount of ^{67}Ga activity, but used less than half of the beam time (7-8 hours).

1.5 OBJECTIVES OF THE THESIS

- To determine distribution coefficients of Ga(III) and contaminant elements in various solvent media on the Amberchrom range of resins.
- To draw up elution curves of Ga(III) and contaminant elements in various solvent media on the Amberchrom range of resins.
- To determine a quantitative separation of synthetic mixtures using the selected resin.
- To develop a purification method to separate the gallium radioisotopes from the tandem ^{nat}Ge / ^{nat}Zn target material by ion exchange chromatography.
- To develop analytical methods, using, flame atomic absorption spectrometry, electrothermal atomisation spectrometry, induced coupled plasma emission spectrometry and / or colorimetric spectrophotometry for the analysis of distribution coefficients, elution curves and the contaminants in the final product, the ^{67}Ga radioisotope.
- To develop a reliable production procedure that requires suitable hot cell facilities and yields consistent carrier-free ^{67}Ga that is within the requirements set by the specifications of the US Pharmacopoeia and British Pharmacopoeia, and can be implemented for routine production of the isotope.

2 LITERATURE SURVEY

2.1 NUCLEAR PHYSICS SURVEY

The production of ^{67}Ga obtained by:

- proton bombardment of natural or enriched zinc,
- deuteron bombardment of natural or enriched zinc,
- alpha-particle bombardment of copper,
- helium (III) bombardment of copper,
- or indirect alpha-particle bombardment of natural or enriched zinc

has been reported in the literature and has been summarized by Helus and Maier-Borst (1973), Thakur (1977) and Bjornstad and Holtebekk (1983).

At the NAC the routine production of radioisotopes is however at present limited to the utilization of a 66 MeV proton beam which is shared with neutron therapy. It is clear from the literature that the proton bombardment of zinc targets is a well established production route for ^{67}Ga, but only at energies below 30 MeV. However the utilization of a 44 MeV proton beam (Bonardi and Birattari, 1983, and Kopecky, 1990) and a higher energy proton beam (Grant et al., 1979, 1982, and Grutter, 1982). has been reported.

The proton bombardment of ^{nat}Ge targets with moderate energies (up to 64 MeV) was also reported to be a suitable method to produce ^{67}Ga (Horiguchi et al., 1983 and

Nortier et al., 1991). However it was reported by Nortier et al., (1991), that substantially higher yields of ^{67}Ga were obtained with a tandem target employing both the ^{nat}Zn and ^{nat}Ge as target material as compared to that of either target. The basis of this study is based on this tandem ^{nat}Ge / ^{nat}Zn target of Nortier et al., (1991) and a more detailed explanation on the targetry design and possible nuclear reactions occurring will follow in section 6.

2.2 NUCLEAR CHEMISTRY SURVEY

Chemical processing involves the separation of radioisotopes from one another and from the target material. Reviews of early chemical separations showed a preference towards classical wet chemical methods such as precipitation (Helus and Maier-Borst, 1973), solvent extraction (Weinreich et al., 1982), distillation (Garrison and Hamilton, 1951), electrodeposition (Hupf and Beaver, 1970) and ion exchange chromatography (Van der Walt and Strelow, 1983). Van der Walt (1984-1998) was the first chemist who had used ion exchange chromatography in South Africa for the separation of radioisotopes from one another and from the target material. Many of these separation methods were published (Van der Walt et al., 1979, 1981, 1982 a, b, 1983 a,b, 1985 a, b, 1987, 1989 a, b, 1994). Ion exchange chromatographic separations can easily be performed in a hot-cell, making it the method of choice at the NAC.

According to the literature, the chemical separation procedures employed for the production of ^{67}Ga from the zinc targets are mainly based on extraction and ion exchange chromatography. The main procedures are:

- solvent extraction with isopropyl ether from strong HCl solutions (Brown, 1971),
- solvent extraction with methyl isobuthyl ketone from a 2 M HCl solution containing a 1 M sulphate (Vlatkovic, 1975),
- solvent extraction with 4-methyl-2-pentatone from 5 M HCl solution, followed by a stripping of water and a subsequent anion exchange step (Hupf and Beaver, 1970),
- adsorbtion on alumina from HCl solution containing nitrate at pH 2.5 (Kopecky and Mudrova, 1975),
- cation exchange from strong HCl solution (Neirincks and Merve, 1971; and Van der Walt and Strelow, 1983),
- anion exchange from HCl and HCl - HF solutions (Kraus et al., 1954; 1960),
- and exchange with an organic polymer containing no ion exchange groups in strong HCl solutions (Brits and Stelow, 1990).

According to the literature, Novgorodov et al., (1988) was the only author that had used the proton bombarded ^{nat}Ge target to produce ^{67}Ga employing a high-temperature method, based on the volatilization of gallium from a solid germanium target in an atmosphere of vapours of hydrofluoric acid at a reduced pressure. The only drawback was the complex experimental set-up and the high production temperature used, which could result in difficulty in controlling surface contamination within the hot cell.

The ^{67}Ga / Zn separation presented by Brits and Strelow, (1990), using an organic polymer containing no ion-exchange groups, Amberlite XAD-7 resin, produced a high

quality ^{67}Ga in good yield with little effort. A similar method using the Amberchrom CG-71cd resin was proposed by Van der Walt (1995) using the tandem ^{nat}Ge / ^{nat}Zn target. Dolly (1995) tested this method, built a hot cell panel and performed a few test runs. Van der Walt (1996) redesigned and simplified the panel. The modified method for the recovery of ^{67}Ga from the tandem ^{nat}Ge / ^{nat}Zn target was thoroughly further investigated and is presented here.

2.3 ION EXCHANGE RESIN SURVEY

Systematic information about the ion exchange behaviour of elements is indispensable for planning separations and estimating optimum conditions. An extensive literature search was done on the anion and cation exchange behaviour of the metals {Ga(III), Ge(IV), Zn(II), Fe(II), Ti(III), As(III), Al(III) and Cu(II)} that may be present in the production.

2.3.1 ANION EXCHANGE RESIN SURVEY

The separation of inorganic elements using anion exchange resins depends on the ability of the elements to form anionic complexes which are adsorbed. The first systematic study of the anion exchange behaviour of a large number of elements in hydrochloric acid was presented by Kraus and Nelson, (1956). They used the strongly basic quaternary ammonium type, Dowex 1-X10 resin (10% crosslinkage). Most other systematic work made use of 8% crosslinked resins, such as the AG 1-X8. Studies of anion exchange behaviour of these metals in different media were

presented in nitric acid (Faris and Buchanan, 1964; Ichikawa, 1961 and Kraus and Nelson, 1958), hydrofluoric acid (Faris, 1960), sulphuric acid (Danielsson, 1965 and Strelow and Bothma, 1967), oxalic acid (Corte et al., 1968), acetic acid (Winkel et al., 1971), hydrobromic acid (Andersen and Knutsen, 1962 and Marsh et al., 1978), hydriodic acid (Marsh et al., 1978), phosphoric acid (Polkowska et al., 1974 and 1977), hydrochloric - hydroflouric acid mixtures (Nelson et al., 1960), hydrochloric - oxalic acid mixtures (Strelow et al., 1972), hydrobromic - nitric acid mixtures (Strelow, 1978) and inorganic acid mixtures with organic solvents (Klakl and Korkish, 1969). Van der Walt et al., (1985) had also presented the adsorption behaviour of some elements using the strongly basic anion exchangers such as the Bio-Rad AG 1-X2, AG 1-X4, AG 1-X8, AG 1-X10 and AG MP-1. Although better exchange kinetics is obtained with the low crosslinked resins as compared to the higher crosslinked resins, large resin columns are often used which results in large elution volumes that are usually required. Serious tailing often occurs when high crosslinked resins are used.

Less attention was however paid to the inorganic analytical use of weakly basic anion exchange resins, probably because of the slow kinetics of the exchange reactions, and of the capability of the ion exchange occurring in a much narrower pH range than the strongly basic resins. The adsorption behaviour of many metals with a phenol condensation type weakly basic anion exchange resin, Amberlite CG-4B, in different media including hydrochloric acid (Kuroda et al., 1968), thiocyanate (Fritz and Kaminski, 1971) and sulphuric acid (Strelow and Bothma, 1967 and Kuroda et al., 1972) were however reported.

2.3.2 CATION EXCHANGE RESIN SURVEY

For the gel-type microporous cation exchangers, such as Bio-Rad AG 50W-X8, systematic information on the adsorption behaviour of a large number of elements {including Ga(III), Ge(IV), Zn(II), Fe(II), Ti(III), As(III), Al(III) and Cu(II)} are available for aqueous hydrochloric acid (Strelow, 1960 and Nelson et al., 1964), nitric acid (Strelow et al., 1965), sulphuric acid (Strelow et al., 1965), hydrobromic acid (Strelow et al., 1975 and Nelson and Michelson, 1966), perchloric acid (Strelow and Sondorp, 1972), hydrochloric acid - perchloric acid mixtures (Nelson and Kraus, 1979), hydrochloric acid - ethanol (Strelow et al., 1969), hydrochloric acid - acetone (Fritz and Rettig, 1962 and Korkisch and Ahluwahla, 1967), hydrobromic acid - acetone (Korkisch and Klaki, 1969) and various other systems. Van der Walt and Strelow, (1983) had also used the Bio-Rad AG 50W-X4 resin for the separation of gallium from other elements in hydrochloric acid, which showed sharp and quantitative separations with insignificant tailing.

It has been shown that in hydrochloric acid the cation exchange separation factor for elements with negligible tendencies to chloride complex formation increases quite considerably with increase in resin crosslinkage (Strelow, 1981). Further increases of separation factors for such elements can be obtained by adding a water-miscible solvent such as methanol or ethanol (Strelow and van Zyl, 1968). Unfortunately when microporous resins are used the exchange rates also become considerably slower with increase in crosslinkage, and further decrease with increasing concentration of the organic solvent.

The so called macroporous or macroreticular cation exchange resin, Bio-Rad AG MP-50, which has a rigid wide open macroporous structure (20 -25% crosslinkage), combines the advantages in selectivity offered by the high crosslinkage with fast exchange rates. This makes the macroreticular resins more suitable for applications in high pressure liquid chromatography procedures for the separation of inorganic ions because of its small change in volume with changes in eluent concentration. Systematic information is found about the cation exchange behaviour of many elements in aqueous nitric acid (Marsh et al., 1978), hydrochloric acid (Strelow, 1984), hydrochloric acid - acetone mixtures (Fritz and Story, 1974), hydrochloric acid - methanol mixtures (Strelow, 1984) and various other systems.

2.3.3 ORGANIC POLYMER RESIN SURVEY

The main disadvantage of using Dowex and Bio-Rad resins, as was encountered by Brits and Strelow, (1990), is that in the separation of nanogram amounts of gallium from macro amounts of the other elements {(Ge(IV), Zn(II), Fe(II), Ti(III), As(III), Al(III) and Cu(II)} as is often encountered in practice, results in excessive tailing, thus requiring the use of relatively large elution volumes for complete recovery. Brits and Strelow (1990), had used an organic polymer containing no ion exchange groups, Amberlite XAD-7 resin, instead of an ion exchange resin, and found that complete separation of gallium from zinc can be obtained at microgram levels. They also determined the flow-through capacities of gallium at various hydrochloric acid concentrations and it was found to be much more superior in the Amberlite XAD-7 resin as compared to the Bio-Rad AG 50W-X4 and AG1-X8 resins. The only

drawback of the Amberlite resins is that the resin had to be dried to a constant weight in a vacuum distilling apparatus, sieved, and a fraction <300 μm in diameter was used for complete separations. We then decided that the Amberchrom range of resins which is very similar in structure to that of the Amberlite resin, but available in <300 μm diameter beads, needed to be investigated. According to a literature study no ion exchange behaviour of the metals {Ga(III), Ge(IV), Zn(II), Fe(II), Ti(III), As(III), Al(III) or Cu(II)} on the Amberchrom resins had been reported and therefore a detailed study was undertaken.

3 ION EXCHANGE CHROMATOGRAPHY

3.1 RESINS

The resins used in this investigation were of the Amberchrom range of resins which were supplied by Tosohaas, Cambridge, UK. Tosohaas is a joint venture of the two well-respected companies: Tosoh Corporation, best known for its popular high performance capillary columns; and Rohm and Haas Company, the leader in polymer design and architecture for purification of biomolecules. The ion exchange behaviour of the Amberchrom resins were compared to the published data of the cation exchange resin (AG 50W-) and anion exchange resin (AG 1-) supplied by the Bio-Rad Laboratories of Richmond, California, and the Amberlite XAD-7 resin supplied by Rohm and Haas.

Amberchrom chromatographic resins are chemically stable, porous and have high surface areas. Two of the resins, Amberchrom CG-161(16% crosslinkage) and Amberchrom CG-162(16% cosslinkage) are based on styrenic polymers, while the Amberchrom CG-71(7% crosslinkage) resin is produced from methacrylate-based polymers as illustrated in Figure 3.1. Amberchrom resins are smaller particle size versions of the commonly used Amberlite XAD adsorbent resins.

Amberchrom resins are manufactured as spherical rigid beads through a polymer technology which enables reproducible production of large batches. They are produced in three particle size ranges, all dry (d): "sd", or superfine (20-50μm), "md",

Figure 3.1 Molecular structure of Amberchrom Resins (Tosohaas, 1996).

Amberchrom CG-161 & Amberchrom CG-162 Resins

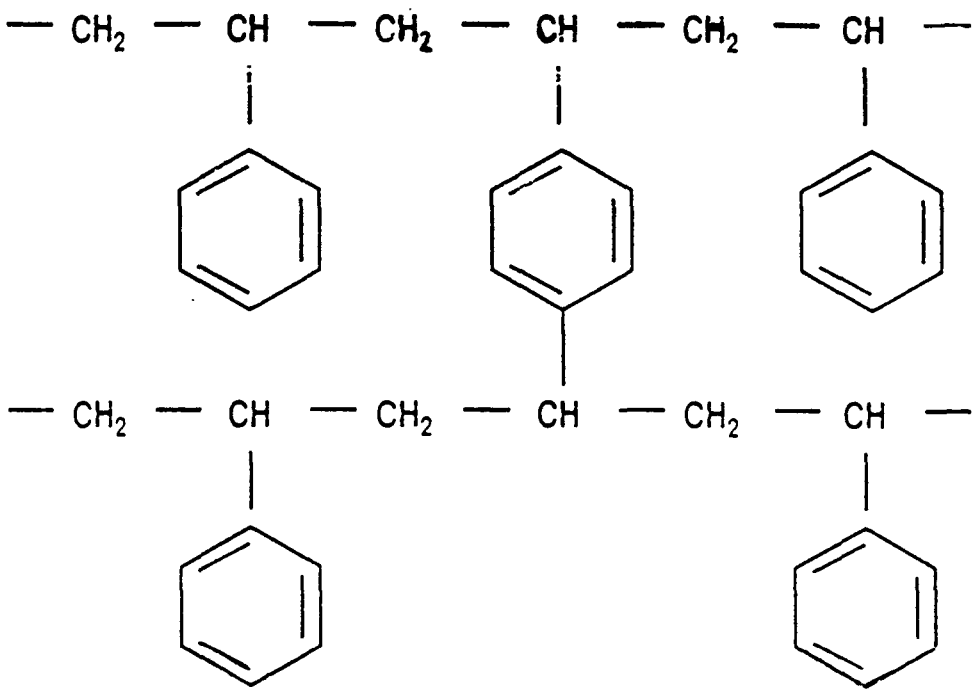

Amberchrom CG-71 Resin

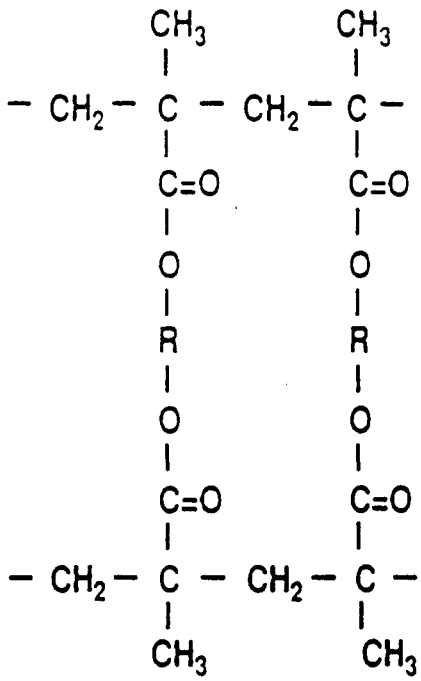

or medium (50-100μm), and "cd", or coarse (80-160μm). The advantages of Amberchrom resins over silica-based resins are due to their physically and chemically stable polymeric structure. Thus Amberchrom resins can offer the following beneficial characteristics for production scale chemical separations: the ability to use aggressive mobile phases for selectivity optimization; they can be cleaned easily with strong acids or bases; they allow thermal or chemical sanitization; they allow gradient elution or cleaning with a broad range of solvents with minimal change in bed volume; they enable repeated cycles with assured column stability and reproducible performance; and the ability to operate at high flow rates, for high throughput with moderate back-pressure. The physical properties of the Amberchrom resins are shown in Table 3.1.

Table 3.1 Physical properties of Amberchrom resins.

Amberchrom resin	Surface Area(m^2/g)	Pore Size(nm)
Styrenic		
CG-161md,cd	800-950	110-175
CG-162sd	200-300	1000-1400
Acrylic		
CG-71sd, md, cd	450-550	200-300

Bio-Rad ion exchange resins have certain common properties. They consist of an insoluble porous lattice with attached functional groups, and are available in the form of beads or more rarely granular particles. For example Figure 3.2, illustrates the crosslinked styrene divinylbenzene lattice which is derivatized with the cationic functional group $CH_2N^+(CH_3)_3$ to form the AG 1 anion exchange resin, or with the anionic functional group SO_3^- to form the AG 50W cation exchange resin.

Figure 3.2 Molecular Structures of Bio-Rad AG 50W and AG 1 resins (Bio-Rad, 1996).

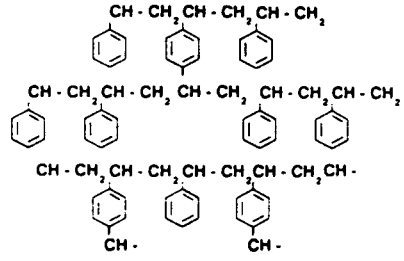

A. Crosslinked styrene divinylbenzene copolymer

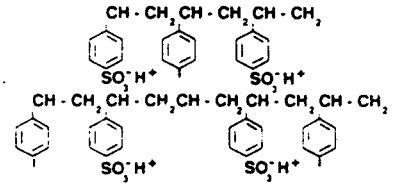

B. AG 50W crosslinked strongly acidic cation exchange resin

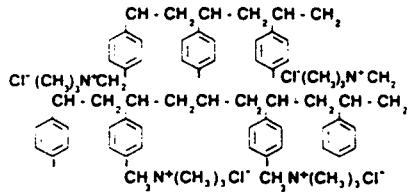

C. AG 1 crosslinked strongly basic anion exchange resin

3.2 ION EXCHANGE THEORY

In ion exchange chromatography, ions are separated according to their charge. The column packing consists of charged functional groups covalently bound to an insoluble support, and mobile counterions which associate with the functional groups because of their opposite charge. When a sample is passed through the column, ions which are neutral or bear the same charge as the functional groups are eluted, while oppositely charged ions compete with the counterions for binding sites on the functional groups. Ions which are more highly charged than the counterions are bound to the matrix and are retained on the column. An eluant with the appropriate ionic strength and pH can then be used to recover the bound sample. The ion exchange principle is illustrated in Figure 3.3

Ion exchange resins are commonly polymers (e.g. polystyrene) with attached ionic groups. The attached group is always an electrolyte, one ion of which is fixed to the resin while the other, of opposite charge, is mobile. The mobile ion is the ion that is exchanged. For example Bio-Rad AG 50W cation exchange resin consists of the resin matrix, styrene divinylbenzene, to which $-SO_3^-H^+$ is attached as the functional group. It is the H^+ of this sulphonic group that is mobile and is exchanged for other cations. Bio-Rad AG 1 anion exchange resin consists of the resin matrix, styrene divinylbenzene, to which $-N^+(CH_3)_3Cl^-$ is attached. The Cl^- is the mobile exchangeable ion. In action, an anion exchange resin will exchange its mobile ions, Cl^- for example, for other anions present in solution around the resin. The resulting equilibria will be influenced by all the usual equlibria factors, for example

Figure 3.3 Theory of ion exchange (Bio-Rad, 1996).

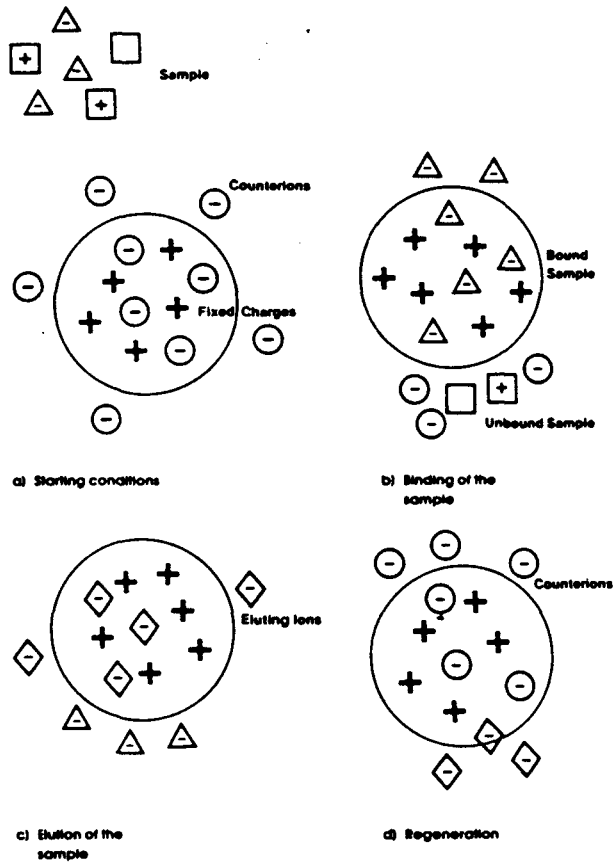

Counterions (⊙) are ionically bound to the fixed charge (+) on the matrix. b) Sample molecules (△) of the opposite charge of the matrix bind displacing the counterions while neutral molecules and molecules of the same charge (□+) as the matrix do not bind (pass straight through). c) The sample is displaced by eluting ions (◇). d) The resin is regenerated by exchanging the eluting ions for the original counterions. The ion exchange resin is ready for re-use.

concentration and mobility of each ion, and time. The factors of equilibria as well as the unique characteristics of each resin will help determine which resin and which particle size is optimum for the separation of elements. The influence of particle size, flow rate, bed volume, cross-sectional area of the bed, crosslinkage of resin polymer matrix, and others will all play a role in the choice of the ion exchange resin.

3.3 ION EXCHANGE RESIN PROPERTIES

Ion exchange resins perform efficiently in a variety of applications in part because of their valuable chemical and physical properties. The physical properties of an ion exchange resin include matrix, functional group, ionic form, particle size distribution, particle shape, swelling, porosity for macroporous resins, permeability for gel type resins and crosslinkage. The chemical properties include exchange capacity, water retention capacity, thermal stability, resistance to reduction and oxidation, solvent stability and response to ionic strength.

Because of the high permeability and high concentration of functional groups within their chemical structure, ion exchange resins normally have a high effective capacity. Small volumes of resin can retain high molecular amounts of ionic material when used for concentrating substances of interest or for scavenging ions to be eliminated from a solution.

Ion exchange resins also provide high resolution chromatographic separations because many interactions take place per unit of column volume. In addition, the remarkable

chemical stability of ion exchange resins makes them usable with a variety of chromatographic conditions including high temperatures, organic solvents and strong reducing and some oxidising agents. The resin matrix remains chemically unchanged by the ionic interactions which take place at the functional groups, and the resins can be regenerated.

3.3.1 PHYSICAL PROPERTIES

3.3.1.1 IONIC FORM

Most resins are available in several ionic forms, and can be converted from one form to another. In the most straightforward case, the resin is used in an ionic form with a lower selectivity for the functional group than the sample ions to be sorbed. The sample ions are then sorbed when introduced, and can be desorbed by introducing an ion with high affinity for the resin, or a high concentration of an ion with equivalent or lower affinity. In many cases a high concentration of the original counterion can be used for desorption, thus regenerating the resin at the same time the sample is eluted. In general, the lower the selectivity of the counterion the more readily it exchanges for another ion of like charge. The order of selectivity can be used to estimate the effectiveness of different ions as eluants, with the most highly selective being the most efficient. The order of selectivity can also be used to estimate the difficulty of converting the resin from one form to another. Conversion from a highly selected to a less highly selected form requires an excess of the new ion.

3.3.1.2 EFFECT OF CROSSLINKAGE

The styrene divinylbenzene ion exchange resins has a relatively rigid gel type structure. The porosity depends upon the hydration of the matrix, which, in turn is controlled by the hydration of the functional groups. Ion exchange resins are most hydrated, therefore most swollen, in water. Their swelling decreases as the ionic strength of the solvent is increased, or as increasingly non-polar solvents are added. Swelling is also affected by the ionic form of the resin, and the hydrophilic nature of the functional group. The copolymer matrix of ion exchange resins consists of polystyrene chains tied together at intervals by divinylbenzene groups. The percentage of crosslinkage used, determines the solubility, swelling, selectivity, as well as other physical and chemical properties for a given type of ion exchanger. As the crosslinkage decreases, the permeability increases, and the ability of the resin to accommodate larger ions is increased. Low crosslinked resins (2%-4% styrene divinylbenzene) have a high degree of permeability, reach equilibrium more rapidly, and are able to accommodate larger ions. They have lower physical resistance to shrinkage and swelling, so that they imbibe more water and swell to a larger wet diameter than a highly crosslinkaged resin of equivalent dry diameter. The wet capacity is lower since the functional groups are, in effect, more dilute; the selectivity for certain ions is reduced; and the physical stability of the resin is decreased.

High crosslinked resins (8%-16% styrene divinylbenzene) exhibit properties in the opposite direction. As the amount of divinylbenzene is increased, the crosslinkages occur at closer intervals and the effective pore size, permeability and tendency of the

resin to swell in solution are all reduced. At the same time, the ionic groups come into effectively closer proximity, resulting in increased sensitivity. Wet volume capacity increases because highly crosslinkaged particles swell only slightly and will, therefore, contain more exchange sites per unit volume than will a resin of low crosslinkage. In addition, the equilibrium rate decreases because ion diffusion through the resin is retarded.

3.3.1.3 EFFECT OF PARTICLE SIZE AND SHAPE

Most Analytical Grade (AG) and Amberchrom resins are available in several particle size ranges, although the ranges in Analytical Grade resins and Amberchrom resins are more precisely controlled than the commonly used Dowex resins. The flow rate in a column increases with increasing resin particle size. The attainable resolution, however, increases with decreasing particle size and with narrow size distribution ranges, i.e. less tailing, are evident.

Analytical Grade resins particle size is generally specified as dry mesh; mesh referring to the number of openings per inch on the screens used to size ion exchange resins. As the particle size of an ion exchanger decreases, the time required to reach equilibrium decreases, the flow rate is reduced, the settling rate of the resin is decreased and the efficiency of a given volume of resin increases.

Generally 200-400 mesh and finer mesh resins are used for high resolution chromatography, 100-200 mesh for general purpose ion exchange techniques, and 50-

100 mesh and coarser meshes for large scale applications and batch operations where the resin and sample are slurred together. The larger meshes are also suitable for small scale applications such as the removal of one cationic species as an anionic complex in the presence of an uncomplexed cation, or in a desalting application.

3.3.1.4 SWELLING AND POROSITY

Ion exchange resins swell or shrink in different aqueous media. Macroporous resins exhibit some volume changes, but only a fraction of those observed in non-macroporous resins. The resin can be thought of as a matrix of insoluble ions. The solubility of a resin is limited by its crosslinked organic backbone. In a specific ionic form, the resin will be swollen to its greatest degree in water. This is caused primarily by the hydration of the functional groups with water which is directly proportional to the number of hydrophilic functional groups on the polymer matrix. Most of the water retained by an ion exchange resin is held internally due to the hydration of the functional group. The amount of water is more or less dependent upon the hydrophobic nature of the functional group and the ionic form of the resin. The porosity of a resin is best defined in terms of the molecular size of the largest ion that is able to penetrate the crosslinked matrix under a given set of conditions. For a specific ionic form of an ion exchange resin, the porosity is greatest in water and decreases rapidly with increasing ionic strength of the solvent.

3.3.2 CHEMICAL PROPERTIES

3.3.2.1 EXCHANGE CAPACITY

The exchange capacity of an ion exchange resin is the number of ion exchange sites per unit mass per volume of resin. The exchange capacity of an ion exchange resin is expressed both as the number of equivalents per gram of oven dried resin and the number of equivalents per unit volume of the hydrated (packed) resin. These data are often expressed as milliequivalents per gram of dry resin (ECD), and milliequivalents per gram of hydrated resin (ECV). For crosslinked polystyrene resins, the ECV for a particular resin type and ionic form increases with crosslinkage, while the ECD is nearly independent of crosslinkage. The ECD for a class of ion exchange resin, for example, AG 1 resin, is relatively constant. When all the water is removed, the dry resin has approximately the same number of functional groups per unit mass of resin, regardless of the degree of crosslinkage.

3.3.2.2 WATER RETENTION CAPACITY

The water retention capacity (WRC) for ion exchange resins is often given as the percentage of water. The WRC varies with crosslinkage and the ionic form. The WRC increases with decreasing crosslinkage because of the reduced physical strength of the crosslinkaged lattice. The resin may be more soluble as crosslinkages decrease and therefore it may be able to absorb more water than increased crosslinkaged resins. If there were no crosslinkage, the resin would be completely soluble in water.

However, the increase in water retention levels of about 8% crosslinkage resins occur, where the increasing physical resistance of the more highly crosslinkaged resin is balanced by its increasingly hydrophilic character as the concentration of functional groups increases.

3.3.2.3 RESPONSE TO IONIC STRENGTH

Ion exchange resins swell and shrink with changes in the ionic strength of the solvent. Resins with high crosslinkage exhibit less volume change with changes in ionic strength than resins with low crosslinkage. These changes are due to osmotic forces. As the concentration of the ions within the resin reaches equilibrium with the ionic media there is a change in the amount of water held by the resin. This chemical property is best explained by the Donnan membrane theory (Samuelson, 1953).

3.3.2.4 CHARGE AND SIZE OF THE SOLUTE

At a given pH, a solute may be positively or negatively charged, with the exception of uncomplexed inorganic ions. If the solute is positively charged and can be made more positively charged by reducing the pH, it will sorb to a cation exchange resin. The opposite is true for a negatively charged solute. Sorption occurs because the charge on the resin is opposite to that of the solute. The solute can be desorbed from the resin by changing the pH until the solute has the same charge as the charge on the resin. In general, if the solute is positively charged and one wants to sorb the solute, a cation exchange resin is often used. If the solute is positively charged and one wants

to change the anionic counterion, an anion exchange resin is often used. As the total number of charges increase on a solute, the sorption increases, provided that the charges have the same sign at a given condition. Some solutes become so strongly sorbed that when desorption is attempted the solute may be denatured. In such cases the choice of an ion exchange resin should be limited to one with low crosslinkage or weak functional groups.

As the molecular size of the solute increases, it experiences great difficulty in penetrating the ion exchange resin. This property is useful for removing small ionic contaminants. However, if sorption and fractionation of large solutes is desired, ion exchange gels should be used. Macroporous resins may be used if the total number of charges on the solute is not too great.

3.3.2.5 SOLVENT STABILITY

Ion exchange resins are generally stable in the presence of strong bases, strong non-oxidising acids and mild oxidising agents. Substantial structural damage occurs with strong oxidizing agents such as permanganate, concentrated nitric acid, hydrogen peroxide etc. Strongly basic anion exchange resins or strongly acidic cation exchange resins can be used to sorb solutes which can tolerate strong acids or bases. In general, if a solute is stable in the pH range of 1-14, a strong acid or base may be used.

Solutes which are not stable over the entire pH range require the use of a resin which functions in a narrow pH range. Conditions for using these resins are mild, and

therefore less severe for the solute. The mechanism for sorption and desorption is similar to that for strong acid and base resins. Structural similarity between the resin matrix and the solute, i.e. aromatic resin and aromatic solute, determines whether adsorption or ion exchange will take place. The use of high ionic strength solvents or the addition of alcohol to the solvent will reduce the degree of the non-ionic adsorption.

3.3.2.6 RADIATION AND THERMAL STABILITY

The effect of ionizing radiation on organic ion exchangers is very similar to that observed on organic polymers except that the presence of functional groups makes radiolytic changes complex. A variety of changes such as scission of chemical bonds, new bond formation, oxidation, gaseous product formation etc., leads to changes in the exchange capacity, crosslinkage, solubility, density porosity, molecular weight and mechanical properties. Pillay (1986) has compiled most of the relevent published data on the limitations of organic ion exchangers.

The thermal stability of an ion exchange resin is lowest when the resin is in a dry state and typical damage is a progressive loss in crosslinkage (Glueckauf, 1955). The trend is for resins of low percentage crosslinkage to be most affected, and in practice if resins have to be dehydrated, the temperature is kept below 60^0C. For the hydrated form of the resin a loss of functional groups rather than crosslinkage occurs, and significant damage has been observed at temperatures above 150^0C (Hall, 1963).

3.4 ION EXCHANGE INTERACTIONS

In addition to true ion exchange, other interactions can take place between the solutes and the resin which may either supplement the ion exchange interaction or be used in place of ion exchange to separate either ionic or non-ionic species.

Adsorption. Aromatic or non-polar interactions between the solute and hydrocarbon matrix of the exchanger have been exploited to separate alcohols, aldehydes, and related compounds by using a salt solution as eluant with either cation or anion exchangers. The salt increases the binding of the non-electrolytes, which are then separated by their degree of attraction for the resin. Adsorption has also been exploited along with other mechanisms to separate such ionic species as aromatic acids. In some cases, however, adsorption interferes with the ion exchange technique, and can be reduced by adding organic solvents such as dioxane or methanol to the eluant.

Complex Formation. A molecule which form a complex with an ion can be separated by ion exchange chromatography. For example, sugars which form complexes with borate have been separated on anion exchangers in the borate form. In this study complex formation played an important role. Amberchrom resins do not have any exchange groups, thus the exchange process takes place to a large extent by complex formation process. The effect of complex formation can be seen by considering a polyvalent ion A^{n+} forming a complex with a ligand (L), as shown in equation 1.

$$A^{n+} + mL^{-} \rightarrow AL_m^{(n-m)+} \quad (1)$$

The complexation reaction in effect removes a portion of the ion (A) from the exchange process , and hence lowers the distribution coefficient. This can be seen where cations such as Ga(III) and Fe(III), which form anionic chloride complexes in HCl solution media, show a decrease in distribution coefficients on a cation exchanger because of the transformation of the cation to an anion and an increase of the H^+ concentration. An increase in the distribution coefficients on an anion exchanger occurs as the negative charge of the complex ion increases.

The effect of complex formation with respect to Ga(III) in HCl as proposed by Brits and Strelow (1990), assumed the interaction of $HGaCl_4$ with the organic skeleton of the resin. This was similar to solvent extraction, where the $HGaCl_4$, at high HCl concentrations preferred the inside of the resin particles for thermodynamic reasons. An extraction-like uptake of $HGaCl_4$ by the hydrophobic resin matrix leads to higher distribution coefficients compared to resins with ion exchange groups (Van der Walt and Strelow, 1983).

Partition. Sugars and other polar non-electrolytes can be separated by partition chromatography between a stationary polar liquid phase held by the ionic functional groups of the resin and a moving non-polar liquid phase used as the eluant. Sugars separate according to their varying degrees of preference for polar over the non-polar solvent.

Ion Exclusion. At low salt concentrations, ionic repulsive forces tend to exclude ions having the same charge as the functional group from the resin. These ions, with an equivalent number of counterions, pass quickly through the column, moving between beads, while non-ionic species, which move freely in and out of the beads, elute more slowly. Ion exclusion has been used primarily to separate electrolytes from non-electrolytes, but it can also separate strong electrolytes from weak electrolytes. For example, ion exclusion has been used to resolve organic acids.

Ligand Exchange. In ligand exchange chromatography, a metal which has been bound to a cation exchanger is used in turn to bind ligands, such as amines or amino acids, which form co-ordination complexes with the metal.

Molecular Sieving. The porous matrix of an ion exchange resin acts as a molecular sieve. It excludes molecules too large to enter the pores and retards the migration of the molecules capable of entering the pores, with the larger molecules eluting first. Sieving effects may improve the resolution of ions which differ in both size and charge. They also limit the size of the ions which can interact with the functional groups of a given exchanger.

4 ION EXCHANGE EQUILIBRIUM

4.1.1 SELECTIVITY COEFFICIENT

The exchange of ions between a solid ion exchange material and a solution is a typically reversible reaction. Suppose a solution containing the cations B^+ is shaken with a solid exchanger AR which contains the cations A^+. Ions B^+ enter the exchanger, while ions A^+ take their place in the solution. After a time, which may range from a few minutes to several days, depending primarily on the solid exchanger, no further change will be observed, and an equilibrium will have been established as seen in equation 1.

$$AR + B^+ \rightarrow BR + A^+ \qquad (1)$$

If the ions are doubly charged the equilibrium will be represented as shown in equation 2.

$$2AR + B^{2+} \rightarrow BR_2 + 2A^+ \qquad (2)$$

To represent the final distribution of concentrations, we write a selectivity coefficient which for the exchanges between ions of equal charge has the form as shown in equation 3.

$$E^B_A = [A^+]\,[BR] \,/\, [B^+]\,[AR] \qquad (3)$$

The symbols [A^+] and [B^+] indicate the molar or molal concentrations in the solution, while [A] and [B] indicate the concentration in the ion exchange resin. It is customary, though not mandatory, to express E^B_A as a number greater than unity. The ion B is considered to be more strongly held than ion A.

In the exchange of ions of equal charge the ratio between the concentrations of A and B does not change with dilution, aside from small effects due to non-ideality. If the ions are of unequal charge, two effects are noted. First, the ion of higher charge is usually more strongly held by the exchanger, and second the distribution shifts with dilution. The more the solution is diluted, the more strongly the ion of higher charge is held by the resin, and vice versa. This effect is sometimes referred to as "electro-selectivity".

4.1.2 THERMODYNAMIC EQUILIBRIUM CONSTANT

A proper representation of the ion exchange equilibrium must recognize that neither the external solution nor that in the ion exchanger is ideal in the thermodynamic sense. The partial molal free energies are not linear functions of the logarithms of concentrations, and this is especially true of the exchange phase, where the ions are much closer together than they are in the external solution. We can take cognizance of non-ideality by introducing activity coefficients and represent the thermodynamic equilibrium coefficient as shown in equation 4.

$$K^B_A = \frac{m_A \bar{m}_B}{m_B \bar{m}_A} \frac{\gamma_A \bar{\gamma}_B}{\gamma_B \bar{\gamma}_A}, \qquad (4)$$

where m and γ represent the molality and activity coefficient respectively.

4.1.3 EQUILIBRIUM DISTRIBUTION COEFFICIENT

The equilibrium of an ion exchange system (analytical species, ion exchanger and electrolyte solution) is usually expressed in terms of the distribution coefficient of the analytical species. For the practical application of this work the distribution coefficient (D) is defined as shown in equation 5,

$$D = \frac{\text{mass of element in resin (g)} \quad x \quad \text{volume of solution (mL)}}{\text{mass of dry resin (g)} \quad x \quad \text{mass of element in solution (g)}} \qquad (5)$$

The distribution coefficient is perhaps one of the most useful tools in ion exchange chromatography since it is used to predict the behaviour of ions and hence the elution order from a column (Smith-Jones and Strelow, 1986).

One of the most fundamental applications of D, given by Mayer (1947), is shown in equation 6

$$V = D \cdot m + V_d \qquad (6)$$

where V is the peak elution volume, that volume of the eluate at which the concentration of the eluted ion reaches the maximum, m is the mass of dry resin in the column and V_d is the dead volume of the column.

Distribution coefficients can be obtained by either **(a)** the batch equilibration method or **(b)** the elution curve method (Smith-Jones and Strelow, 1986). In practice the former is mostly used.

- **(a)** Distribution coefficients were obtained by equilibrating 100 mL HCL (at various concentrations) or a mixture of HCl-HF solution (at specified concentration ratio's) containing various concentration (0.1-1.0 mmole) of the specific element to be determined with 1 g of dry Amberchrom resin by shaking for 24 hours in a mechanical shaker at 20^{0}C. After equilibration the resin was separated from the aqueous phase by filtration and the amounts of the specific element in the aqueous phase were determined by one of flame atomic absorption spectrometry, electrothermal atomisation spectrometry, induced coupled plasma emission spectrometry and / or colorimetric spectrophotometry. Reference solutions containing the same amounts of the specific element for equilibration were used to calculate the amount of the element retained by the resin. The distribution coefficients were calculated using equation (5).

- **(b)** The elution curve method used resin columns as described in section 4.3. The resin columns prior to the sorption step were equilibrated with the relevant acid media. The solution with the specific element was passed through the resin column, and was followed up with the relevant wash solution. This was followed by the elution solution. Fractions (10 ml in volume) were collected from the beginning of the sorption step. The excess acid was evaporated on a water bath, and the amounts of elements in each fraction were determined by methods

described above. The distribution coefficients could be determined using equation (6).

4.1.4 SEPARATION FACTOR

The separation of an ion pair, A and B, is determined by the relationship of the distribution coefficient, D^A and D^B, in a specific experimental environment and the separation factor is then expressed as shown in equation 7:

$$\alpha_A{}^B = D^B / D^A \qquad (7)$$

The greater $\alpha_A{}^B$ differs from 1 for a given ion pair, the easier the two ions will separate on an ion exchange column.

4.2 RESIN PREPARATION

The Amberchrom resins are supplied as dry, free flowing solids. These resins must thus be thoroughly hydrated with deionised water prior to use. This is accomplished by ensuring that the hydration solution is of the same solvent concentration, otherwise a mismatch in solvent concentration may result in poor packing of the column. The following procedure was utilised:

- A quantity of the dry resin sufficient to produce the desired column volume, was weighed out.

- The resin was slowly added to three resin volumes of hydration solvent and mixed gently with overhead stirring while adding the resin.
- The resin was allowed to hydrate overnight (18-24 hours) to ensure that the resin is completely hydrated and free of entrapped air.
- The supernatant was decanted and fresh hydration solvent added. The process was repeated until all the fines in the gel slurry were removed. These may clog filters and increase the pressure across the column.

4.3 COLUMN PREPARATION

Figure 4.1 illustrates a typical resin column used in this work, and the packing of the resin in the column were accomplished as follows:

- Polyethylene tubes (6 mm inner diameter and 41 mm length) fitted with 70 μm polyethylene frits at the bottom were used as ion exchange columns.
- The resin slurry was slowly poured down the inside of the column to prevent air entrapment and ensure homogeneity, until the settled resin had reached a mark indicating a volume of 5 mL. A 70 μm polyethylene frit was placed on top of the resin of the column.
- A plunger made of a teflon rod (6 mm diameter and 41 mm long with a 1.0 mm bore hole drilled through the length, fitted with an O-ring near the bottom and a Luer-fitting at the top) was used to seal the column at the top end.

Figure 4.1 Typical resin column.

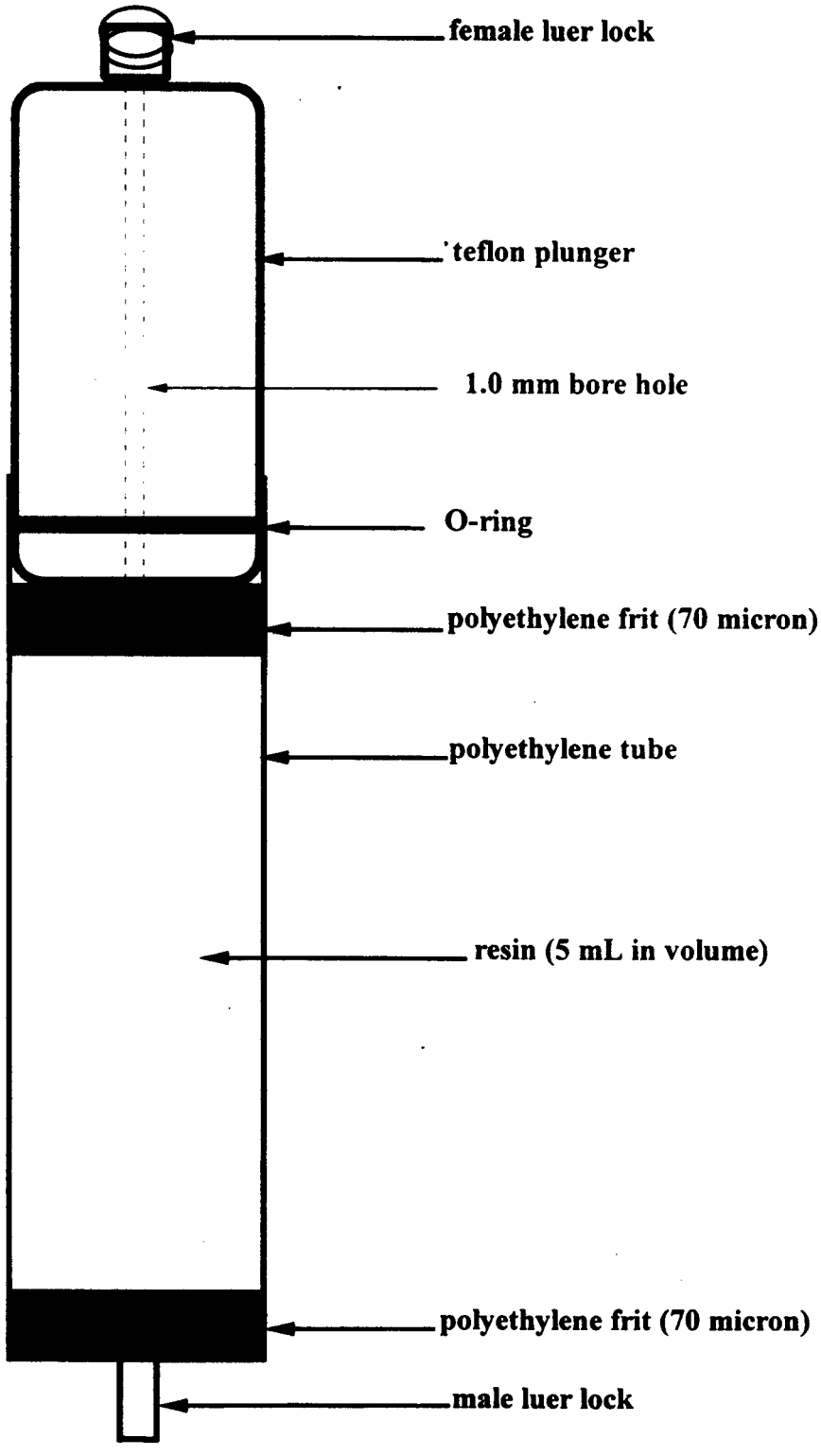

Scale: 3 mm :1 mm

5 ANALYTICAL TECHNIQUES

5.1 INTRODUCTION

The chemical quality control of radiopharmaceuticals is essentially an important step in the production of radioisotopes. Since the radioisotope is injected into humans for in vivo diagnostic investigations, it must fulfil the stringent requirements of a registered medicine of the South African Medical Control Board. The development of analytical methods for the determination of very low levels of trace metals was therefore needed. Extensive literature on trace analysis is documented (Skoog and West, 1982), so there is no need to expand on the theoretical background of analytical principles. The procedures outlined in this section focus chiefly on the optimisation of instrument parameters that would produce reduced interferences and good sensitivity for the specific elements to be analysed.

The determination of the elements at microgram levels in the eluates or the fractions when determining the distribution coefficients, elution curves, quantitative separations of synthetic mixtures, and the final product ^{67}Ga analysis, were done with the following analytical instruments: a Varian AA600 flame atomic absorption spectrophotometer, coupled to a Varian GTA100 graphite tube atomizer, a Perkin Elmer 400 inductively coupled plasma emission spectrometer, and / or a Shimadzu 265 UV-VIS recording spectrophotometer. The methods were developed according to the guidelines of the different instruments instruction and procedure manuals (Varian AA600, 1989; Varian GTA100, 1988; Perkin Elmer 400, 1990 and Shimadzu 265,

1992) and adapted according to the matrix of the radioisotope or metal to be investigated.

The radionuclidic purity of the ^{67}Ga final product was determined using a high, resolution γ-ray spectrometry using a high purity germanium detector and a multichannel analyzer.

5.2 FLAME ATOMIC ABSORPTION SPECTROMETRY

In the flame atomic absorption spectrometry analysis, the determination of Ga, Ge, Zn, Al, Fe, Co, Ni, Cu, Cd and In were developed and the recommended instrument parameters are illustrated in Table 5.1 (calibration curves, Appendix 1). For metals Al, Fe and Ge better sensitivity and considerably less background interferences were found using an acetylene-nitrous oxide flame than with the normally used acetylene-air flame. However these metals are partially ionised using the high temperature acetylene-nitrous oxide flame, but this ionisation can be suppressed by adding an appropriate volume of KCl solution to the eluate containing the metal, having a concentration of 2.0 mg of potassium per millilitre. The addition of a readily ionised element such as potassium created an excess of electrons in the flame and effectively suppressed ionisation of the analyte (Varian AA600, 1989). The working range of the various metals extended from 0.1 μg / mL - 300 μg / mL and were therefore not sensitive enough for the analysis of metals in the ng / mL range, as is often required in the analysis of contaminants present in the ^{67}Ga final product.

Table 5.1 Varian AA600 instrument parameters for flame atomic absorption methods.

Element	Wavelength (nm)	Slit Width (nm)	Lamp Current (mA)	Working Range (μg / ml)	Flame
Ga	294.4	0.5	4	1.0 – 200	acetylene-air (oxidising)
Ge	265.1	1.0	5	2.0 – 300	acetylene-nitrous oxide (reducing)
Zn	213.9	1.0	5	0.1 - 2.0	acetylene-air (oxidising)
Al	309.3	0.5	10	0.3 – 250	acetylene-nitrous oxide (reducing)
Fe	248.3	0.2	5	0.1 - 15.0	acetylene-nitrous oxide (reducing)
Co	240.7	0.2	7	0.1 - 15.0	acetylene-air (oxidising)
Ni	352.4	0.2	4	1.0 – 100	acetylene-air (oxidising)
Cu	324.7	0.5	4	0.1 - 10.0	acetylene-air (oxidising)
Cd	228.8	0.5	4	0.1 - 3.0	acetylene-air (oxidising)
In	303.9	0.5	5	0.4 – 40	acetylene-air (oxidising)

5.3 ELECTROTHERMAL ATOMISATION SPECTROMETRY

Graphite furnace atomic absorption methods for sub-micro level analysis were developed for Ge, Zn, Al and Fe, the only major contaminants found in the ^{67}Ga final product. The recommended instrument parameters are illustrated in Table 5.2 (calibration curves, Appendix 2).

Table 5.2 Varian GTA100 instrument parameters for electrothermal atomisation methods.

Element	Lamp Current (mA)	Slit Width (nm)	Wavelength (nm)
Ge	5	1.0	265.2
Zn	5	1.0	213.9
Al	10	0.5	396.2
Fe	5	0.2	248.3

All the standards and the solutions to be analysed were in a 0.1% HNO_3 matrix, and the pyrolytic coated partitioned graphite tube was used in all analysis. A palladium solution (500 μg / mL - 2000 μg / mL) plus a reducing agent such as ascorbic acid was often used to permit the use of a higher ashing temperature. This palladium modifier also resulted in the enhancement of the analyte signal, and thereby improved the sensitivity. Nitrogen gas was used in the ashing step and argon gas during the atomisation step (Varian GTA100, 1988).

5.4 INDUCED COUPLED PLASMA SPECTROMETRY

The induced coupled plasma emission methods were developed whenever a large amount of a specific metal was needed to be analysed because of the better sensitivity it had over a large working range (1 μg / mL - 9000 μg / mL). This minimised sample dilutions, thereby minimising sample handling errors as compared to flame methods. More importantly, with the induced coupled plasma emission method, one was able to do multi-elemental analysis. The matrix of the standards and samples were in a 0.5 M HNO_3 medium. The recommended instrument parameters for the methods developed for Ga, Ge, Zn, Al, Fe, Co, Ni, Cu, Cd, In and Ti are illustrated in Table 5.3 (calibration curves, Appendix 3). The only drawback of using the induced coupled plasma emission technique was the use of the larger sample volumes that were required as compared to the electrothermal atomisation techniques (Perkin Elmer 400, 1990).

5.5 ULTRA VIOLET - VISIBLE SPECTROPHOTOMETRY

As mentioned before it is vitally important to know the specifications of the ^{67}Ga final product before it is despatched. However problems such as gas depletion and / or vacuum problems could arise when using the above techniques. This then prompted us to develop procedures using the ultra violet - visible spectrophotometric techniques for both Ge and Zn, the major chemical contaminants in the ^{67}Ga final product.

Table 5.3 Perkin Elmer 400 instrument parameters for induced coupled plasma emission methods.

Element	Wavelength (nm)	Primary Line (μg / mL)
Ga	417.206	0.065 - 3250
Ge	265.118	0.13 - 6500
Zn	213.856	0.009 - 450
Al	396.152	0.0015 - 750
Fe	259.941	0.0015 - 750
Co	228.616	0.050 - 2500
Ni	231.604	0.060 - 3000
Cu	324.754	0.020 - 1000
Cd	228.802	0.015 - 750
In	325.609	0.18 - 9000
Ti	334.941	0.006 - 300

5.5.1 Ge SPECTROPHOTOMETRIC ANALYSIS

Germanium is determined spectrophotometrically via the phenylfluorone-germanium complex (red), which is stabilised in solution with a cationic surfactant, cetyltrimethylammonium bromide. The presence of this surface active agent increases the sensitivity and the rate of reaction of the germanium and xanthone of the reagent as well as dispersing the suspended water insoluble germanium-phenylfluorone complex. Analysis can be performed directly on the ^{67}Ga-citrate final product as there are no interferences that may arise from the citrate at the pH of the analysis, at *ca* 1.6 M HCl (Fries and Getrost, 1977).

Reagents

- **Ge standard (1000 μg / mL):** Dissolve 1.00 g metallic Ge in a teflon beaker with 20 mL HF (22 M). Add 5 mL H_2O_2 (30%) in 1 mL increments while heating at 100^{0}C. The solution is then transferred into a 1 litre polyethylene volumetric flask and made up to the mark with deionised water. Standards of 1, 3 and 5 μg / mL were then prepared using 2.6% sodium citrate as a dilution medium.
- **0.001 M phenylfluorone (2,6,7-tri-hydroxy-9-phenyl-3H-xanthen-3-one):** Dissolve 0.08 g of phenylfluorone in 100 mL absolute ethanol, add 4 mL HCl (12 M) and dilute with deionised water to the 250 mL mark of a volumetric flask.
- **0.9% cetyltrimethylammonium bromide:** Dissolve 2.3 g cetyltrimethyl-ammonium bromide in 150 mL deionised water and dilute to the 250 mL mark of a volumetric flask.
- **10% ascorbic acid:** Dissolve 10 g ascorbic acid in 100 mL deionised water.

Procedure

A 0.25 mL sample of the blank citrate, standards, and final product were added into separate vials. Deionised water (1.75 mL), 10% ascorbic acid (0.4 mL), concentrated HCl (0.6 ml) and 0.9% cetyltrimethylammonium bromide (0.4mL) were added sequentially to each vial with mixing. Thereafter 0.4 mL phenylfluorone solution was added to each vial to initiate colour development. The solutions were then analysed on a Shimadzu 265 UV-VIS spectophotometer at a absorbance wavelength of 507 nm after 10 minutes. The calibration curve as illustrated in Appendix 4, obeyed the Beer's law (Fries and Getrost, 1977).

5.5.2 Zn SPECTROPHOTOMETRIC ANALYSIS

Zinc is determined spectrophotometrically via the stable PAR - zinc complex (yellow) which is formed in a buffered solution at pH 9. Metals such as Fe, Co, Cd, Ni, Sn, and Ti may interfere in a citrate medium. This often resulted in an increase in the absorbance signal. However it was determined that the citrate solution could be stabilised, when 0.1% hydrazine hydrate solution was used, and this nullified any interferences.

Reagents

- **Zn standard (1000 µg / mL):** Dissolve 1.00 g zinc in a teflon beaker with 20 ml HCl (12 M). The solution was then transferred into a 1 litre volumetric flask and made up to the mark with deionsed water. Standards of 1, 5, 7 and 10 µg / mL were then prepared using 2.6% sodium citrate as a dilution medium.

- **0.001 M 4-(2-pyridylazo) resorcinol monosodium salt (PAR):** Dissolve 0.0255 g 4-(2-pyridylazo) resorcinol monosodium salt in 100 mL deionised water.
- **Potassium hydrogen phthalate buffer (pH 9):** Dissolve 5.0 g potassium hydrogen phthalate in 50 mL deionised water. Adjusted the pH of the solution to 9 with 1.0 M NaOH. Thereafter transferred the solution into a 100mL volumetric flask and made up to the mark with deionised water.
- **1% hydrazine hydrate solution:** 1.25 mL of 80% hydrazine hydrate is diluted with deionised water to the 100 ml mark of a volumetric flask.

Procedure

A 0.2 mL sample of the blank citrate, standards, and final product were added into separate vials. 1% hydrazine hydrate (0.1 mL) and potassium hydrogen phthalate (2.0 mL) were added to each vial sequentially and mixed. Thereafter the colour reagent (0.2 ml) was added to each vial and mixed to initiate colour development. The solutions were then analysed on a Shimadzu 265 UV-VIS spectophotometer at an absorbance wavelength of 495 nm after 10 minutes. The calibration curve, as illustrated in Appendix 4 obeyed the Beer's law (Fries and Getrost, 1977).

6 TARGETRY

6.1 NUCLEAR DATA

At the NAC, where a 66 MeV proton beam is available for neutron therapy and the routine production of radioisotopes, either ^{nat}Zn or ^{nat}Ge can be considered as target material for the large scale production of ^{67}Ga suitable for medical use, since the thick target yields expected for these two materials are very similar. However, a substantially higher yield compared to that of either target can be obtained with a tandem target employing both the ^{nat}Zn and ^{nat}Ge as target materials.

Thick target production rate curves for all the radiogallium nuclides of interest were derived from measured excitation functions for the proton bombardment of ^{nat}Zn and ^{nat}Ge up to 100 MeV (Nortier et al., 1991). Since the half-lives of the radiogallium contaminants are significantly shorter than that of ^{67}Ga, a product of any desired radioisotopic purity can always be obtained by allowing an appropriate decay time before calibration. Current medical standards for ^{67}Ga require a radionuclidic purity of > 99% at the time of calibration. Hence, the above mentioned curves were used to construct thick target yield curves for 99% radioisotopically pure ^{67}Ga for both target materials as seen in Figure 6.1. In the case of ^{nat}Zn, ^{66}Ga was found to be predominant in determining the decay time required to reach the 99% purity level at each specific incident proton energy, while both ^{66}Ga and ^{72}Ga had to be considered in the case of the ^{nat}Ge. It is clear from Figure 6.1 that at lower incident energies the slope of

Figure 6.1 **Thick target yield curves for ^{67}Ga of 99% radioisotopic purity expected for ^{nat}Zn + p and ^{nat}Ge + p *(top)*, and the corresponding calculated decay times after EOB required to achieve this purity level *(bottom)* (Nortier et al., 1991).**

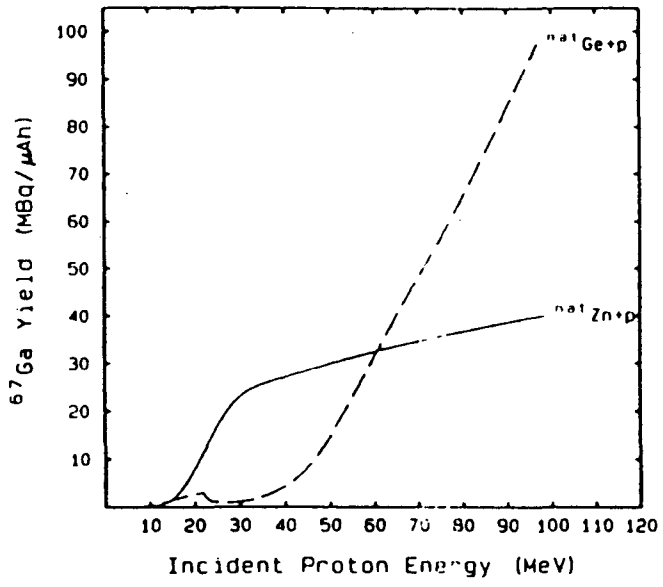

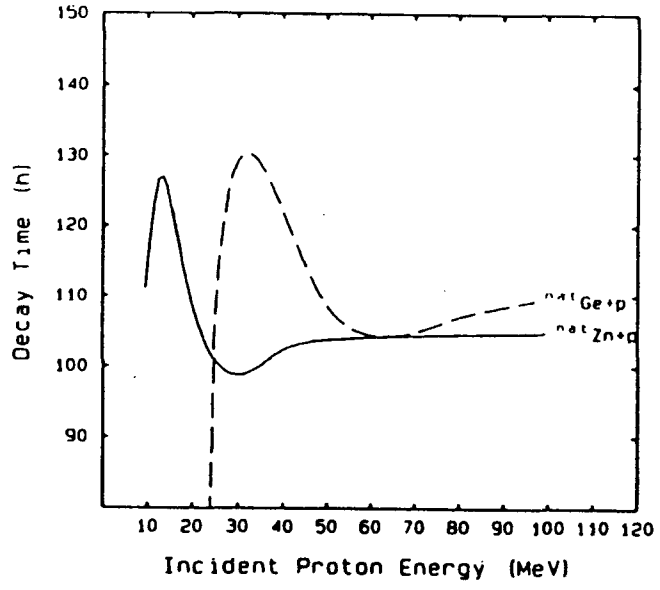

the ^{67}Ga (99%) yield curve for ^{nat}Zn is steeper than for ^{nat}Ge, while the opposite is true at higher energies. This implies that, with a primary beam of 66 MeV protons, the best ^{67}Ga (99%) yield will be obtained by bombardment of a tandem target, with the ^{nat}Zn and ^{nat}Ge utilizing the lower and higher energy regions, respectively. It is also obvious that an optimum proton energy value for the Ge / Zn interface of such a tandem target can be determined (Nortier et al., 1991).

As is illustrated in Figure 6.2, this optimum was found to be at about 35 MeV. Figure 6.2 also shows that the ^{67}Ga (99%) yield of the tandem target is not very sensitive to the exact position of the interface. In the final design, the Ge and Zn target materials utilize the 60.7 - 38.7 MeV and 34.3 - 18.1 MeV proton energy windows respectively. The important radioactive isotopes produced during proton activation of the ^{nat}Ge / ^{nat}Zn target along with γ ray energy's are shown in Table 6.1 (Nortier et al., 1991).

6.2 BOMBARDMENT CONFIGURATION

For bombardment at high intensities, the target was mounted in a standard Al holder, which was then loaded in a target station and secured outside the beamline vacuum as seen in Figure 6.3. Thin layers (1 mm thick) of cooling water, flowing at a high velocity across the target faces, are employed to ensure proper cooling of the targets. Material thickness upstream of the Ge target (which determine the incident energy of 60.7 MeV) as well as those between the two targets are kept to a minimum. The choice of 18.1 MeV for the exit energy is based on radiation dose considerations.

Figure 6.2 **Dependence of the ^{67}Ga (99%) yield of a tandem target as illustrated the position of the Ge / Zn interface (in MeV) (Nortier et al., 1991).**

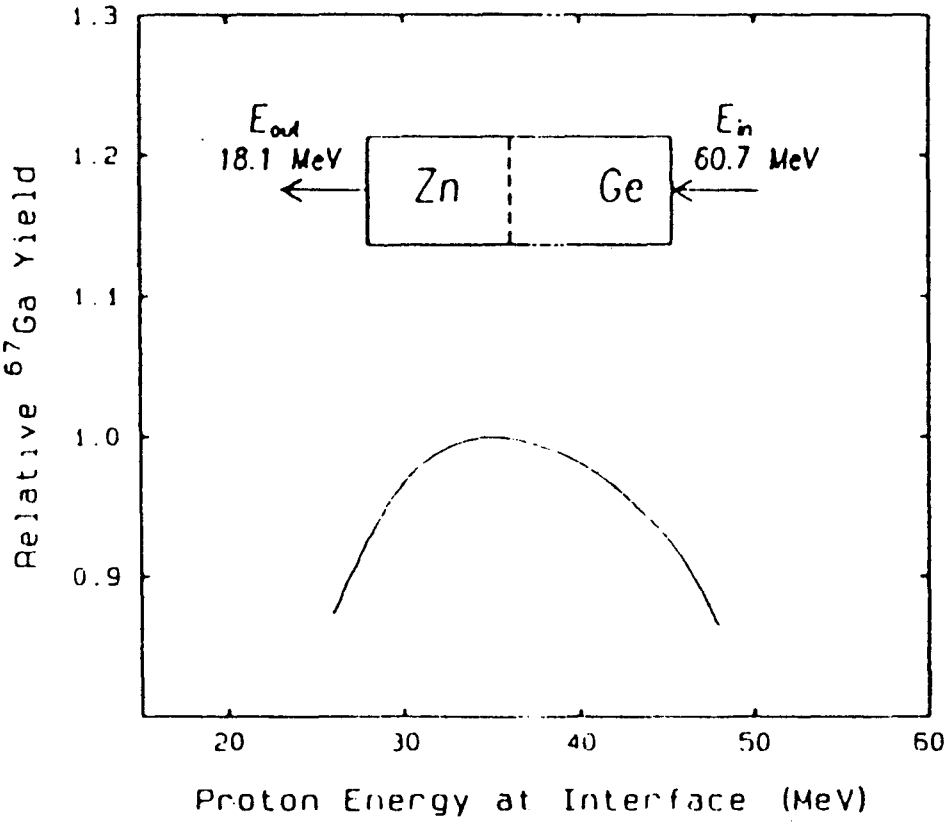

Table 6.1 Important radioisotopes and their major γ rays (Nortier et al., 1991).

Radioisotope	Half-life (Days)	Energy (keV)	Abundance (%)
^{66}Ga	0.40	1039	37.9
^{67}Ga	3.26	184	20.4
^{67}Ga	3.26	300	16.6
^{72}Ga	0.59	630	24.4
^{72}Ga	0.59	834	95.6
^{67}Cu	2.58	184	48.6
^{71}As	2.70	174	83.1
^{72}As	1.08	834	79.5
^{74}As	17.78	595	60.2
^{69}Ge	1.63	1107	36.0
^{65}Zn	244.10	1115	50.8

Figure 6.3 Schematic diagram of the ^{nat}Ge / ^{nat}Zn tandem target configuration in the bombardment position (Nortier et al., 1991).

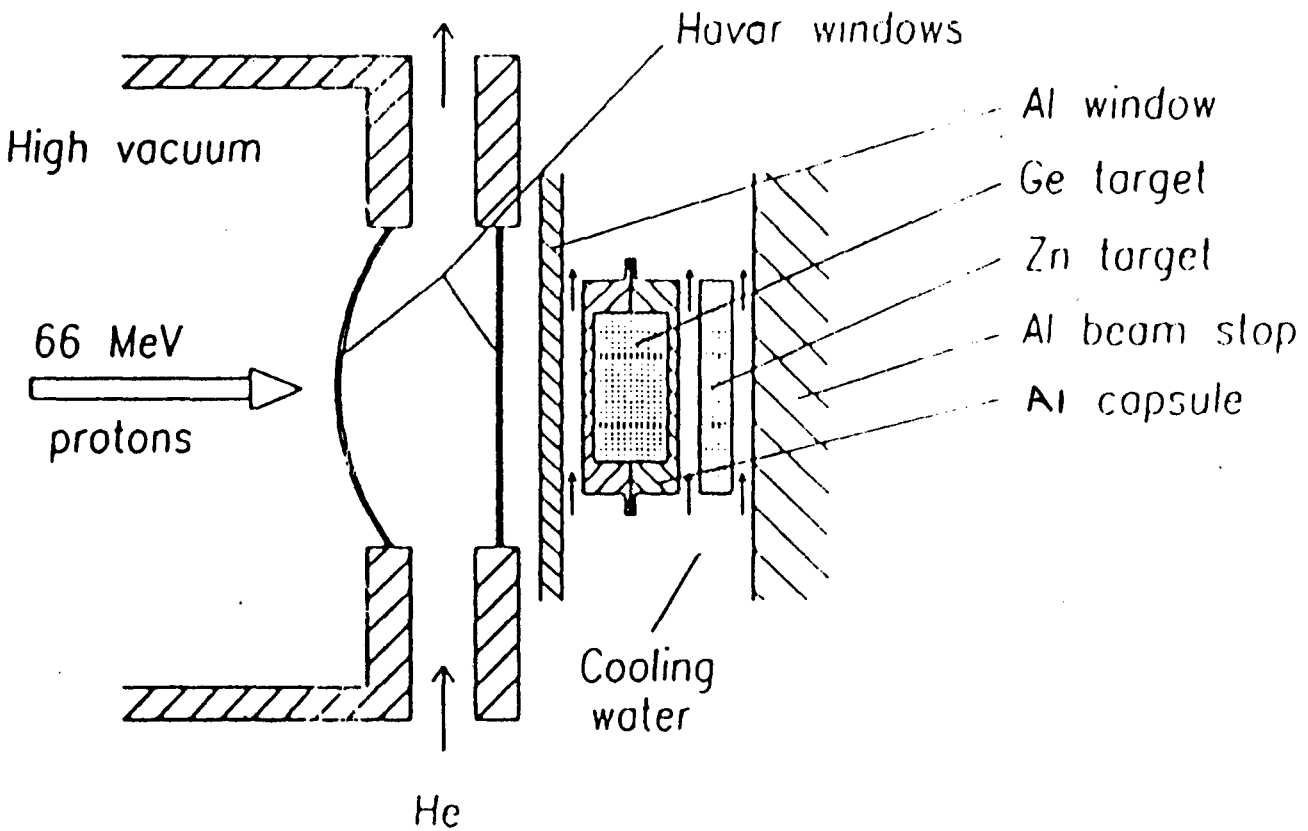

6.3 TARGET PREPARATION

The germanium metal and zinc metal of high purity (99.9+ %) were supplied by Goodfellow Metals UK and Koch Chemicals UK respectively.

The Ge target (8.0 g, diameter 20 mm) owing to its low thermal conductivity and its brittleness, is encapsulated in an aluminium canister (inner diameter 21 mm, inner thickness 6 mm) for bombardment. A casting method was developed for the manufacturing of Ge targets. Powder, obtained by grinding lumps of polycrystalline Ge metal, was poured into a special graphite mould, machined from high quality pyrocarbon as shown in Figure 6.4, and heated in a muffle furnace for 2.0 hour at 1050^{0}C to allow the Ge to melt. Disposable graphite rings ensured the trouble-free removal of the Ge metal disk castings afterwards. The Ge metal disk was then encapsulated in an aluminium canister which was then sealed by electron beam welding.

The Zn target (4.4 g, diameter 20 mm) was prepared by unaxial pressing of ^{nat}Zn metal powder at a pressure of 523 MPa under vacuum by means of a suitable punch and die set machined from a high carbon , high chromium tool steel as shown in Figure 6.4. The metal disc of 95 % theoretical maximum density were removed from the die and was annealed / sintered in an oven for 0.5 hour at 400^{0}C, an operation which was found to be necessary in order to prevent the cracking of the target under bombardment (Nortier et al., 1991).

Figure 6.4 **Graphite mould *(top)* and the punch and die set *(bottom)* for the preparation of Ge / Zn targets, respectively, (Nortier et al., 1991).**

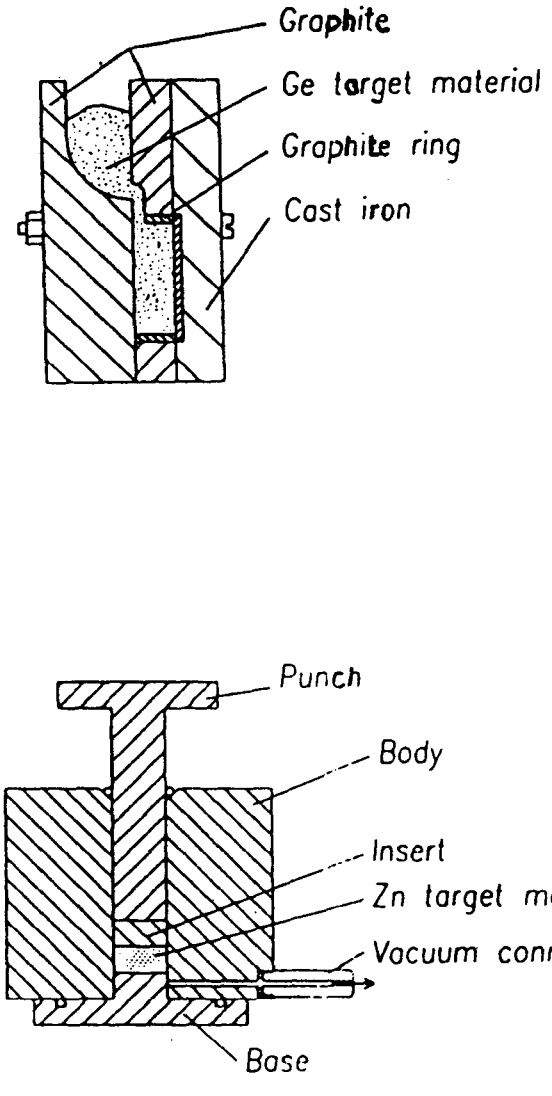

7 CHEMICAL PROCESSING OF ^{nat}Zn TARGETS

7.1 DISTRIBUTION COEFFICIENTS FOR Ga(III) IN HCl

Distribution coefficients for Ga(III) (1 mmole / g resin) on Amberchrom CG-71cd, Amberchrom CG-161cd, Amberchrom CG-162sd, Amberlite XAD-7 and Bio-RAD AG 50W-X4 resins in various HCl concentrations were determined and compared to published distribution coefficients for Ga(III) (0.08 mmole / g resin) on Amberlite XAD-7 (Brits and Strelow, 1990) and Bio-Rad AG 50W-X4 (Van der Walt and Strelow, 1983) resins as shown in Table 7.1. Clearly the distribution coefficients for Ga(III) on the Amberchrom range of resins were higher than that of the polymeric XAD-7 and the cation exchange AG 50W-X4 resin, even though a higher concentration of Ga(III) was used in the determination of the Amberchrom range of resins. The Amberchrom resins were then selected for further investigation. As shown in Table 7.1, both the Amberchrom CG-161cd and Amberchrom CG-162sd showed higher distribution coefficients for Ga(III) in 7 M HCl and 9 M HCl, but the elution of Ga(III) from the resin with 0.5 M HCl showed serious tailing as shown in Figure 7.1 and Figure 7.2 and this was due to the increased crosslinkage (16%) of the resin. Elution with dilute nitric acid or acetic acid did not lead to any reduction of tailing. The Amberchrom CG-71cd, with a 7% crosslinkage, was then chosen for further investigation. The distribution coefficients of Ga(III) (0.01 mmole) as a function of HCl concentration as shown in Figure 7.3 were determined, to find the optimal HCl concentration that could be used in the separation of Ga(III) from other metals.

Table 7.1 Distribution coefficients for Ga(III) (1.0 and 0.08 mmole / g resin) on various resins in 3 M HCl, 5 M HCl and 9 M HCl.

Resin	Ga(III) (mmole/ g resin)	3 M HCl	7 M HCl	9 M HCl
Amberchrom CG-71cd	1.0	20	1400	1300
Amberchrom CG-161cd	1.0	15	1560	1701
Amberchrom CG-162sd	1.0	14	1610	1819
Amberlite XAD-7	1.0	4	310	517
Amberlite XAD-7 (a)	0.08	9	625	1000
Bio-Rad AG 50W-X4	1.0	16	25	55
Bio-Rad AG 50W-X4 (b)	0.08	nd	96	130

(a) Brits and Strelow, 1991

(b) Van der Walt and Strelow, 1983

nd not determined

Figure 7.1 Elution curve for Ga(III) on the Amberchrom CG-161cd resin in 7 M HCl (column length 41 mm, i.d. 6 mm).

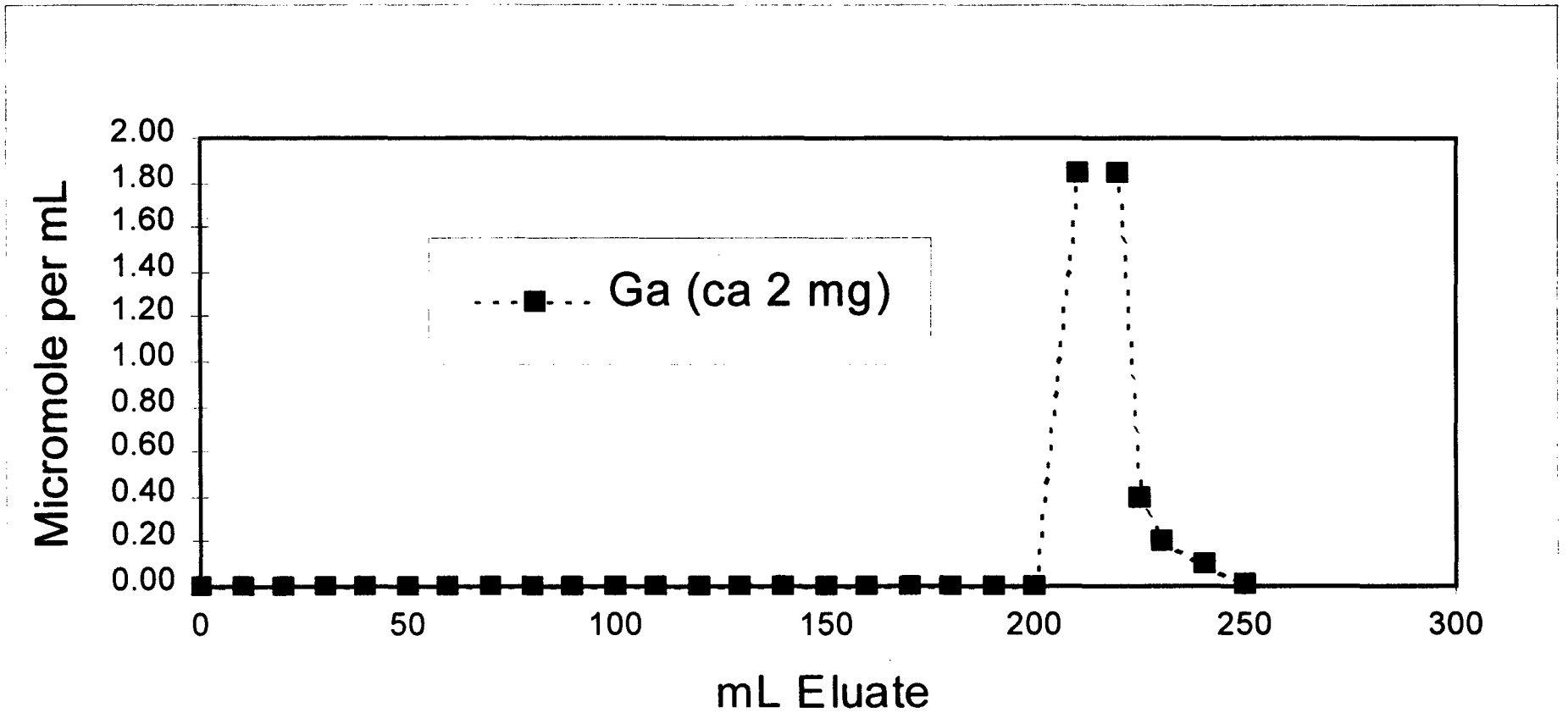

Figure 7.2 Elution curve for Ga(III) on the Amberchrom CG-162sd resin in 7 M HCl (column length 41 mm, i.d. 6 mm).

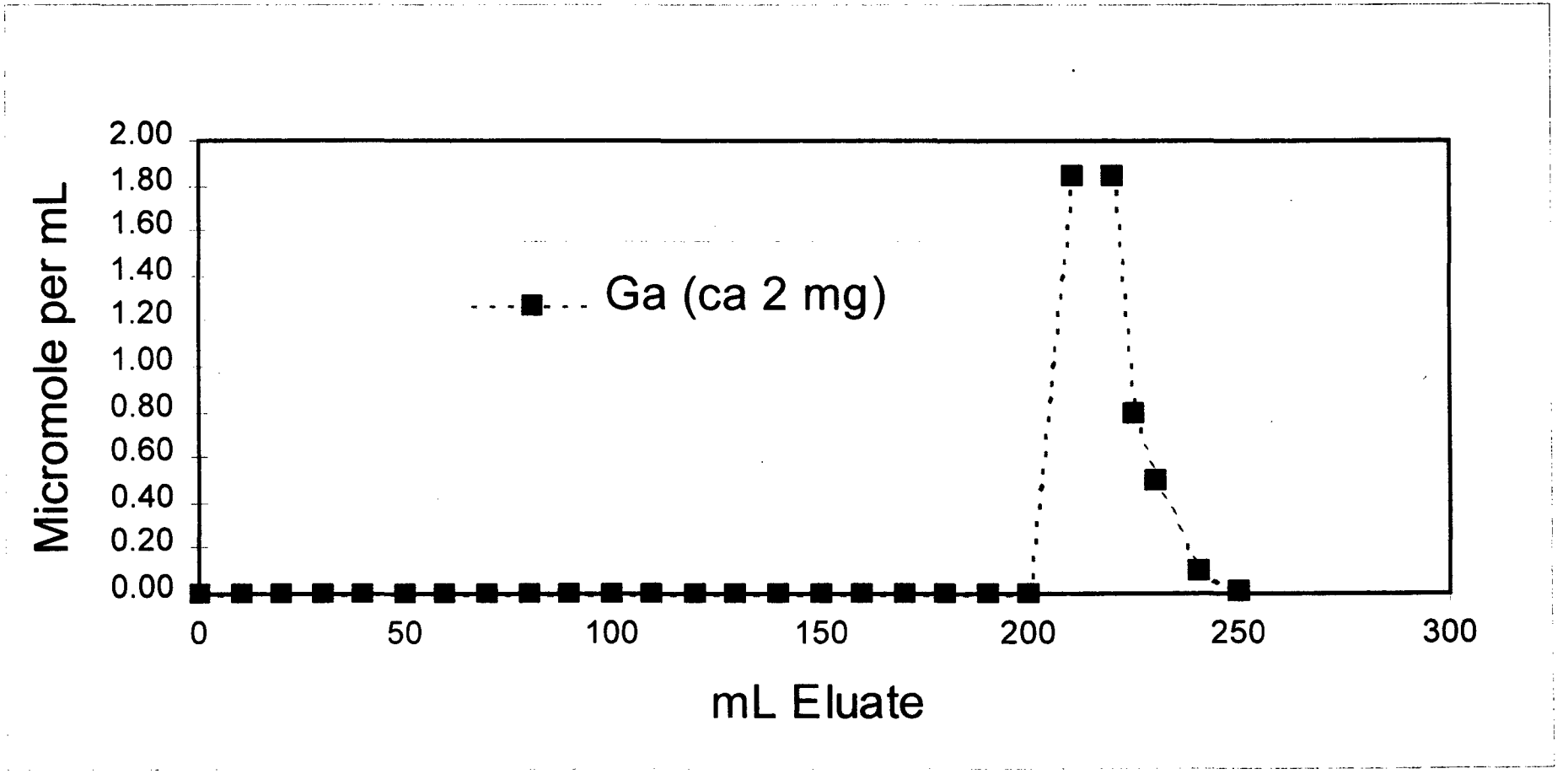

Figure 7.3 **Distribution coefficients for Ga(III) (0.01 mmole / g resin) on the Amberchrom CG-71cd resin as a function of HCl concentration.**

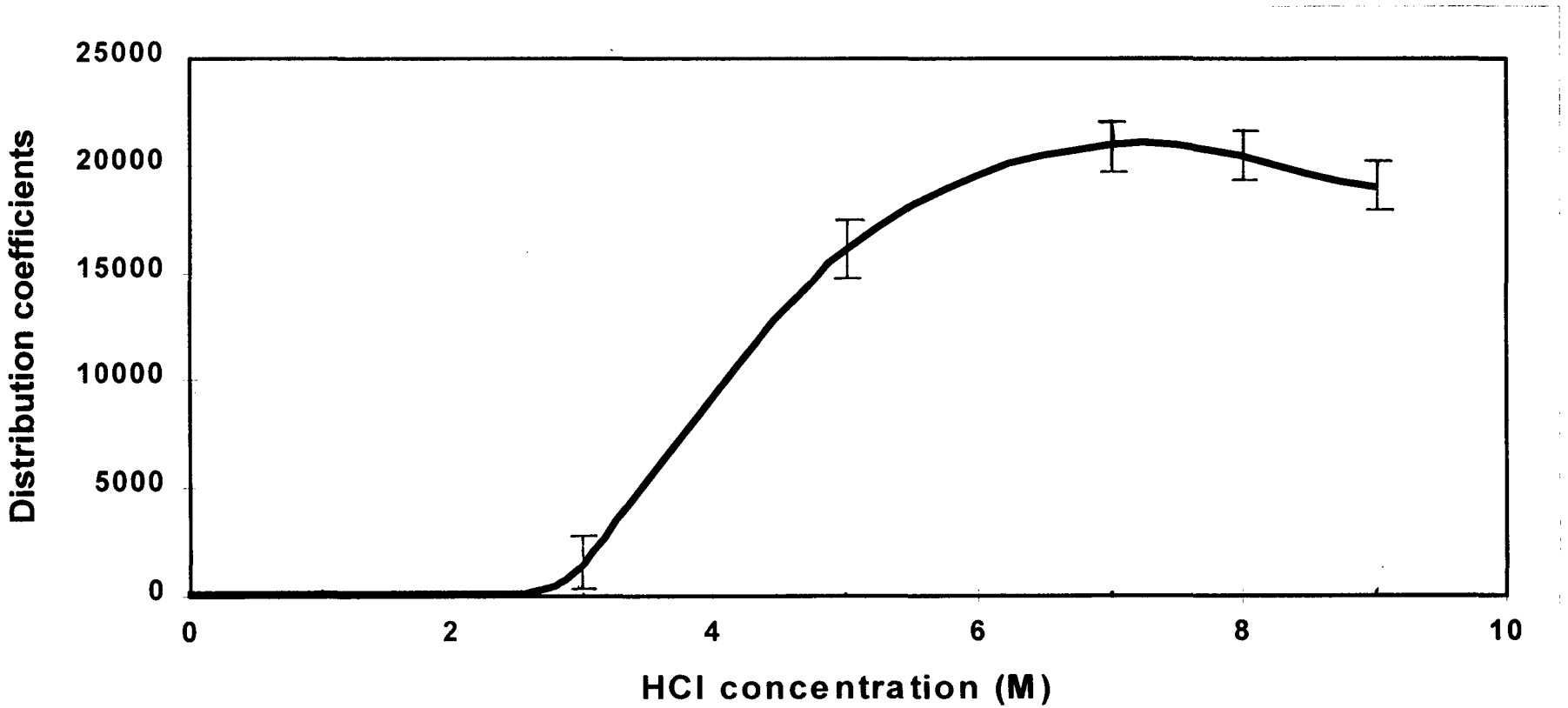

7.3 ELUTION CURVES

In elution curve determinations, resin columns as described in section 4.3 were used.

(a) ***Elution curve for 4.0 g Zn(II), 2.0 g Cu(II) and 2.0 mg Ga(III) on 1.0 g Amberchrom CG-71cd resin.*** The resin column was equilibrated by passing 50 mL of 7 M HCl through the resin column. A solution containing 4.0 g Zn(II), 2.0 g Cu(II) and 2.0 mg of Ga(III) in a volume of 50 mL 7 M HCl was prepared and passed through the resin column. The elements were washed onto the resin with small portions of 7 M HCl and the Zn(II) and Cu(II) was eluted with 150 mL of 7 M HCl altogether. The Ga(III) were eluted with 50 mL 0.5 M HNO_3. The flow rate was 3.0 mL per minute. Fractions (5 mL in volume) were collected from the sorption step and the excess acid was evaporated on a water bath. The amounts of elements in each fraction were determined by flame atomic absorption spectrometry, electrothermal atomisation spectrometry, induced coupled plasma emission spectrometry and / or colorimetric spectrophotometry as outlined in section 5. The amount of Zn(II) and Cu(II) was found to be less than 10 ppm in the Ga(III) eluate. The elution curve as shown in Figure 7.4, indicates the quantitative separation of Zn(II) and Cu(II) from Ga(III).

(b) ***Elution curve for 2.0 g Fe(II) and 2.0 mg of Ga(III) on 1.0 g of Amberchrom CG-71cd resin.*** The resin column was equilibrated by passing 50 mL of 7 M HCl through the resin column. A solution containing 2.0 g Fe(III) and 2.0 mg of Ga(III) in

Figure 7.4 Elution curve for Ga(III)-Zn(II) and Ga(III)-Cu(II) on the Amberchrom CG-71cd resin in 7M HCL (col. 41 mm/i.d. 6 mm).

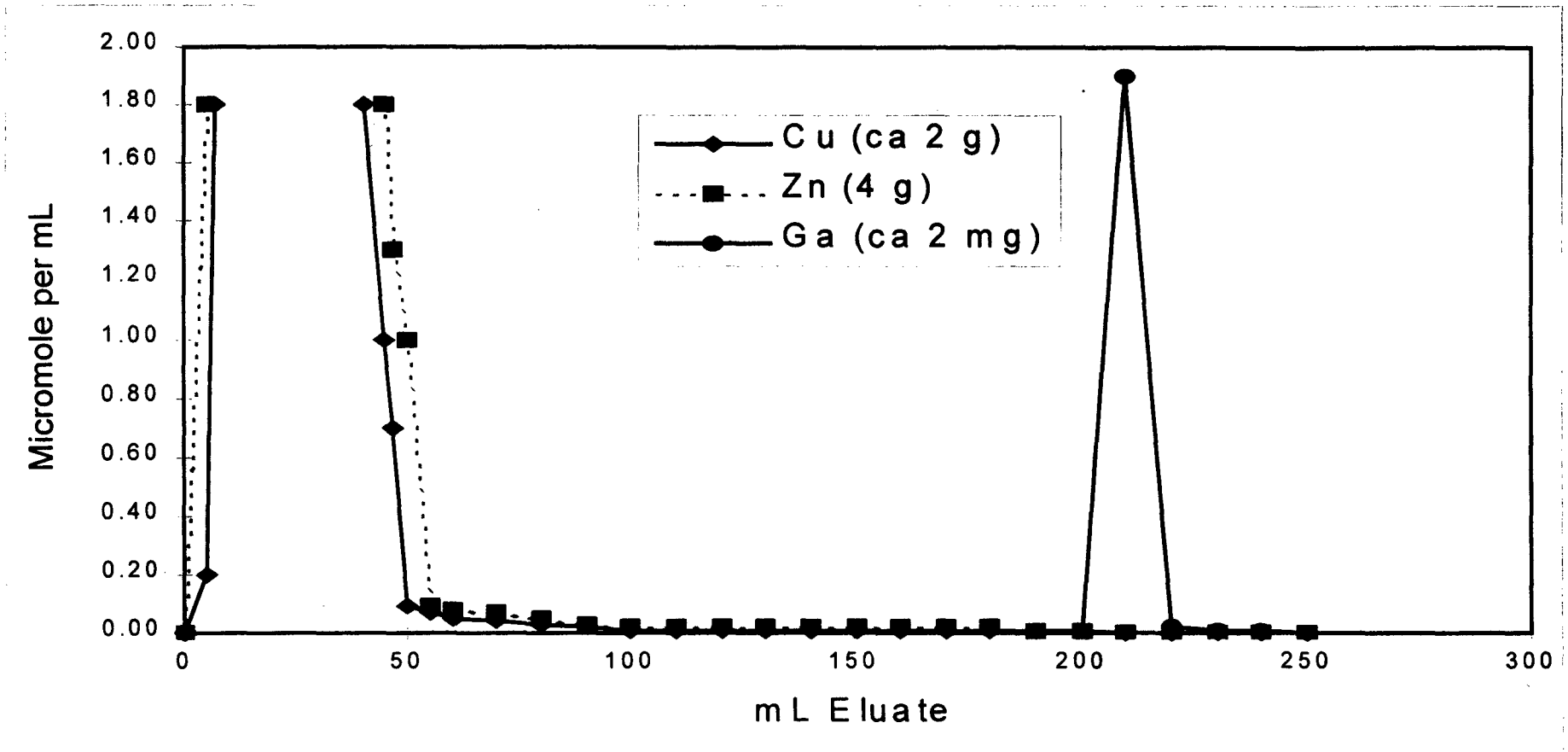

50 mL of 7 M HCl which included 0.3 % $TiCl_3$ (1.0 g) to reduce any Fe(III) to the divalent state. The solution was passed through the resin column which was equilibrated with 7 M HCl. The elements were washed onto the resin with small portions of 7 M HCl and the Fe(II) together with Ti(III) was eluted with a total volume of 150 mL 7 M HCl. Finally the Ga(III) was eluted with 50 mL 0.5 M HNO_3. The flow rate, collection of fractions and the analysis of amounts of elements in each fraction were determined as described above. The elution curve is shown in Figure 7.5. It was found that less than 5 ppm Fe(II) and less than 1 ppm Ti(III) was found in the Ga(III) eluate. It is evident that the quantitative separation of Zn(II), Fe(II) and Ti(III) from Ga(III) is obtainable at microgram amounts which is useful for the separation of carrier-free radioisotopes of Ga from irradiated ^{nat}Zn targets.

7.4 CHEMICAL SEPARATION OF THE ^{67}Ga FROM THE ^{nat}Zn TARGET MATERIAL

The bombarded zinc target was dissolved in concentrated HCl containing 500 μg $TiCl_3$ to yield a solution containing 1.4 M $ZnCl_2$ and 7 M HCl. The column containing 1.0 g Amberchrom CG-71cd resin in 7 M HCl was packed as described in section 4.3. A peristaltic pump was used to pump the solution through the column at a flow rate of 3.0 mL / min. The resin containing the absorbed ^{67}Ga and other Ga isotopes were washed with 200 ml 7 M HCl to remove residual Zn and traces of Ti. Finally the ^{67}Ga was eluted with 30 ml 0.5 M HNO_3, and the solution was evaporated to incipient dryness. Concentrated HNO_3 (2.0 mL) was added to convert $GaCl_3$ to the less volatile nitrate

Figure 7.5 Elution curve for Ga(III)-Fe(II) and Ga(III)-Ti(III) on the Amberchrom CG-71cd in 7M HCl (col. 41 mm / i.d. 6 mm).

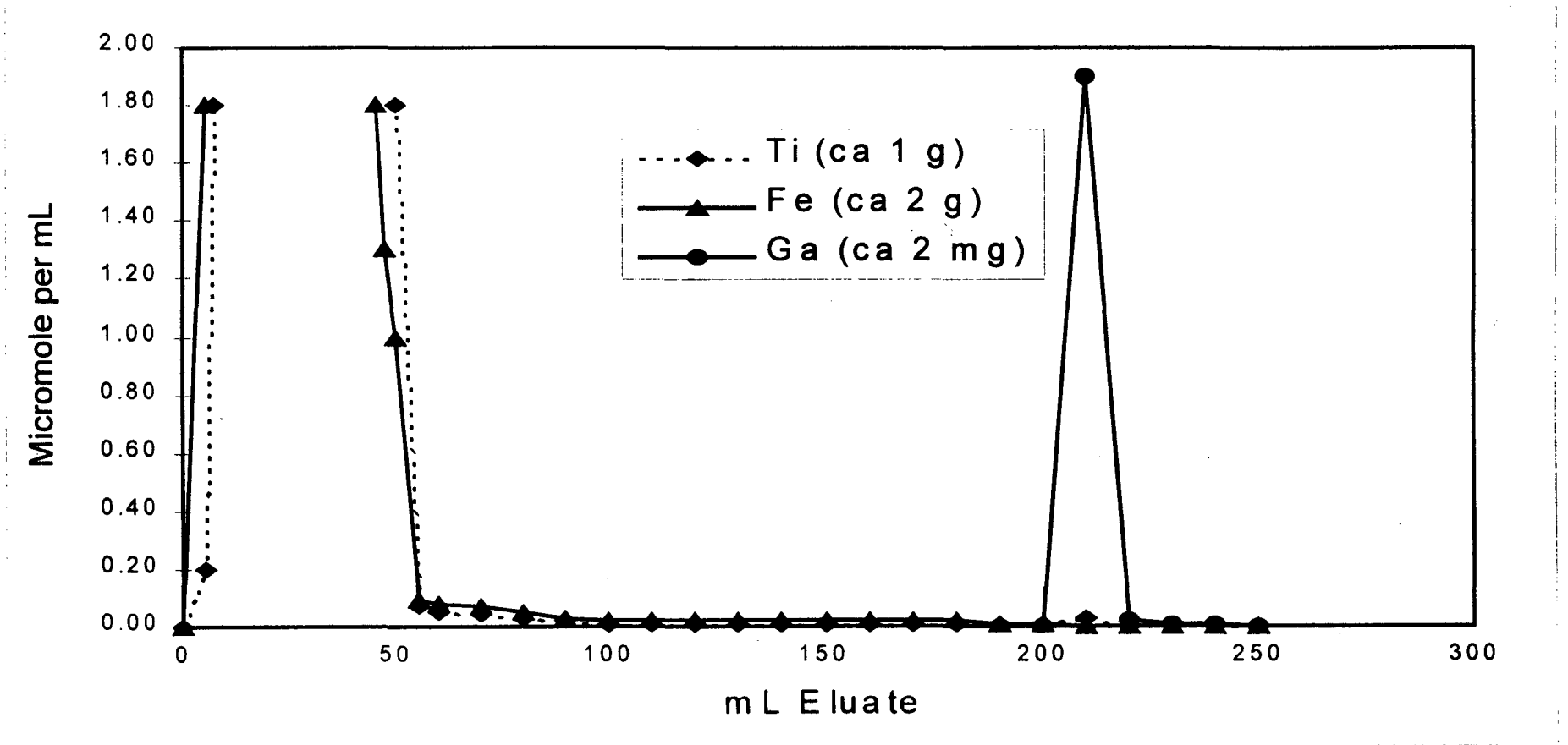

and heated to boiling point to destroy traces of organic material present. The excess acid was also evaporated to incipient dryness. Deionised water (2.0 mL) was added to the evaporator and also evaporated to incipient dryness to remove traces of the acid. The ^{67}Ga salts remaining were dissolved in 10 mL 2.6% sodium citrate solution which was transferred to a sealed sterile sample vial for further processing in the dispensary laboratory. A schematic diagram of the ^{nat}Zn target chemical process is illustrated in Figure 7.6.

Figure 7.6 Schematic diagram of the ^{nat}Zn target chemical process.

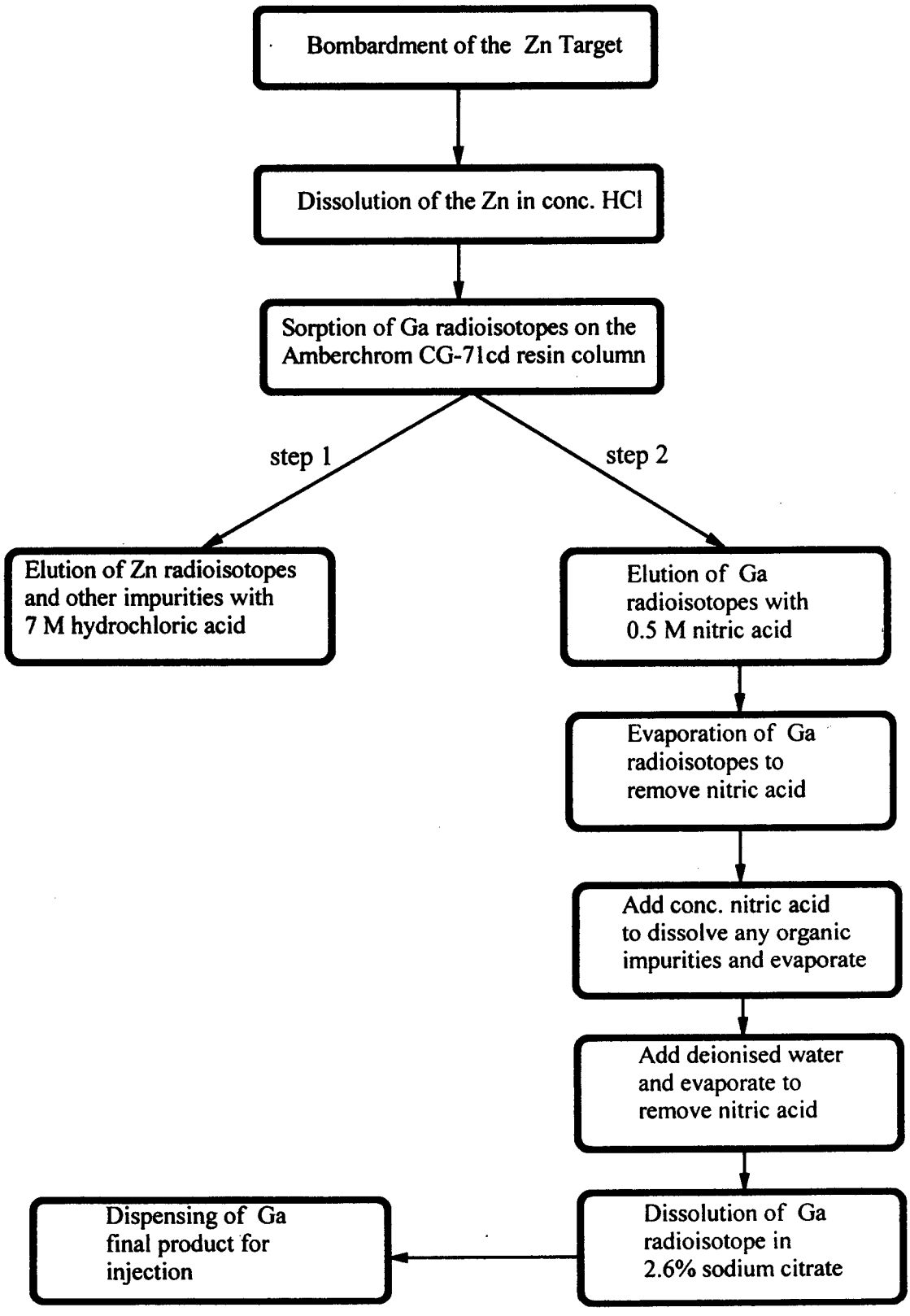

8 CHEMICAL PROCESSING OF ^{nat}Ge TARGET

8.1 TARGET DISSOLUTION DEVELOPMENT

Unlike the ^{nat}Zn target, the ^{nat}Ge is encapsulated in an aluminium canister, and this canister is normally mechanically removed by cutting it open to expose the actual ^{nat}Ge disc. However in this case, it was not a viable option because of two important factors:

- Ge becomes molten under bombardment, bonding physically to the front of the aluminium canister where the beam strikes the target.
- Ge is a hard metal, yet very brittle, with a tendency to break under physical duress (e.g. temperature cycling), together with the formation of metal dust presenting a substantial threat to contamination.

It was decided to process the encapsulated ^{nat}Ge as a whole target and the following approach was utilised:

8.1.1 DISSOLUTION OF THE ALUMINIUM CANISTER

Dissolving the aluminium canister was accomplished with a mixture of 5 M HCl (150 mL) and 40% HF (20 mL), using 30% H_2O_2 (10 mL) as an oxidant. Hydrofluoric acid is necessary to ensure that the dissolved alloy is stabilised in solution as a soluble fluoride or chloro-fluoro complexes. Elimination of this solvent will cause aluminium to be oxidised to the insoluble aluminium oxide. Hydrogen peroxide is added to

ensure a vigorous oxidative environment, in contrast to the mildly reducing nature of the hydrochloric acid. The reaction is extremely rapid and exothermic. The solution is removed and discarded and the exposed ^{nat}Ge target is washed with deionised water to remove traces of aluminium.

8.1.2 DISSOLUTION OF THE ^{nat}Ge TARGET

Germanium metal is not readily soluble in common acids and alkalis, even at elevated temperatures. Various dissolution methods were investigated:

- The dissolution with aqua regia had a drawback of a slow reaction and the formation of GeO_2 in solution.
- The dissolution with 40% HF - 70% HNO_3 (3:1 by volume) mixture with heat exhibited a lag phase before the reaction proceeded.
- Substituting 70% HNO_3 with fuming HNO_3 resulted in a spontaneous reaction, but fuming HNO_3 is extremely corrosive for the hot cell facilities and the generation of large volume of noxious red gas NO_2 was not suitable.
- In comparison 40% HF - 30% H_2O_2 mixture (1:1 by volume) which required stepped heating up to 100^{0}C, proceeded smoothly and efficiently. Removal of excess peroxide is accomplished by heating to decomposition or simply allowing it to react with hydrochloric acid to produce chlorine. The mechanism of dissolution is proposed to be via free-radicals, since many reactions involving H_2O_2 and O_2 in solution involve free radicals. The only drawback with this

method is the lengthy time consumed during dissolution. However more importantly complete dissolution is obtained.

8.2 DISTRIBUTION COEFFICIENTS FOR Ga(III) IN HCl - HF MEDIUM

Since the dissolution medium had a high concentration of HF and HCl, distribution coefficients for Ga(III) in this particular medium had to be investigated. According to the literature survey as discussed in section 2.3, no distribution coefficients for Ga(III) and other elements on a polymeric resin in HCl - HF medium were available. Distribution coefficients for Ga(III) (1 mmole / g resin) on the Amberchrom CG-71cd resin as a function of varying HCl - HF concentration were then determined, to obtain the optimal conditions required for the adsorption of Ga on the Amberchom CG-71cd resin column. It is illustrated in Table 8.1 that very high distribution coefficients are obtained in 5 M HF containing 5 M HCl, 6 M HCl and 7 M HCl.

The 5 M HCl - 5 M HF mixture was then selected for this work because of the fairly high distribution coefficients it showed with Ga(III), and the less corrosive environment it exhibits during chemical separation as compared to the 6 M HCl - 5 M HF and 7 M HCl - 5 M HF mixtures. The distribution coefficients for Ga(III) (1 mmole / g resin) on the Amberchrom CG-71cd in 5 M HCl - 5 M HF did show a decrease as expected, when the concentration of the competing ion, Ge(IV), increased from 0 to 1.5 M as illustrated in Table 8.2. This behaviour was very similar to the effect Zn, as a competing ion, had on Ga(III) (section 7.1).

Table 8.1 **Distribution coefficients for Ga(III) (1 mmole / g resin) as a function of HCl - HF concentration on Amberchrom CG-71cd resin.**

HCl - HF concentration	Distribution coefficients for Ga(III)
3 M HCl-3 M HF	39
4 M HCl-4 M HF	610
5 M HCl-5 M HF	6900
6 M HCl-5 M HF	7200
7 M HCl-5 M HF	7400

Table 8.2 **Distribution coefficients for Ga(III) (1 mmole / g resin) on Amberchrom CG-71cd resin in 5 M HCl - 5 M HF at varying Ge(IV) (0.5 - 1.5 M) concentrations.**

Ge(IV) concentration (M)	Distribution coefficients for Ga(III)
0	6900
0.5	4210
1.0	2980
1.5	1110

Distribution coefficients of various eluents on the Amberchrom CG-71cd were also determined for both Ga(III) (0.01mmole) and Ge(IV) (0.01mmole) to obtain the optimal conditions required to remove the Ge(IV) from the resin column without having any effect on the Ga(III) retained on the resin column. Table 8.3 showed that Ga(III) had higher distribution coefficients in HCl - HF mixtures than in HCl. For the purpose of this work the 6 M HCl - 0.5 M HF mixture was then selected as the eluent to be used in future work, because of the satisfactory results obtained during the chemical processing of the ^{nat} Ge target, which will be discussed later.

Table 8.3 Distribution coefficients for Ga(III) and Ge(IV) (1 mmole / g resin) on the Amberchrom CG-71cd resin as a function of varying HCl and HCl - HF mixtures.

Acid concentration	Distribution coefficient of Ga(III)	Distribution coefficient of Ge(IV)
5 M HCl	580	1.6
5 M HCl-0.5 M HF	780	1.1
6 M HCl	690	1.2
6 M HCl-0.5 M HF	850	0.5
7 M HCl	760	1.1
7 M HCl-0.5 M HF	870	0.4

8.3 DISTRIBUTION COEFFICIENTS FOR ELEMENTAL CONTAMINANTS IN HCl - HF MEDIUM

Distribution coefficients for elemental contaminants such as Al(III), Ge(IV), Fe(II), Fe(III), and Ti(III) {0.01 - 1.0 mmole / g resin} that may arise from the chemical processing were also determined on the Amberchrom CG-71cd resin in the 6 M HCl - 0.5 M HF mixture.

As is illustrated in Table 8.4 it was found that Al(III), Ge(IV), Fe(II), and Ti(III) showed very low distribution coefficients, and therefore these elements could be easily eluted from an Amberchrom CG-71cd resin column. Iron(III) followed a similar behaviour to that of Ga(III) in the 6 M HCl - 0.5 M HF mixture. It was therefore again necessary to reduce the iron from a trivalent state to a divalent state using $TiCl_3$ as a reducing medium.

Table 8.4 Distribution coefficients for Al(III), Fe(II), Fe(III), Ti(III) and Ge(IV) on the Amberchrom CG-71cd resin in 6M HCl - 0.5M HF mixture.

mmole	Al(III)	Fe(II)	Fe(III)	Ti(III)	Ge(IV)
0.01	0.2	0.9	190	0.1	0.11
0.02	0.2	1.0	195	0.1	0.15
0.05	0.5	1.2	196	0.1	0.2
0.10	0.8	1.2	254	0.1	0.3
0.20	0.9	1.4	269	0.2	0.4
1.00	1.0	1.4	283	0.2	0.5

8.4 ELUTION CURVES

The same resin column parameters and conditions were employed as discussed in section 4.3.

(a) ***Elution curve for 4.0 g Ge(IV) and 2.0 mg Ga(III) on 1.0 g Amberchrom CG-71cd resin.*** The resin column was equilibrated by passing 50 mL of 6 M HCl - 0.5 M HF through the resin column. A solution containing 4.0 g Ge(IV) and 2.0 mg Ga(III) in a volume of 50 mL 5 M HF - 5 M HCl was prepared and passed through the resin column. The elements were washed onto the resin with small portions of 6 M HCl - 0.5 M HF and the Ge(IV) was eluted with 150 mL 6 M HCl - 0.5 M HF mixture. The Ga(III) was eluted with 50 mL 0.5 M HNO_3. The flow rate, collection of fractions, and the analysis of amounts of elements in each fraction were determined using the spectrophotometric methods as described in section 5. The elution curve shown in

Figure 8.1 is evident of a quantitative separation of Ge(IV) from Ga(III) in microgram levels. The amount of Ge(IV) found in the Ga(III) eluate was less than 25 ppm.

(b) ***Elution curve for 2.0 g Al(III) and 2.0 mg Ga(III) on 1.0 g Amberchrom CG-71cd resin.*** The resin column was equilibrated by passing 50 mL 6 M HCl - 0.5 M HF. A solution containing 2.0 g Al(III) and 2.0 mg Ga(III) in a volume of 50 mL 5 M HF - 5 M HCl was prepared and passed through the resin column. The elements were washed onto the resin with small portions of 6 M HCl - 0.5 M HF and the Al(III) was eluted with 150 mL 6 M HCl-0.5 M HF mixture. The Ga(III) was eluted with 50 mL 0.5 M HNO_3. The flow rate, collection of fractions, and the analysis of amounts of elements in each fraction were determined using the spectrophotometric methods as described in section 5. The elution curve shown in Figure 8.2 is evident of a quantitative separation of Al(III) from Ga(III) in microgram levels. The amount of Al(III) found in the Ga(III) eluate was less than 20 ppm.

It is evident that both of the elution curves had shown a sharp and quantitative separation of Ga(III) from the major contaminants, Ge(IV) and Al(III), and the retained Ga(III) could be effectively eluted with a small volume of 0.5 M HNO_3.

Figure 8.1 Elution curve for Ga(III)-Ge(IV) and Ga(III)-Ti(III) on Amberchrom CG-71cd in 6 M HCl-0.5 M HF (col. 41mm / 6 mm).

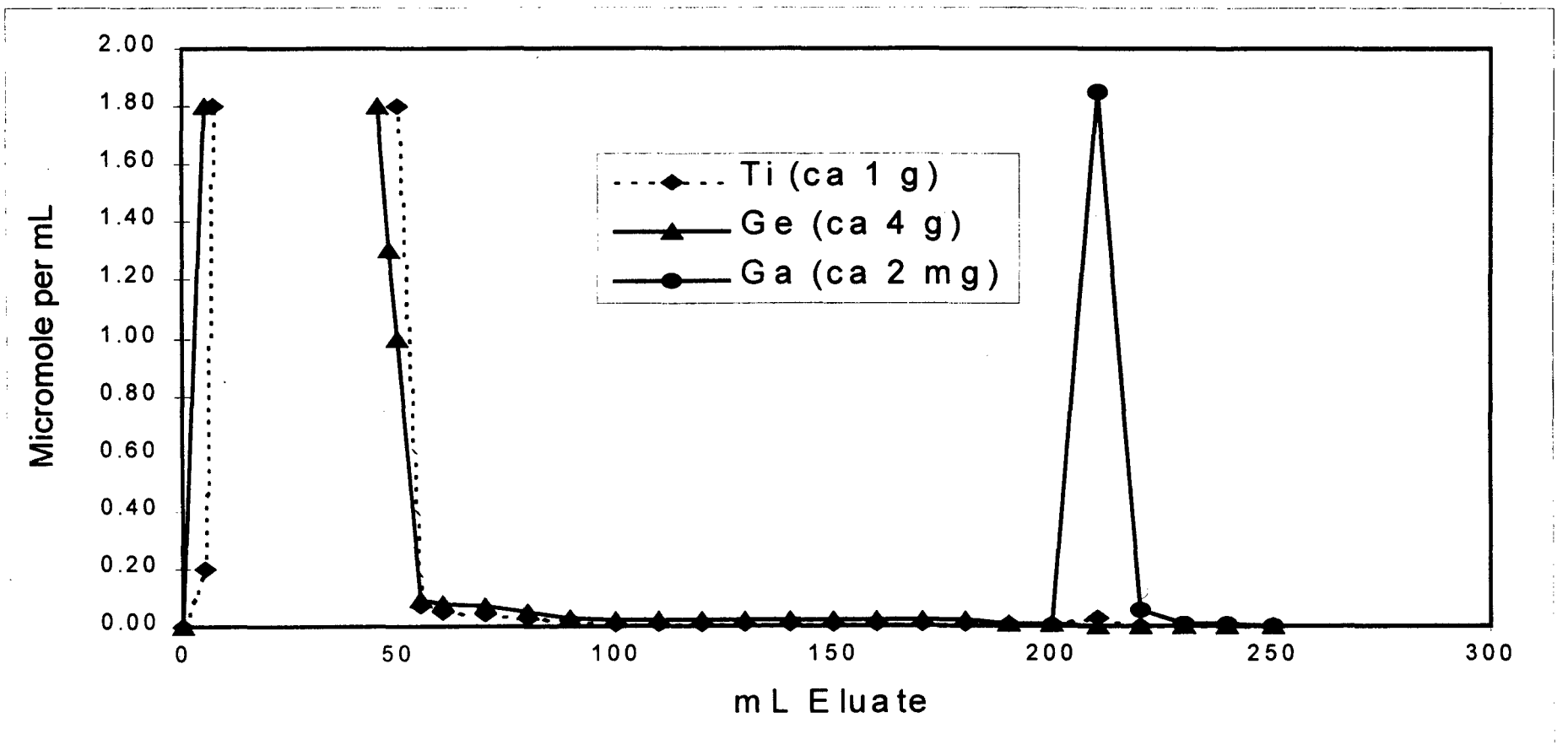

Figure 8.2 Elution curve for Ga(III)-Al(III) on the Amberchrom CG-71cd resin in 6 M HCl - 0.5 M HF (col. 41 mm / i.d. 6 mm).

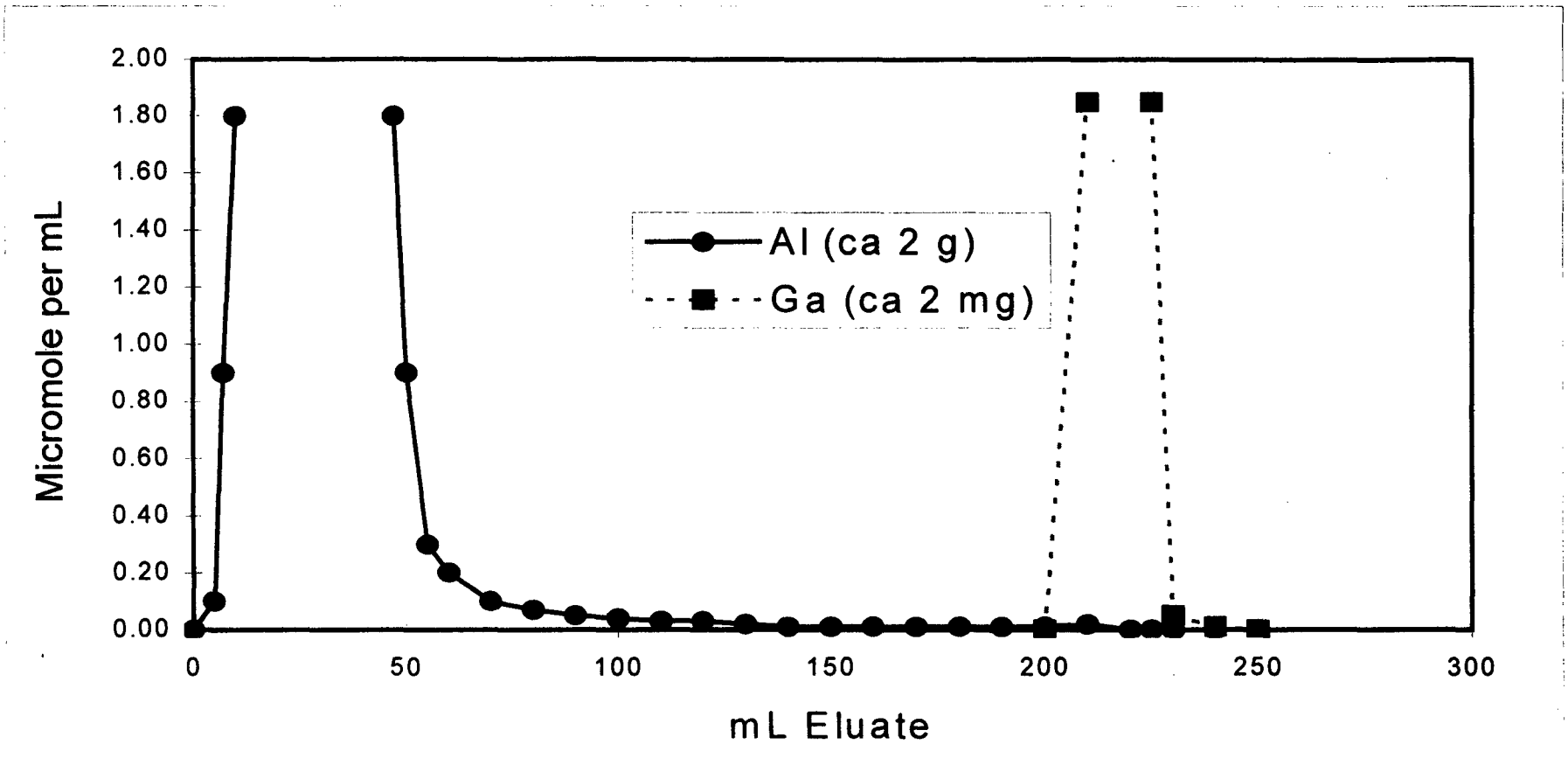

8.5 QUANTITATIVE SEPARATIONS OF SYNTHETIC MIXTURES

According to a literature survey, quantitative separations of Ga(III) from other elements was done on a cation exchange resin or an anion exchange resin (Van der Walt and Strelow, 1983 and Kuroda et al., 1968). The elution of the elements were done in a strong HCl medium. However no literature was available on the quantitative separation of Ga(III) from other elements using a polymeric resin. This prompted us to study the quantitative separation of Ga(III) from other elements such a . Ge(IV), Zn(II), Fe(II), Cu(II), Al(III), In(III), Cd(II), Ni(II), and Co(II) on a polymeric Amberchrom CG-71cd resin in a 6 M HCl - 0.5 M HF mixture.

A series of 1.0 g Amberchrom CG-71cd resin columns were prepared as described in section 4.3. Appropriate volumes of standard solutions of Ga(III) {10 μg or 100 μg} and one other element such as Ge(IV), Zn(II), Fe(II), Cu(II), Al(III), In(III), Cd(II), Ni(II), and Co(II) {10 μg or 100 μg} were accurately measured out in triplicate, mixed, and adjusted to a volume of about 50 mL containing a 6 M HCl - 0.5 M HF mixture. When 5.0 g of Ge(IV) or 5 g of Zn(II) was present, a volume of 100 mL was used. The standard solution of Fe(II) in the 6 M HCl - 0.5 M HF was treated with $TiCl_3$ before it was made up to volume. Three equivalent aliquots of each solution were measured out and kept separately as standards for comparison with the solutions obtained after separations, using similar dilutions or volumes for the final determinations of the elements in the standards and separated solutions. The mixed solutions were passed through the equilibrated resin columns and washed onto the resin with small portions of 6 M HCl - 0.5 M HF mixture, 50 mL in total. When

separating 5 g of Ge(IV) from Ga(III) a total volume of 100 mL of 6 M HCl - 0.5 M HF mixture was used. The same condition was applied when separating 5 g of Zn(II) from Ga(III). When Fe(II) was separated from Ga(III), the elements were washed onto the resin with small portions of 6 M HCl - 0.5 M HF containing 0.30% $TiCl_3$. The Ti(III) was then eluted with a further 50 mL of 6 M HCl - 0.5 M HF mixture.

The Ga(III) was eluted with 50 mL 0.5 M HNO_3. The different fractions were collected from the beginning of the sorption step, and, after the excess acid had been removed by evaporation, they were made up to convenient volumes, ready for flame atomic absorption spectrometry, electrothermal atomisation spectrometry, induced coupled plasma emission spectrometry and / or colorimetric spectrophotometry analysis.

As is illustrated in Table 8.5 and 8.6 excellent quantitative separations of Ga(III) from other elements such as Ge(IV), Zn(II), Fe(II), Cu(II), Al(III), In(III), Cd(II), Ni(II), and Co(II) were possible. The separations were sharp and the recoveries of the Ga(III) were between 99.1% and 100%. No significant difference was encountered in the separation of Ga(III) from the other elements when using a 10 μg Ga(III) instead of the 100 μg Ga(III) stock sample. Therefore the quantitative separation of Ga(III) from other elements on a 1.0 g Amberchrom CG-71cd resin at submicrogram amounts of Ga(III) is possible. This made it viable to develop a method for the separation of carrier-free radioisotopes of Ga from irradiated cyclotron targets such as the ^{nat}Zn or ^{nat}Ge targets.

Table 8.5 Results of quantitative separation of synthetic mixtures using the 10 μg Ga(III) stock solution.

Other Element	Amount taken in μg		Amount found in μg (a)		Amount of other element found in Ga(III) fraction in μg
	Ga(III)	other element	Ga(III)	other element	
Ge(IV)	10 μg	100 μg	9.1 ± 0.5	99.3 ± 0.5	0.3- 0.5
Zn(II)	10 μg	100 μg	9.2 ± 0.3	99.4 ± 0.3	0.2 - 0.5
Al(III)	10 μg	100 μg	9.1 ± 0.5	99.1 ± 0.5	0.4 - 0.7
Fe(II)	10 μg	100 μg	9.3 ± 0.4	99.3 ± 0.4	0.3 - 0.6
Co(II)	10 μg	100 μg	9.4 ± 0.4	99.6± 0.3	0.1 - 0.3
Ni(II)	10 μg	100 μg	9.5 ± 0.5	99.6 ± 0.3	0.1 - 0.4
Cu(II)	10 μg	100 μg	9.7 ± 0.4	99.8 ± 0.2	0.1 - 0.2
Cd(II)	10 μg	100 μg	9.9 ± 0.1	99.9 ± 0.1	0.1 - 0.3
In(III)	10 μg	100 μg	10.0 ± 0.3	99.5 ± 0.4	0.1 - 0.2
Ge(IV)	10 μg	5.003 g	9.3 ± 0.6	5.002 ± 0.003	0.4 - 0.6
Zn(II)	10 μg	5.001 g	9.4 ± 0.6	5.001 ± 0.003	0.5 - 0.7

(a) = Results are the means of triplicate runs.

Table 8.6 Results of quantitative separation of synthetic mixtures using the 100 μg Ga(III) stock solution.

Other Element	Amount taken in μg		Amount found in μg (a)		Amount of other element found in Ga(III) fraction in μg
	Ga(III)	other element	Ga(III)	other element	
Ge(IV)	100 μg	100 μg	99.3 ± 0.5	99.3 ± 0.5	0.3 - 0.6
Zn(II)	100 μg	100 μg	99.4 ± 0.3	99.4 ± 0.3	0.4 - 0.6
Al(III)	100 μg	100 μg	99.1 ± 0.5	99.1 ± 0.5	0.3 - 0.7
Fe(II)	100 μg	100 μg	99.3 ± 0.4	99.3 ± 0.4	0.2 - 0.6
Co(II)	100 μg	100 μg	99.4 ± 0.3	99.6± 0.3	0.1 - 0.3
Ni(II)	100 μg	100 μg	99.6 ± 0.3	99.6 ± 0.3	0.1 - 0.3
Cu(II)	100 μg	100 μg	99.8 ± 0.2	99.8 ± 0.2	0.1 - 0.2
Cd(II)	100 μg	100 μg	99.9 ± 0.1	99.9 ± 0.1	0.1 - 0.2
In(III)	100 μg	100 μg	100.0 ± 0.3	100.0 ± 0.3	0.1 - 0.2
Ge(IV)	100 μg	5.001 g	99.3 ± 0.4	5.001 ± 0.002	0.6 - 0.9
Zn(II)	100 μg	5.001 g	99.4 ± 0.3	4.999 ± 0.003	0.6 - 0.9

(a) = results are the means of triplicate runs.

8.6 CHEMICAL SEPARATION OF THE ^{67}Ga FROM THE ^{nat}Ge TARGET MATERIAL

After dissolution of the ^{nat}Ge target a small volume of concentrated HCl was added to the hot Ge solution (100^{0}C) to destroy the excess peroxide. The chlorine gas produced was removed via vacuum. After cooling the dissolution mixture, $TiCl_3$ was added to induce a reductive environment and suffucient concentrated HCl was added to obtain a *ca* 5 M HCl – 5 M HF media. The dissolution solution was sorbed onto a 1.0 g Amberchrom CG-71cd resin column, and the excess Ge remaining on the column was eluted with a 6 M HCl - 0.5 M HF mixture.

Elution of the ^{67}Ga was obtained by eluting the resin column with 0.5 M HNO_3, which was transferred into an evaporator where it was evaporated to dryness. Concentrated HNO_3 was then added into the evaporator and also evaporated to dryness to destroy any organic material that may arise during the chemical separation. Thereafter deionised water was added into the evaporator and also evaporated, in order to remove the last traces of the nitric acid.

The ^{67}Ga was then taken up by 2.6% sodium citrate (10 mL) and transferred from the evaporator into a sterile vial, for further processing in the dispensary laboratory. A schematic diagram of the chemical processing of the ^{nat}Ge target is illustrated in Figure 8.3.

Figure 8.3 Schematic diagram of the ^{nat}Ge target chemical process.

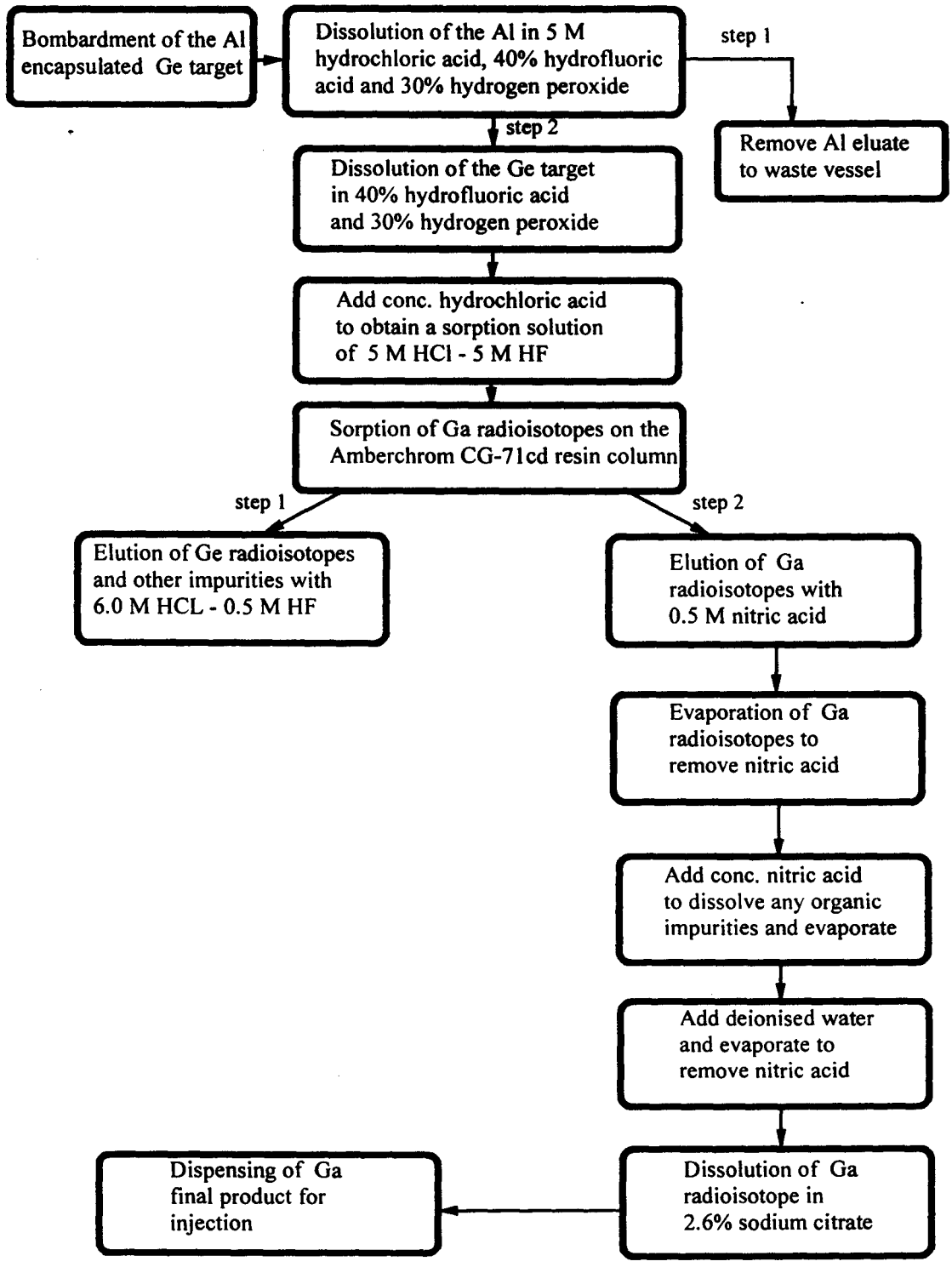

9 PRODUCTION RUNS

9.1 HOT CELL PROCEDURE

(a) Reagents

Analytical reagent grade chemicals supplied by Merck (SA) and Saarchem Holpro (SA) were used. Deionised water was obtained from a Milli-Q reagent grade water system.

Stock solutions

- HCl (hydrochloric acid)
- HNO_3 (nitric acid)
- H_2O_2 (hydrogen peroxide)
- HF (hydroflouric acid)
- $TiCl_3$(titanium chloride)
- $N_2H_4.H_2O$ (hydrazine hydrate)
- $(NH_4)_2S$ (ammonium sulphide)
- $Na_2CO_3.H_2O$ (sodium carbonate monohydrate)
- $Na_3C_6H_5.2H_2O$ (tri-sodium citrate dihydrate)

Prepared solutions

- Al dissolution: 5 M HCl (300 mL)
- Ge eluting solution: 6 M HCl - 0.5 M HF (500mL)
- Zn eluting solution: 7 M HCl (250 mL)

- Ga eluting solution: 0.5 M HNO_3 (100 mL)
- Arsenic trap solution: 140 mL 5 M HCl + 1 mL $(NH_4)_2S$
- Acid scrubber solution: 26 g $Na_2CO_3.H_2O$ + 45 mL H_2O + 45 mL 80% $N_2H_4.H_2O$

Column preparation

The Amberchrom CG-71cd resin supplied in a dry form was hydrated with deionised water and the column (5 mL in volume) was packed with 70 μm polyethylene frits at the top and bottom of the column, as described in section 4.3.

(b) Hot cell preparation

(Refer to Figure 9.1, a schematic diagram of hot cell panel)

Pump cassette: load line 1 = L1

load line 2 = L2

wash line 1 = W1

wash line 2 = W2

1. The entire system was rinsed with deionised water using cassette pump L1, L2, W1 and W2.
2. The evaporator was cleaned with deionised water.
3. The scrubber solution and arsenic trap solution were placed in the relevant holders as indicated on the schematic.
4. Two 5 micron filters were placed in position.

5. Weighed Ge and Zn mother solution sample bottles were placed in position.
6. The column was placed in position and equilibrated with 30 mL 6 M HCl - 0.5 M HF just before the sorption step of the separation, using cassette pump W1 and taps 1, 2, 3, 4, 9, 10, 11, 12, 13, 14 and 16.

(c) Processing of ^{nat}Ge target

Al encapsulation dissolution

1. The vacuum pump was connected to the reaction vessel 1 via the arsenic trap: V1, V2 and V3.
2. The target was transferred into reaction vessel 1 and the stirrer was activated.
3. 5 mL 30% H_2O_2 was added to the reaction vessel 1 from the outside line using cassette pump W1 and taps 1, 2, 3, 4, 5 and 6.
4. After 10 minutes, 10 mL 40% HF was pumped via the outside line as in (3) and stirred.
5. After 5 minutes, an additional 50 mL 5 M HCl was pumped via the outside line as in (3) and stirred.
6. After 5 minutes, 10 mL 40% HF was pumped via the outside line as in (3) and stirred.
7. After 5 minutes, an additional 50 mL 5 M HCl was pumped via the outside line as in (3) and stirred.
8. After 5 minutes, 10 mL 30% H_2O_2 was added to reaction vessel 1 at 1 minute intervals via the outside line as in (3) and stirred.

9. After complete dissolution of the Al encapsulation, the solution was pumped from reaction vessel 1 to the waste vessel using cassette pump L1 and taps 0, 7, 8, 17, 18, 19, 20, 21, 15 and 16.

10. The reaction vessel 1 was washed with 2 x 150 mL deionised water by pumping deionised water into reaction vessel 1 from the outside as in (3) and thereafter pumping it out to waste as in (9).

Ge dissolution

11. Thereafter 40 mL 40% HF + 10 mL 30% H_2O_2 was added into reaction vessel 1 as in (3), and the temperature was set at 70^0C.

12. After 15 minutes, 10 mL 30% H_2O_2 was added into reaction vessel 1 as in (3), and the temperature was set at 75^0C.

13. After 15 minutes, 10 mL 30% H_2O_2 was added into reaction vessel 1 as in (3), and the temperature was set at 85^0C.

14. After 15 minutes, 10 mL 30% H_2O_2, was added into reaction vessel 1 as in (3), and the temperature was set at 95^0C.

15. After 15 minutes, 10 mL 40% HF was added into reaction vessel 1 as in (3), and the temperature was set at 100^0C.

16. After 15 minutes, 10 mL 30% H_2O_2 was added into reaction vessel 1 as in (3), and the temperature was maintained at 100^0C.

17. The temperature was maintained for a further 15 minutes, and thereafter the heat and vacuum was switched off, while the stirrer was kept on for mixing to ensure complete dissolution of the Ge target.

(wait for 1 hour to ensure complete dissolution)

18. Reaction vessel 1 solution was again heated to 80^0C for 10 minutes.

19. Thereafter 100 mL 32% HCl was added into reaction vessel 1 as in (3).
20. The Ga / Ge solution was pumped from reaction vessel 1 via a 5 micron filter to reaction vessel 2 using cassette pump L2 and taps 0, 7, 8, 17, 18, 19, 20, 21 and 15.
21. Thereafter 50 mL 32% HCl was added into reaction vessel 1 from the outside as in (3) and thereafter pumped to reaction vessel 2 as in (20).
22. Thereafter 5 mL $TiCl_3$ was added into reaction vessel 2 from the outside using cassette pump W1 and taps 1, 2, 3, 4 and 5.
23. The resulting solution was pumped from the reaction vessel 2 to the equilibrated column using cassette pump W1 and taps 2, 3, 4, 9, 10, 11, 12, 13, 14 and 16.
24. The Ge sample (2 mL) was taken by toggling tap 11 in the sample position.
25. The column was washed from the outside with 450 mL 6 M HCl - 0.5 M HF by using cassette pump W2 and taps 1, 3, 4, 9, 10, 11, 12, 13, 14 and 16.
26. The ^{67}Ga was eluted from the column to the evaporator with 25 mL 0.5 M HNO_3 by using cassette pump W2 and taps 1, 3, 4, 9, 10, 11, 12, 13 and 21.
27. Evaporation of ^{67}Ga in the evaporator was temperature controlled between 100^{0}C - 150^{0}C with the vacuum activated via V1 only.
28. 1 mL 70% HNO_3 was added from holder 1 into the evaporator, using tap 23, and the solution was evaporated to dryness.
29. 1 mL deionised water was added from holder 2 into the evaporator, using taps 23 and 24, and the solution was evaporated to dryness.
30. 10 ml 2.6% sodium citrate was added from holder 3 into the evaporator using taps 23, 24 and 25, and the solution was heated at 50^{0}C for 1 minute and the heat was then switched off.

31. The concentrated ^{67}Ga final product was pumped into a sterile vial via cassette pump P1.
32. The ^{67}Ga final product vial was then forwarded to the dispensing laboratory for further processing.

(d) Processing of ^{nat}Zn target

Before the processing of the Zn target, the column was cleaned by pumping from the outside the hotcell, 50 mL 1 M HNO_3, followed by 30 mL deionised water, and thereafter the column was equilibrated with 50 mL 7 M HCl [cassette pump and taps as in (25) above].

1. The Zn target was transferred into reaction vessel 1 and 45 mL 32% HCl with 2 ml $TiCl_3$ was added into reaction vessel 1 from the outside, using casette pump W1 and taps 1, 2, 3, 4, 5 and 6.
2. The vacuum and the stirrer was activated, and no heat was required.
3. The sorption solution was pumped from the reaction vessel 1 via a filter to the equilibrated column using casette pump L1 and taps 0, 7, 8, 17, 18, 19, 20, 21, 9, 10, 11, 12,13, 14 and 16.
4. A 2 mL Zn sample was taken by toggling tap 10 to the sample position.
5. The column was washed from the outside with 150 mL 7 M HCl, using cassette pump W2 and taps 1, 3, 4, 9, 10, 11, 12, 13, 14 and 16.
6. The elution of the ^{67}Ga final product from the column to the evaporator was done with 25 mL 0.5 M HNO_3 using cassette pump W2 and taps 1, 3, 4, 9, 10, 11, 12, 13, and 21.

7. Evaporation of ^{67}Ga in the evaporator was temperature controlled between 100^{0}C - 150^{0}C with the vacuum activated in position V1 only.
8. Thereafter 1 mL 70% HNO_3 was added from holder 1 into the evaporator, using taps 23, and the solution was evaporated to dryness.
9. Thereafter 1 mL deionised water was added from holder 2 into the evaporator, using taps 23 and 24, and the solution was evaporated to dryness.
10. Thereafter 10 ml 2.6% sodium citrate was added from holder 3 into the evaporator using tap orientation 23, 24 and 25 and the solution was heated at 50^{0}C for 1 minute and the heat was then switched off.
11. The concentrated ^{67}Ga final product was pumped into a sterile vial via cassette pump P1.
12. The ^{67}Ga final product vial was then forwarded to the dispensing laboratory for further processing.

(e) Production clean-up

1. All the lines were rinsed with deionised water as soon as the production yield was calculated.
2. The waste was drained to the basement.
3. The vacuum, stirrer, heaters, etc. were switched off.
4. The hot cell lights were switched off.

Figure 9.1 Schematic diagram of the hot cell panel for ^{67}Ga production from a tandem ^{nat}Ge / ^{nat}Zn target.

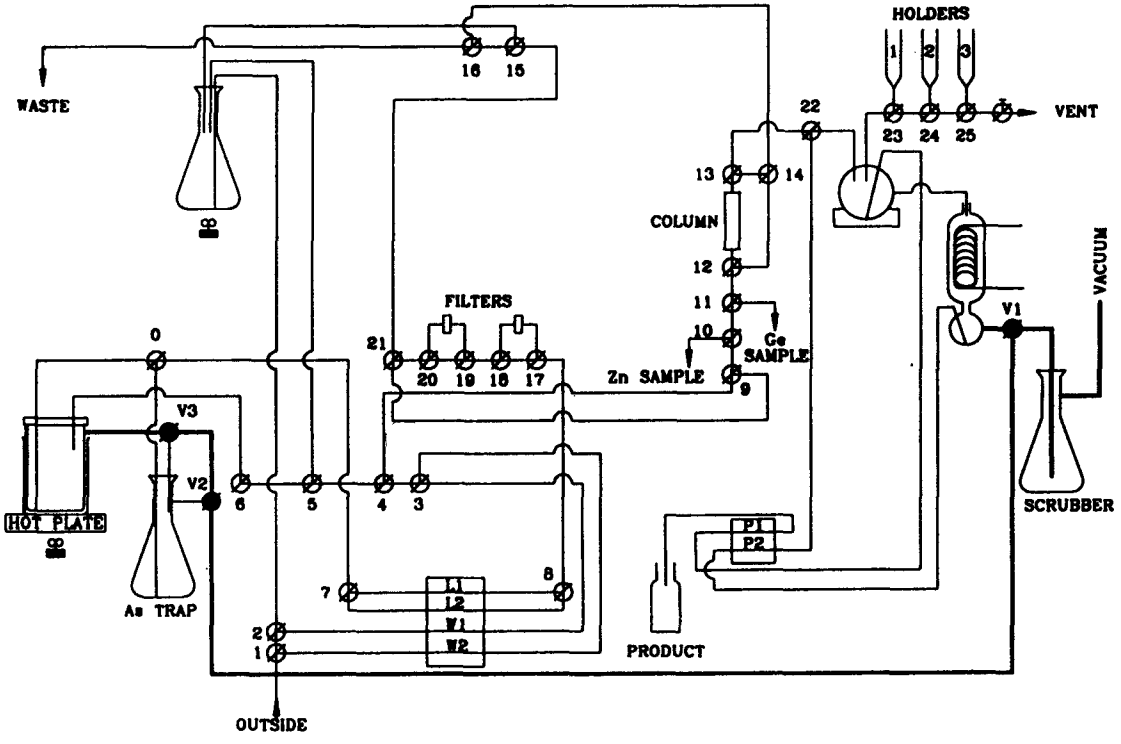

10 RESULTS AND DISCUSSION

According to the distribution coefficients, elution curves and quantitative separation study done on the Amberchrom CG-71cd with Ga(III) and other contaminant elements, in the different acid media, one expected to produce a chemical separation of a carrier-free ^{67}Ga radioisotope from the tandem ^{nat}Ge / ^{nat}Zn target with ease.

As is illustrated in Table 10.1 the production runs to date had shown reproducible results. Firstly the chemical impurities found in the ^{67}Ga final product, was minimal, and had contaminant levels of only Fe(II) (< 3 ppm), Ti(III) (< 1 ppm), Al(III) (< 0.1 ppm), Ge(IV) (< 5 ppm), Cu(II) (< 0.05 ppm) and Zn(II) (< 6 ppm) in the product, which was within the human toxicity limits (Casarett and Doull, 1975).

According to Table 10.1 it was also noticeable that as the irradiation time increased on the tandem target, there was a slight decrease in the yield mCi / μAh at EOB. For example a target exposed to an irradiation charge of 10 μAh, resulted in a yield of 3.05 mCi / μAh at EOB. Compared to this, a target exposed to a charge of 435 μAh, resulted in a yield of 2.59 mCi / μAh at EOB. This may be due to the ^{67}Ga spreading out onto the front of the Al canister, the hot spot of the target when under irradiation. The longer the radiation time the greater the spread. This then resulted in a loss of ^{67}Ga activity when the Al canister was dissolved in the strong acid and the solution was thereafter removed to the waste vessel and not passed through the column. It may

Table 10.1 **^{67}Ga final product analysis for a tandem ^{nat}Ge / ^{nat}Zn target.**

Run	Charge (μAh)	EOB (mCi/μAh)	Contaminants (ppm) at calibration time					
			Ge(IV)	Zn(II)	Al(III)	Fe(II)	Ti(III)	Cu(II)
1	1	3.24	1	5	< 0.1	1	< 1	< 0.05
2	10	3.05	1	4	< 0.1	2	< 1	< 0.05
3	207	2.39	2	3	< 0.1	1	< 1	< 0.05
4	200	2.99	1	1	< 0.1	2	< 1	< 0.05
5	139	3.42	1	5	< 0.1	1	< 1	< 0.05
6	20.6	2.66	2	4	< 0.1	1	< 1	< 0.05
7	94.6	2.94	2	2	< 0.1	3	< 1	< 0.05
8	113	2.7	2	3	< 0.1	2	< 1	< 0.05
9	250	3.20	1	4	< 0.1	2	< 1	< 0.05
10	435	2.59	3	5	< 0.1	1	< 1	< 0.05
Toxicity Limit (Casarett and Doull, 1975)			< 300	< 20	< 0.2	< 10	< 3	< 0.1

also be as a result of the irradiation or the beam sweep on the target being irregular, and therefore not producing the expected theoretical yield.

The time of bombardment for a tandem ^{nat}Ge and ^{nat}Zn target compared to the ^{nat}Zn target alone was however reduced by less than half the time, even though the same amount of ^{67}Ga radioisotope was produced. The production activity of the final product ^{67}Ga (mCi) as per bombardment time (μAh) was considerably higher for the tandem ^{nat}Ge and ^{nat}Zn targets (3 mCi / μAh at EOB) as compared to the ^{nat}Zn target (1.5 mCi / μAh at EOB) (Nortier et al., 1991).

According to Table 10.2 the radionuclidic impurity of the final product ^{67}Ga had shown satisfactory results. The radionuclidic impurity found in the ^{67}Ga final product at calibration time was found to be ^{66}Ga(< 0.8%), ^{72}Ga(< 0.1%), ^{71}As(< 0.1%) and ^{67}Cu (< 0.1%). Neither ^{69}Ge nor ^{65}Zn radioisotopes were found present in the final product ^{67}Ga. The ^{67}Ga therefore had a radionuclidic purity of > 99.00% at calibration which was well within the specifications required by the British Pharmacopoeia (1993) and US Pharmacopoeia (1995).

The production runs to date had shown a high percentage yield of ^{67}Ga activity of 90 - 95%. The activity loss, could be attributed to ^{67}Ga lost during the sorption step (< 5%), or the Al dissolution step (< 2%) or the various wash solution steps (< 1%). The high loss in the sorption step is due to the high Ge concentration and also to the difficulty in assessing the exact molarity of the HCl - HF mixture after the dissolution

Table 10.2 Radionuclidic analysis of the production runs.

Run .	Charge (μAh)	^{67}Ga and radionuclidic impurities (%) at calibration time						
		^{67}Ga	^{66}Ga	^{72}Ga	^{69}Ge	^{65}Zn	^{71}As	^{67}Cu
1	1	99.11	0.39	0.07	0	0	0.30	0.01
2	10	99.23	0.67	0.06	0	0	0.04	0.01
3	207	99.21	0.71	0.05	0	0	0.03	0.01
4	200	99.43	0.45	0.06	0	0	0.05	0.01
5	139	99.69	0.28	0.01	0	0	0.01	0.01
6	20.6	99.39	0.49	0.07	0	0	0.05	0.01
7	94.6	99.35	0.53	0.07	0	0	0.03	0.01
8	113	99.33	0.53	0.08	0	0	0.06	0.01
9	250	99.11	0.74	0.08	0	0	0.07	0.01
10	435	99.12	0.74	0.08	0	0	0.06	0.01
British Pharmacopoeia		> 99%	other radionuclidic impurities < 1%					
US Pharmacopoeia		> 99%	other radionuclidic impurities < 1%					

of the Ge target. An excess concentrated HCl is added and it is assumed to be greater than the *ca* 5 M HCl - 5 M HF mixture required for complete sorption of the Ga.

If the beam sweep on the tandem target is incorrect, the Al dissolution, which is normally removed to the waste vessel, will have a high percentage of ^{67}Ga entrapped in the solution. Steps to have a consistent beam sweep on the tandem target are needed to be instituted, to remove any activity loss incurred.

11 CONCLUSION

Distribution coefficients for elements such as Ga(III), Ge(IV), Zn(II), Fe(III), Fe(II), Al(III), Cu(II) and Ti(III) {0.01 - 1.00 mmole}, on the Amberchrom CG-71cd resin in various acid concentrations (HCl, HCl - HF mixture) were determined. The distribution coefficients for Ga(III) on the Amberchrom CG-71cd resin in high HCl concentrations and high HCl -HF mixtures were found to be much higher than that of the elemental contaminants such as Ge(IV), Zn(II), Fe(II), Al(III), Cu(II) and Ti(III). However the Fe(III) contaminant was found to follow a similar behaviour to that of the Ga(III) on the Amberchrom CG-71cd resin, and it was therefore necessary to reduce the Fe(III) to the Fe(II) state with $TiCl_3$.

The elution curves for Ga(III)-Zn(II), Ga(III)-Cu(II), Ga(III)-Fe(II) and Ga(III)-Ti(III) in 7 M HCl and elution curves for Ga(III)-Ge(IV) and Ga(III)-Al(III) in 6.0 M HCl - 0.5 M HF mixtures, showed a complete separation of the Ga(III) from the contaminant elements. The eluting solutions used to remove the contaminant elements from the resin column were found to be small in volume.

A study on a quantitative separation of synthetic mixtures was undertaken, and illustrated the separation capabilities of the Amberchrom CG-71cd resin with other elements. Excellent quantitative separations of Ga(III) from other elements such as Ge(IV), Zn(II), Fe(II), Cu(II), Al(III), In(III), Cd(II), Ni(II), or Co(II) were obtained. The separations were sharp and the recoveries of the Ga(III) were between 99.1% and 100%. No significant difference was encountered in the separation of Ga(III) from

the other elements when using a 10 μg Ga(III) stock solution instead of the 100 μg Ga(III) stock sample. Therefore the quantitative separation of Ga(III) from other elements on a 1.0 g Amberchrom CG-71cd resin at submicrogram amounts of Ga(III) was possible.

The purification of ^{67}Ga from the proton bombarded tandem ^{nat}Ge and ^{nat}Zn target material was easily accomplished using the column chromatographic method. The dissolution of the ^{nat}Zn target with concentrated HCl proved to be easily accomplished as compared to the dissolution of ^{nat}Ge target. The dissolution of the ^{nat}Ge target could not be accomplished with a single strong acid or a base. However complete dissolution of the ^{nat}Ge target was accomplished with a 40% HF - 30% H_2O_2 mixture which was then adjusted to the *ca* 5 M HCl mixture by addition with concentrated HCl. Both the ^{67}Ga dissolution mixtures were easily absorbed onto an Amberchrom CG-71cd resin column with minimal ^{67}Ga breakthrough.

A chemical separation which was adapted for hot cell facilities as outlined in section 9, has thus far yielded satifactory results of the ^{67}Ga final product during routine production runs, which is well within the limits of the requirements of the British Pharmacopoeia and US Pharmacopoeia. The final product ^{67}Ga (> 99.0 % radionuclidic purity), only had chemical contaminant levels of Fe(II) (< 3 ppm), Ti(III) (< 1 ppm), Al(III) (< 0.1 ppm), Ge(IV) (< 5 ppm), Cu(II) (< 0.05 ppm) and Zn(II) (< 6 ppm) which was far below the human toxicity limits.

Analytical methods such as spectrophotometry and electrothermal atomisation spectrometry, were developed for the determination of the contaminant elements found in the ^{67}Ga final product as shown in section 5. The ultra violet - visible spectrophotometric method for Ge(IV) and Zn(II) used phenylfluorone and 4-(2-pyridylazo) resorcinol monosodium salt, as organic reagents, respectively.

The time of bombardment for a tandem ^{nat}Ge and ^{nat}Zn target compared to the ^{nat}Zn target alone was reduced by less than half the time, to produce the same amount of ^{67}Ga activity. The production activity of the final product ^{67}Ga (mCi) as per bombardment time (μAh) was considerably higher for the tandem ^{nat}Ge / ^{nat}Zn target (3 mCi / μAh at EOB) as compared to the ^{nat}Zn target (1.5 mCi /μAh at EOB).

Since it is estimated that irradiation time per hour could be as high as R1 200, the production cost of the ^{67}Ga radioisotope would therefore be substantially reduced due to the shorter irradiation time and therefore more time would be available to produce other radioisotopes of interest.

The transformation from the ^{nat}Zn target to the tandem ^{nat}Ge / ^{nat}Zn target will take place as soon as the toxicity studies and registration of the final product ^{67}Ga radioisotope with the South African Medical Control Board is complete.

12 APPENDIX

12.1 APPENDIX 1

Varian AA600 atomic absorption (AA) spectrometric calibration curves for the metals investigated.

Figure 12.1.1 **AA calibration curve for Ga.**

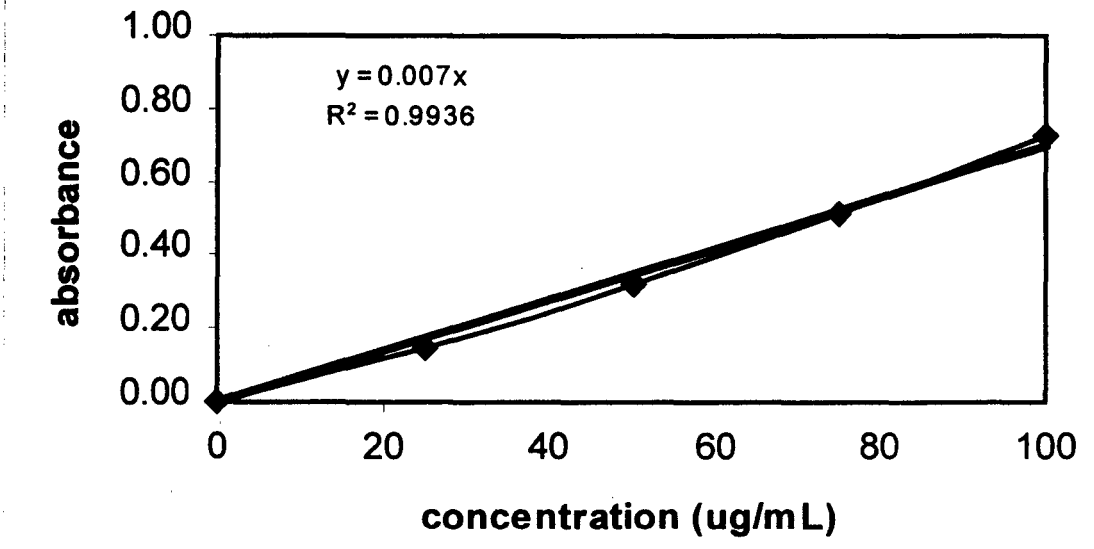

Figure 12.1.2 **AA calibration curve for Ge.**

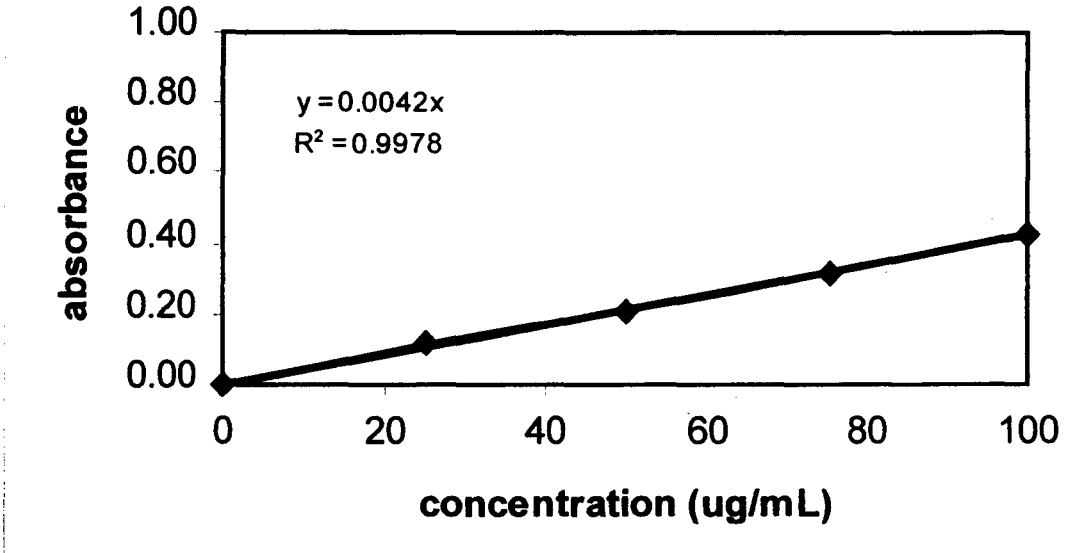

Figure 12.1.3 **AA calibration curve for Zn.**

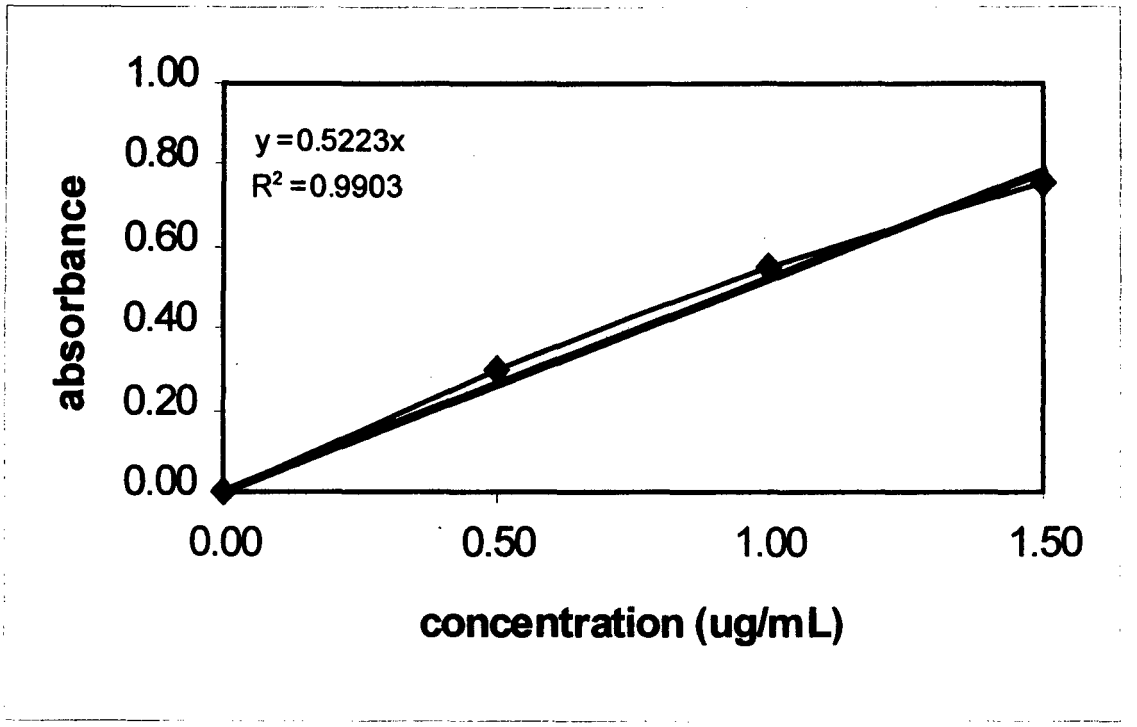

Figure 12.1.4 **AA calibration curve for Al.**

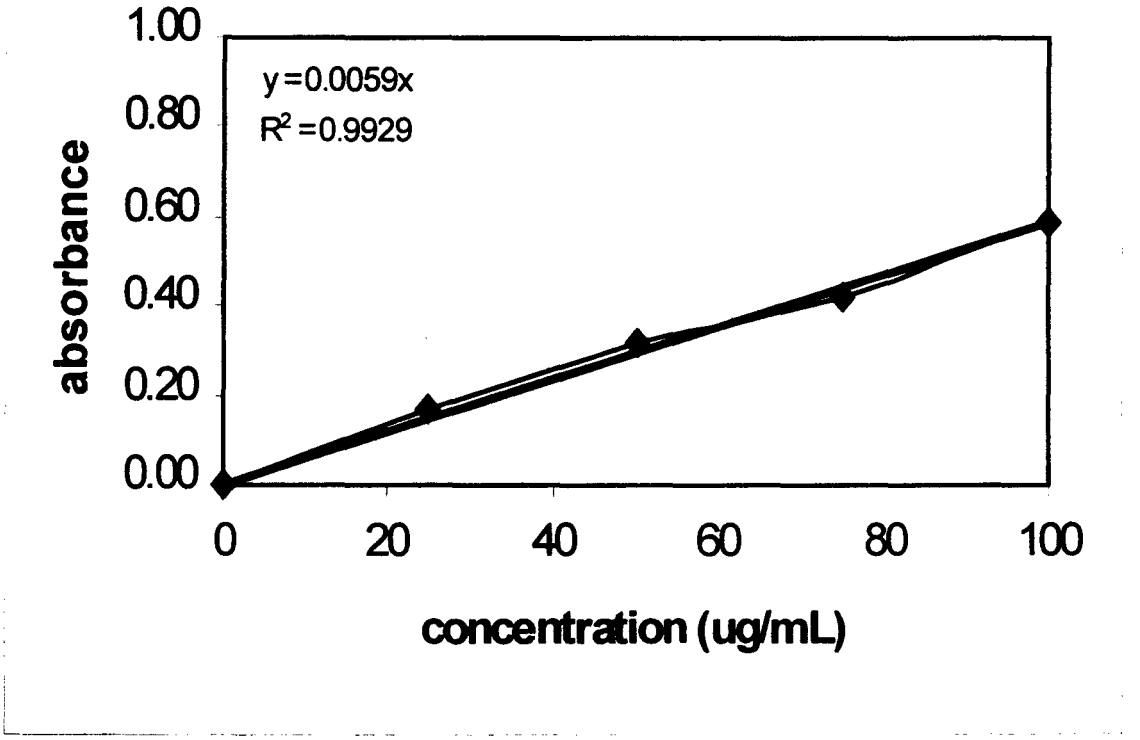

Figure 12.1.5 **AA calibration curve for Fe.**

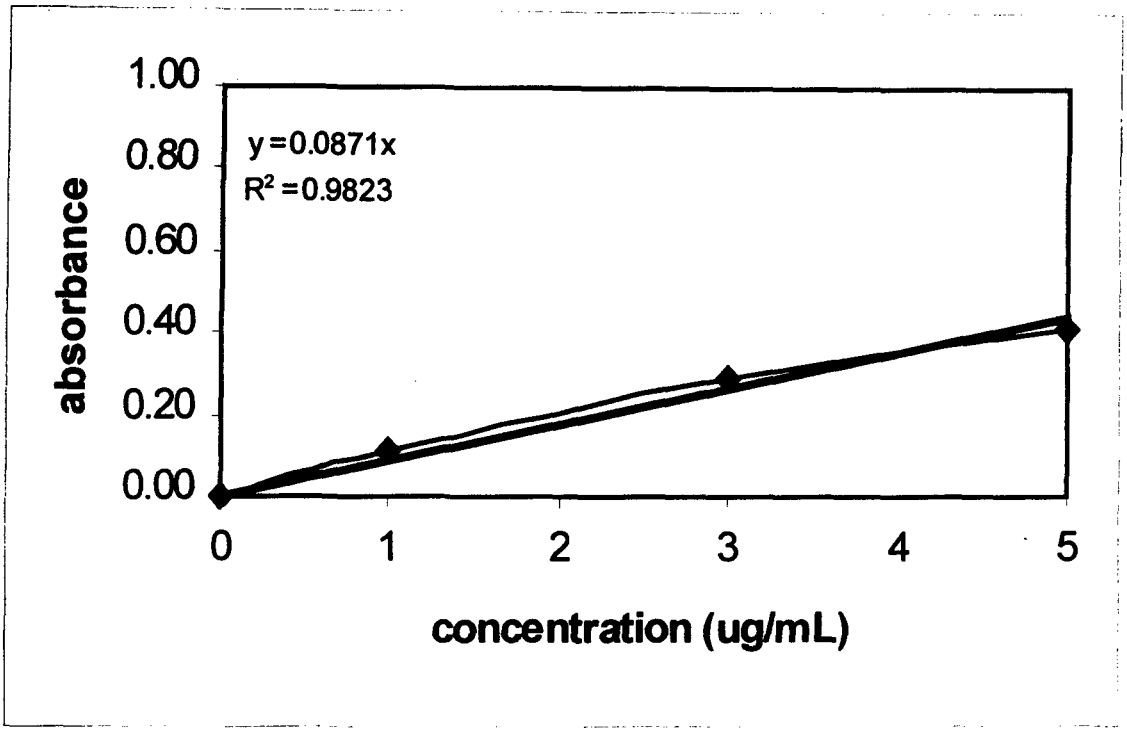

Figure 12.1.6 **AA calibration curve for Co.**

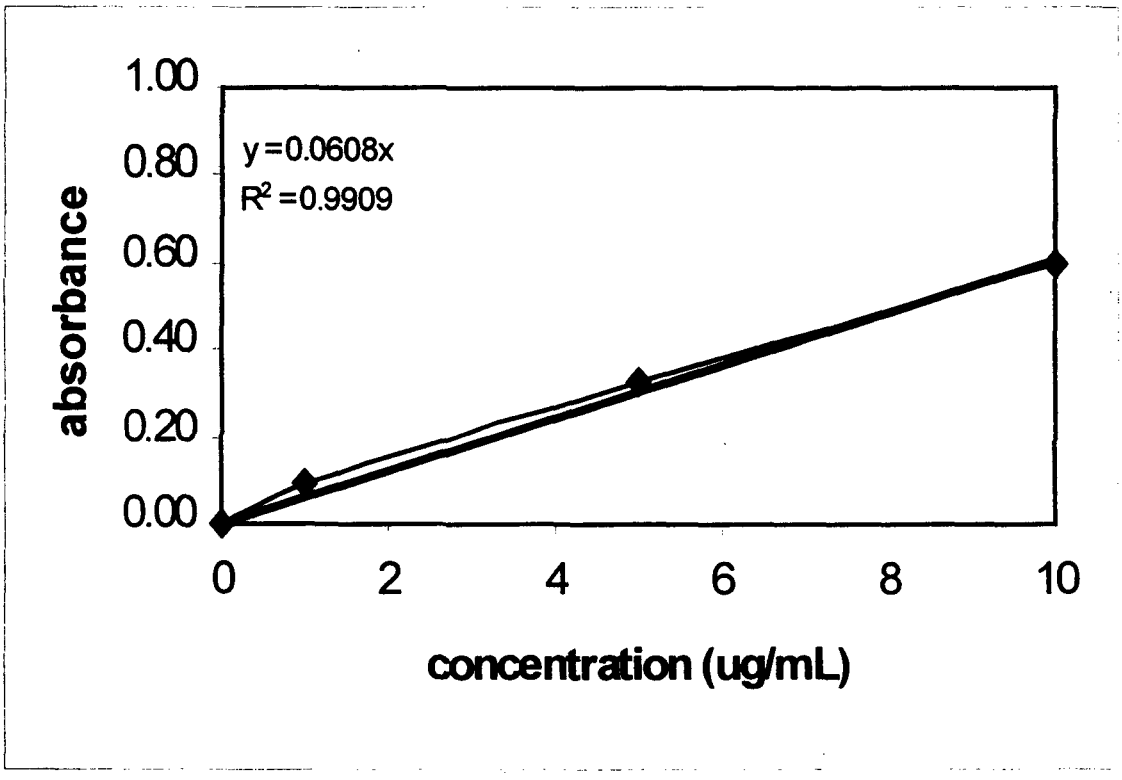

Figure 12.1.7 **AA calibration curve for Ni.**

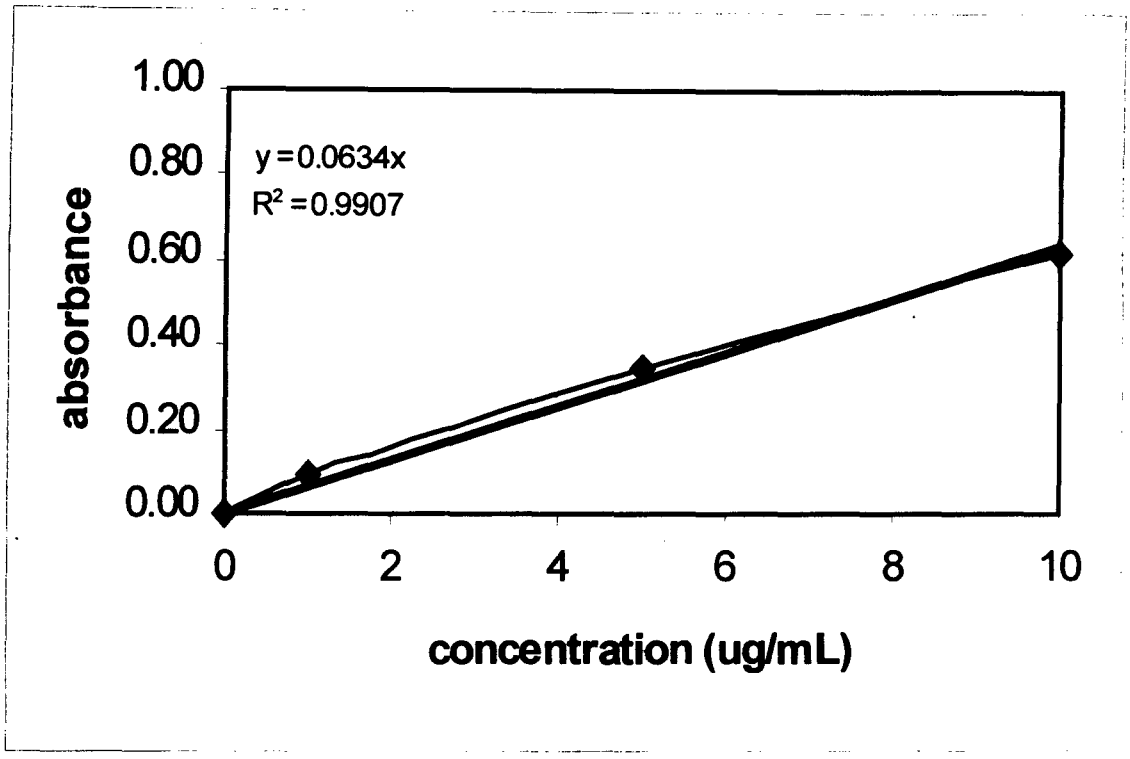

Figure 12.1.8 **AA calibration curve for Cu.**

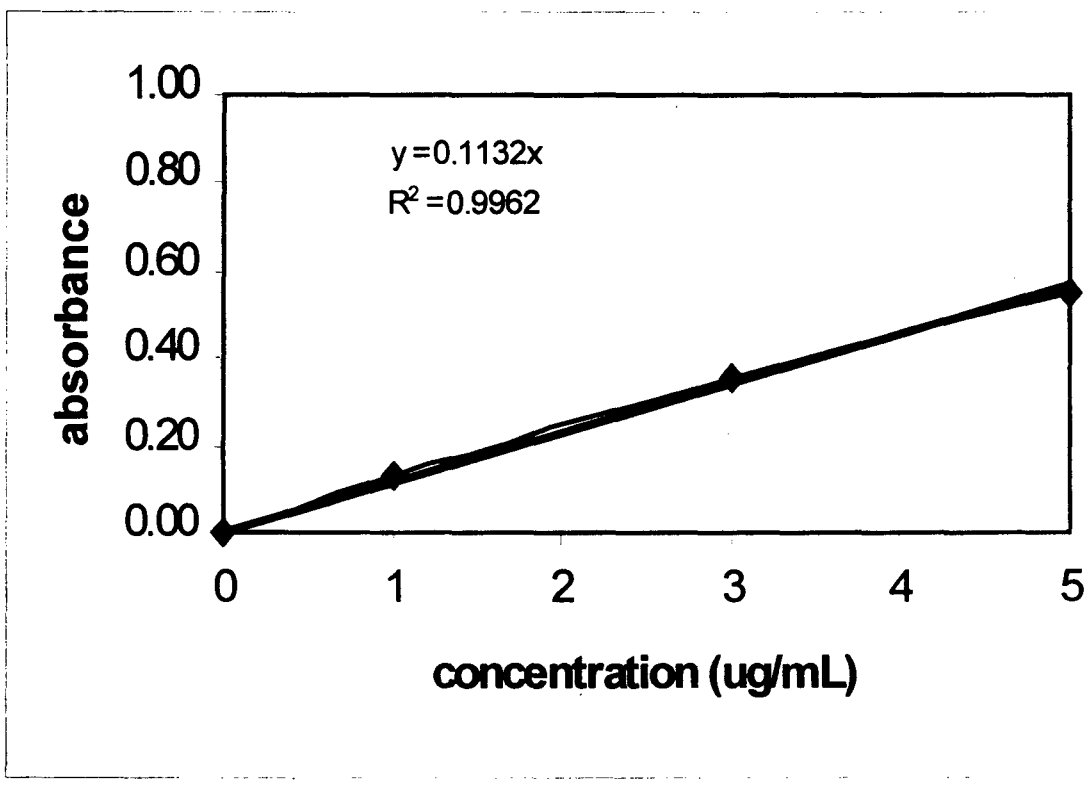

Figure 12.1.9 **AA calibration curve for Cd.**

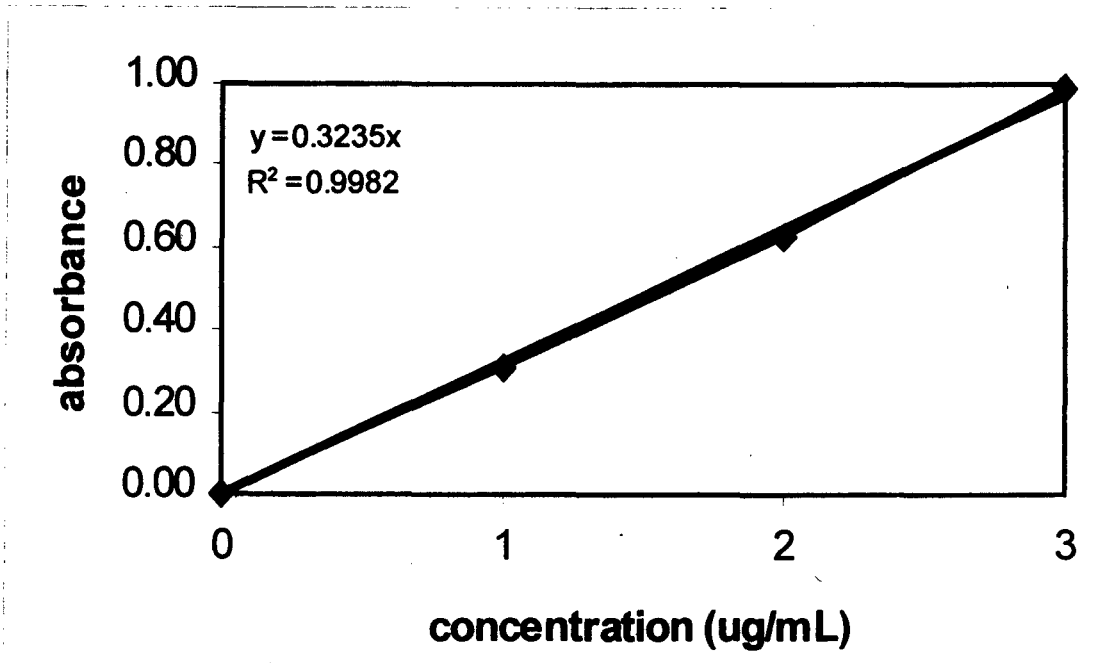

Figure 12.1.10 **AA calibration curve for In.**

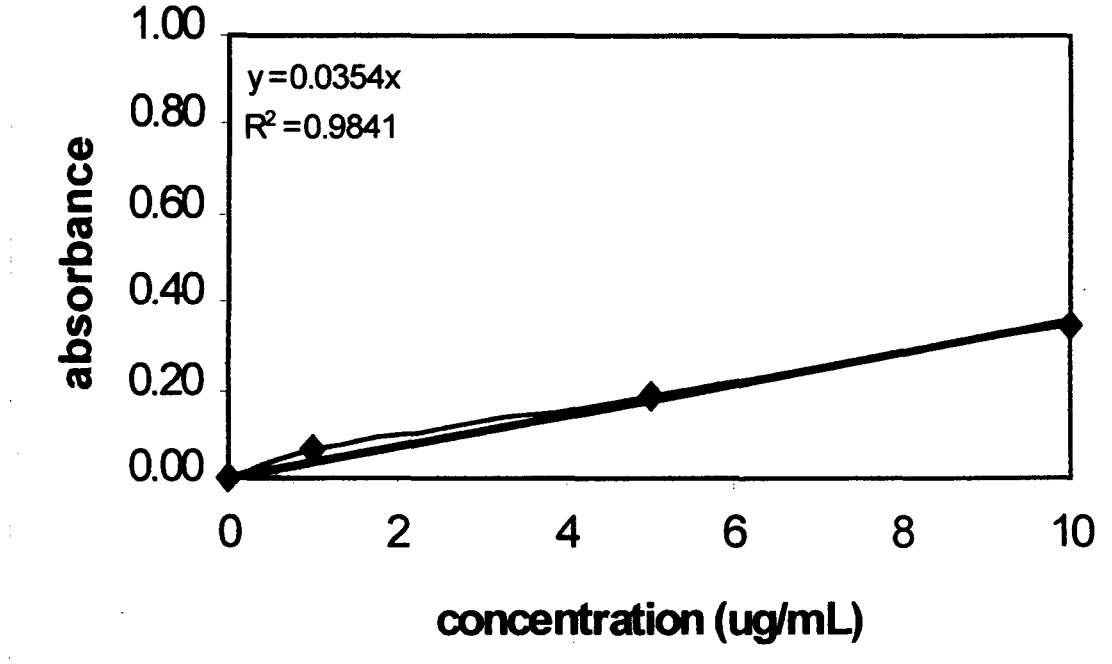

12.2 APPENDIX 2

Varian GTA100 electrothermal atomisation (ETA) spectrometric calibration curves for the metals investigated.

Figure 12.2.1 ETA calibration curve for Ge.

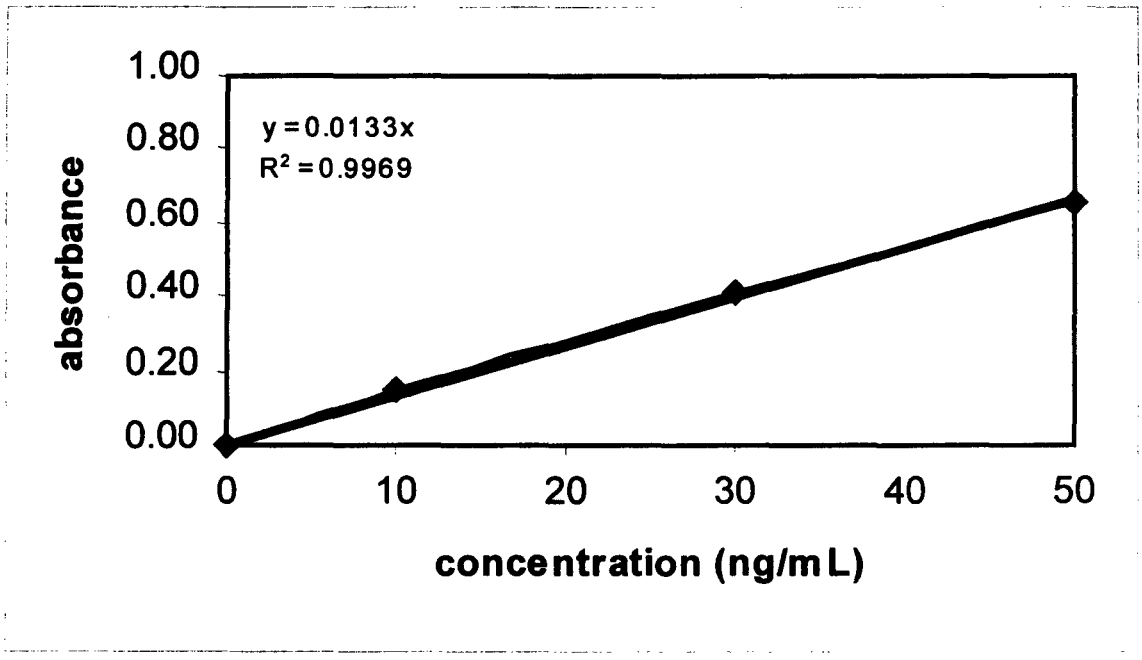

Figure 12.2.2 ETA calibration curve for Zn.

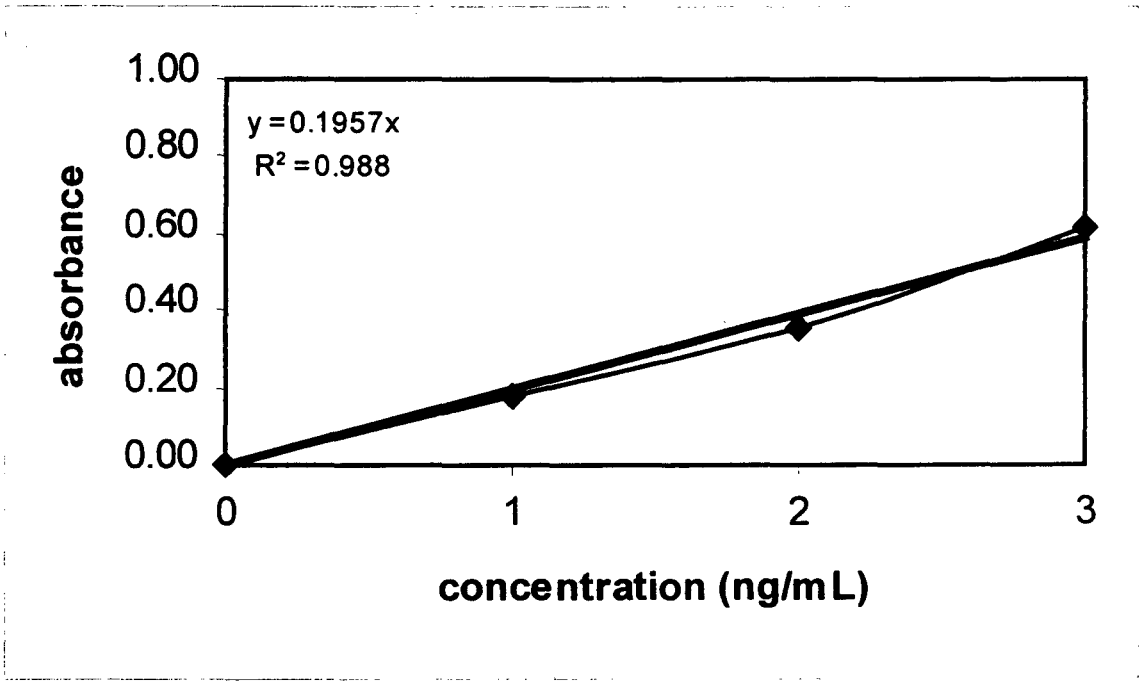

Figure 12.2.3 **ETA calibration curve for Al.**

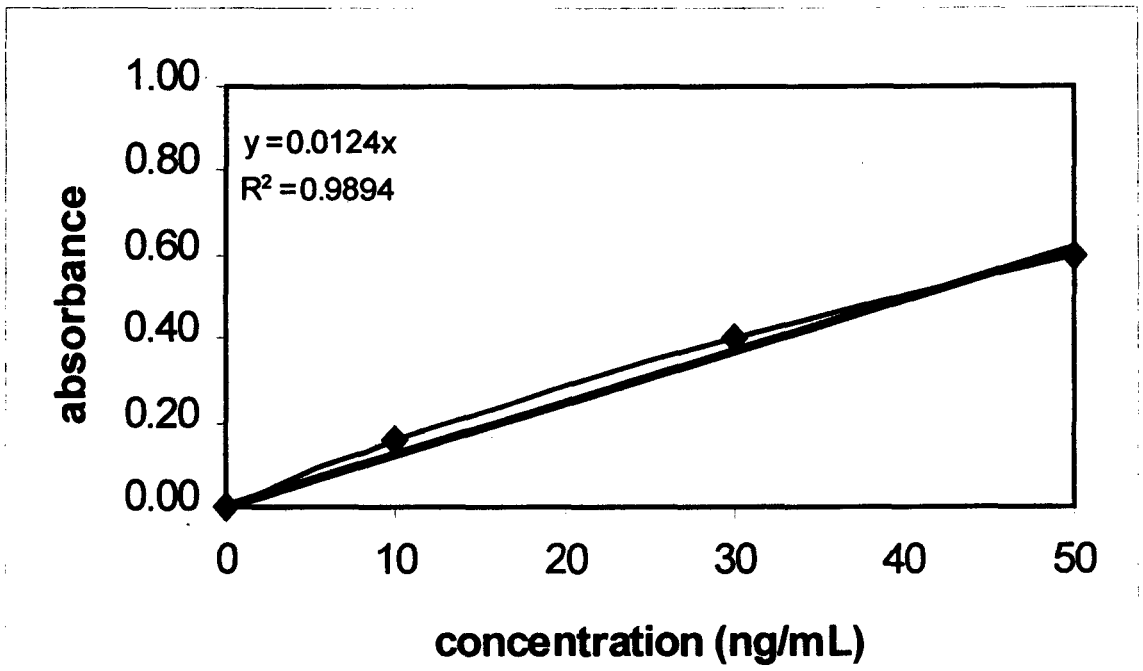

Figure 12.2.4 **ETA calibration curve for Fe.**

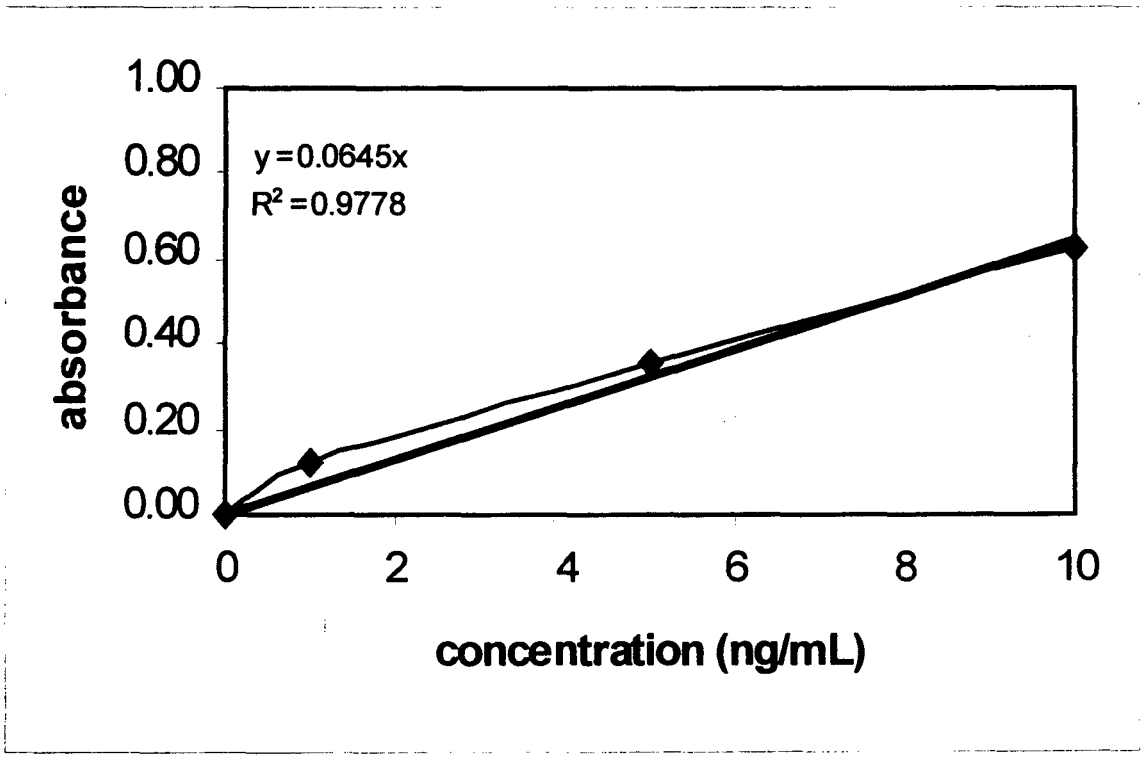

12.3 APPENDIX 3

Perkin Elmer 400 induced coupled plasma (ICP) spectrometric calibration curves for the metals investigated.

Figure 12.3.1 **ICP calibration curve for Ga.**

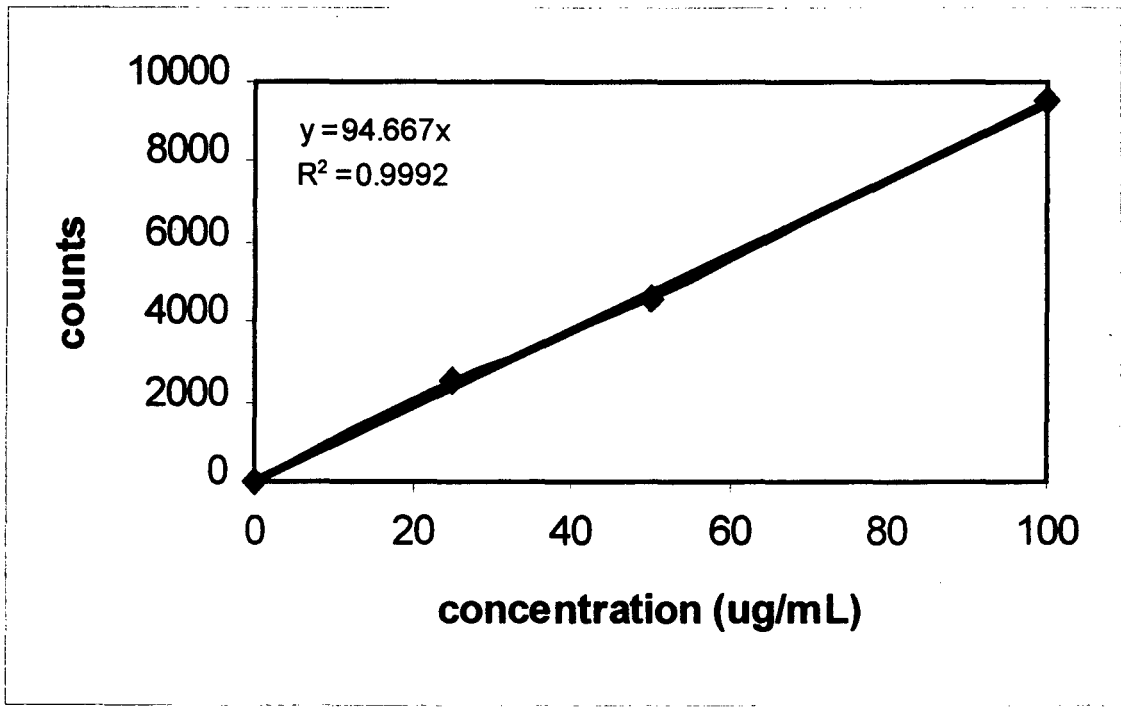

Figure 12.3.2 **ICP calibration curve for Ge.**

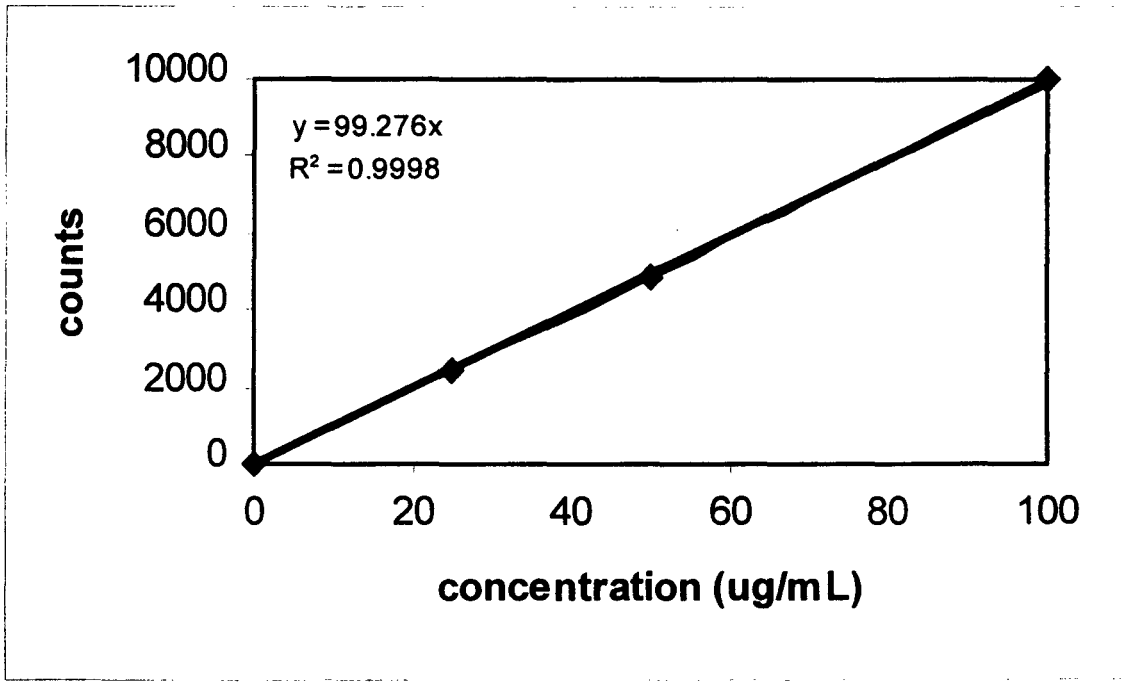

Figure 12.3.3 **ICP calibration curve for Zn.**

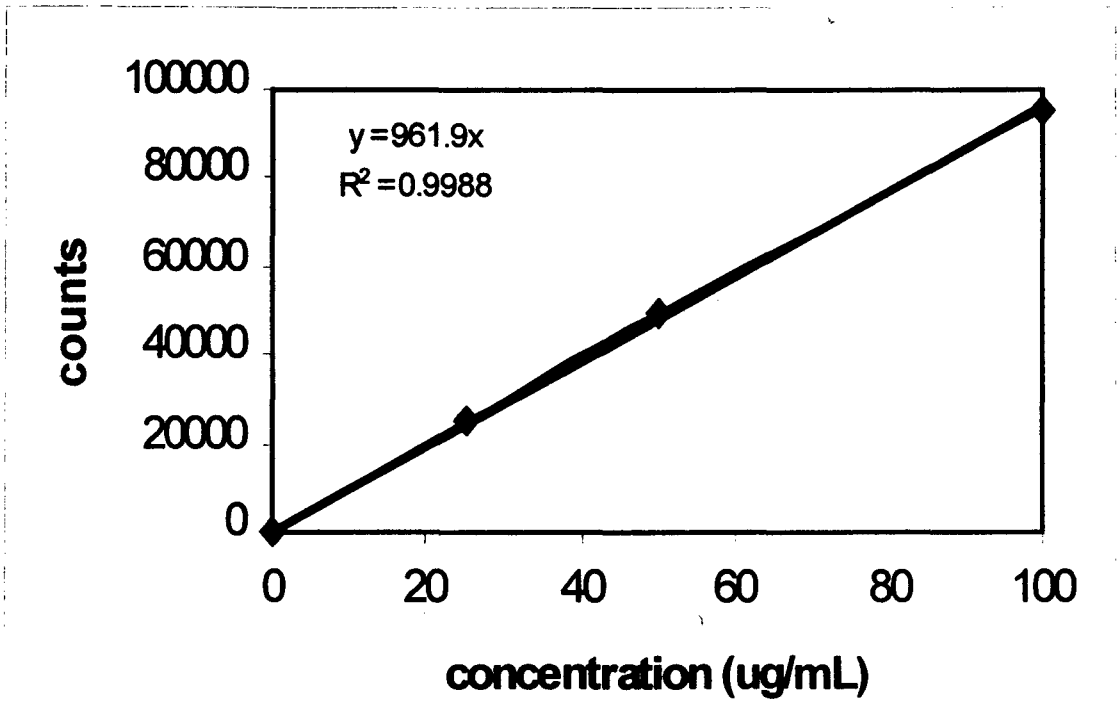

Figure 12.3.4 **ICP calibration curve for Al.**

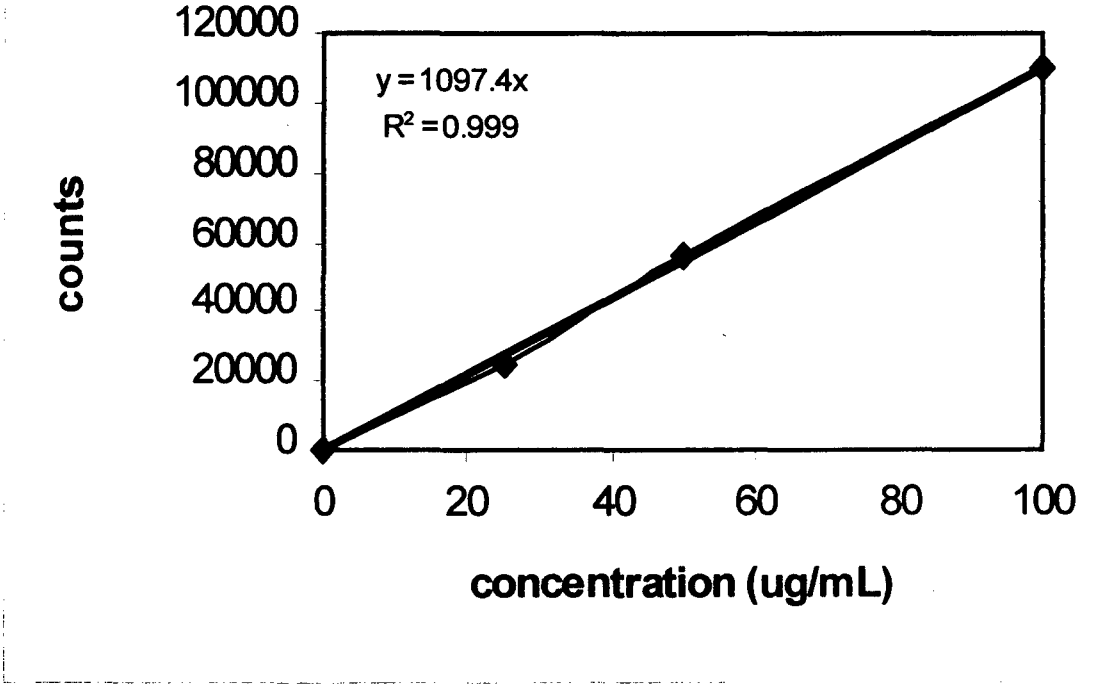

Figure 12.3.5 **ICP calibration curve for Fe.**

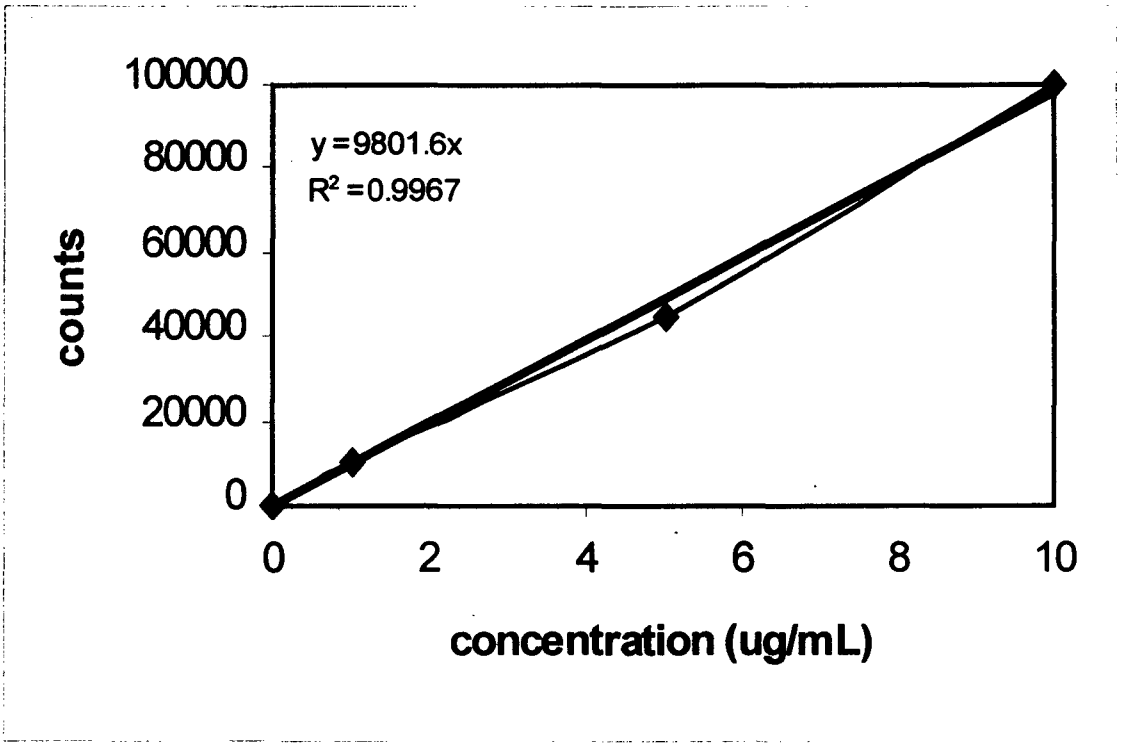

Figure 12.3.6 **ICP calibration curve for Co.**

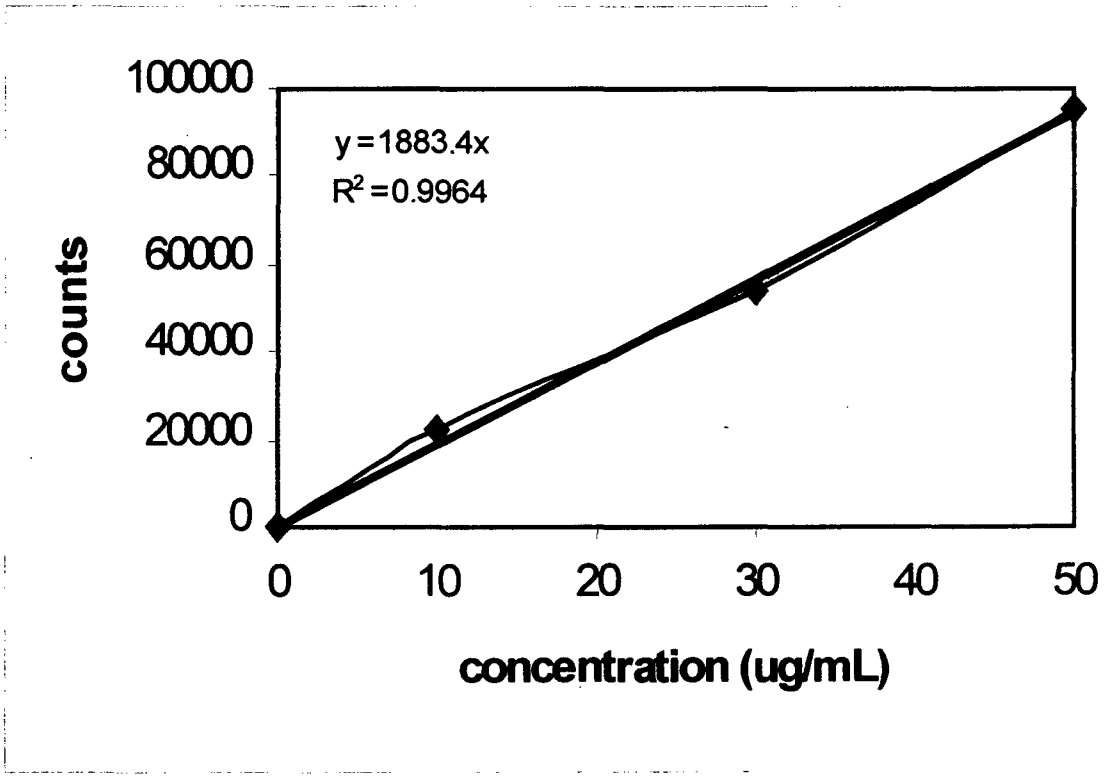

Figure 12.3.7 **ICP calibration curve for Ni.**

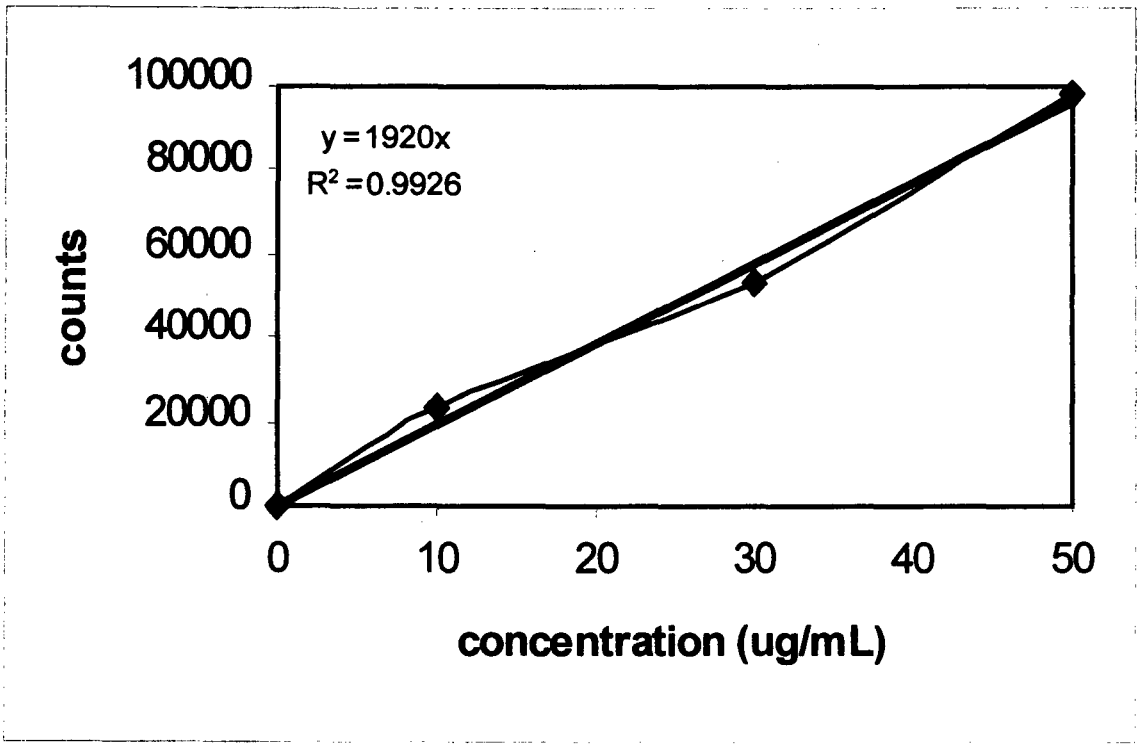

Figure 12.3.8 **ICP calibration curve for Cu.**

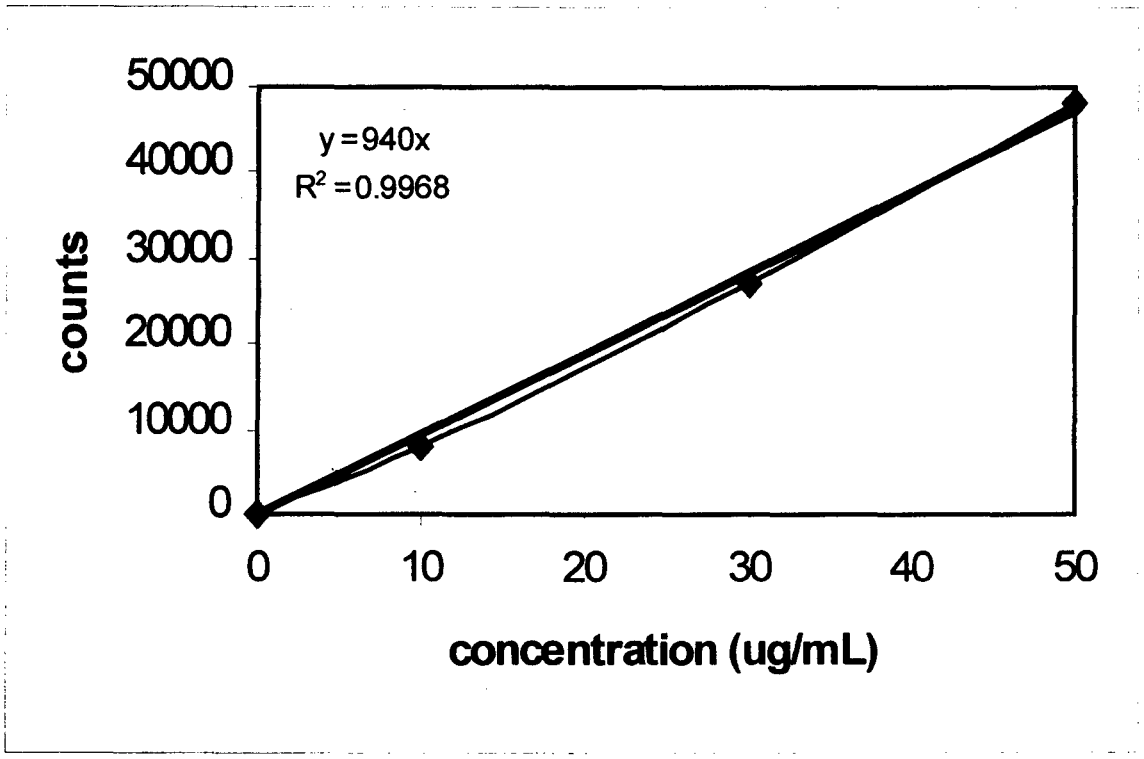

Figure 12.3.9 **ICP calibration curve for Cd.**

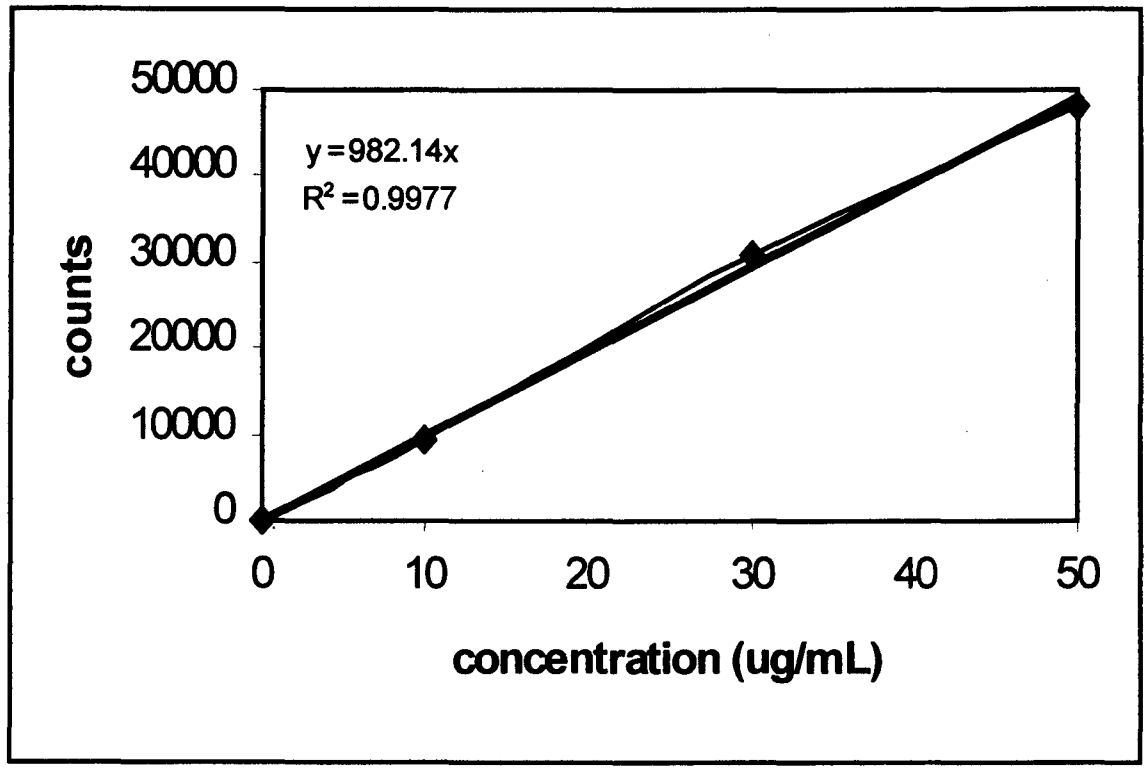

Figure 12.3.10 **ICP calibration curve for In.**

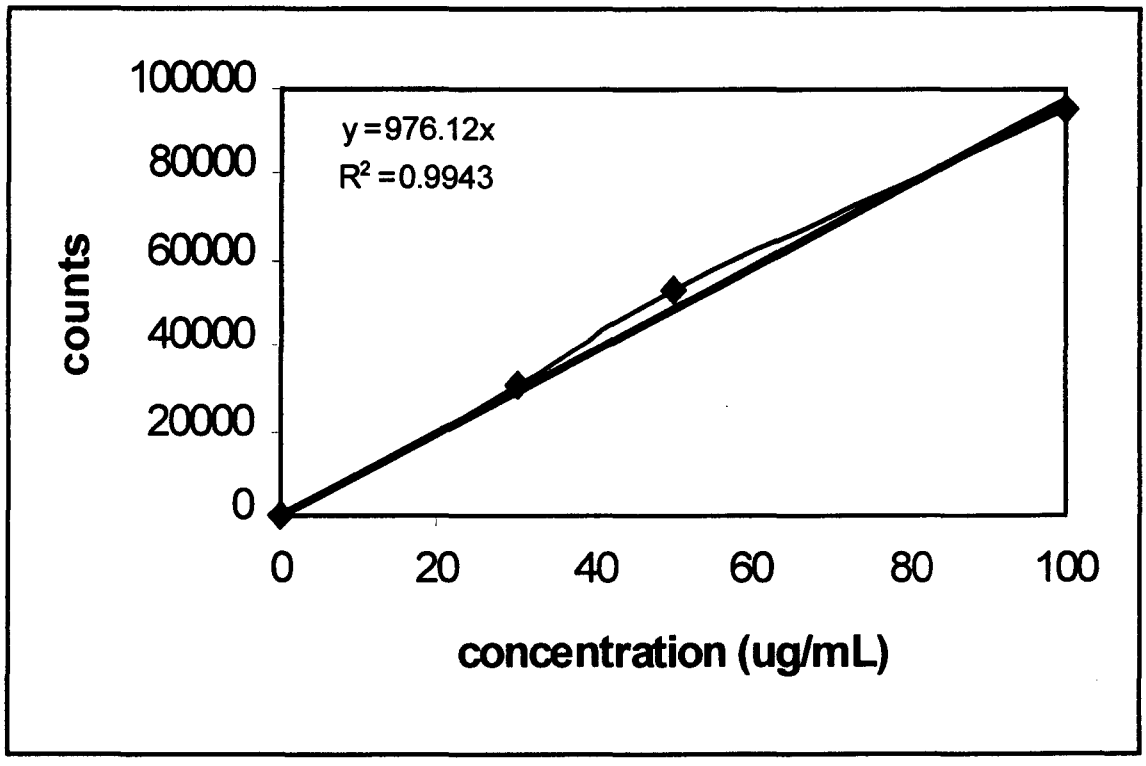

Figure 12.3.11 **ICP calibration curve for Ti.**

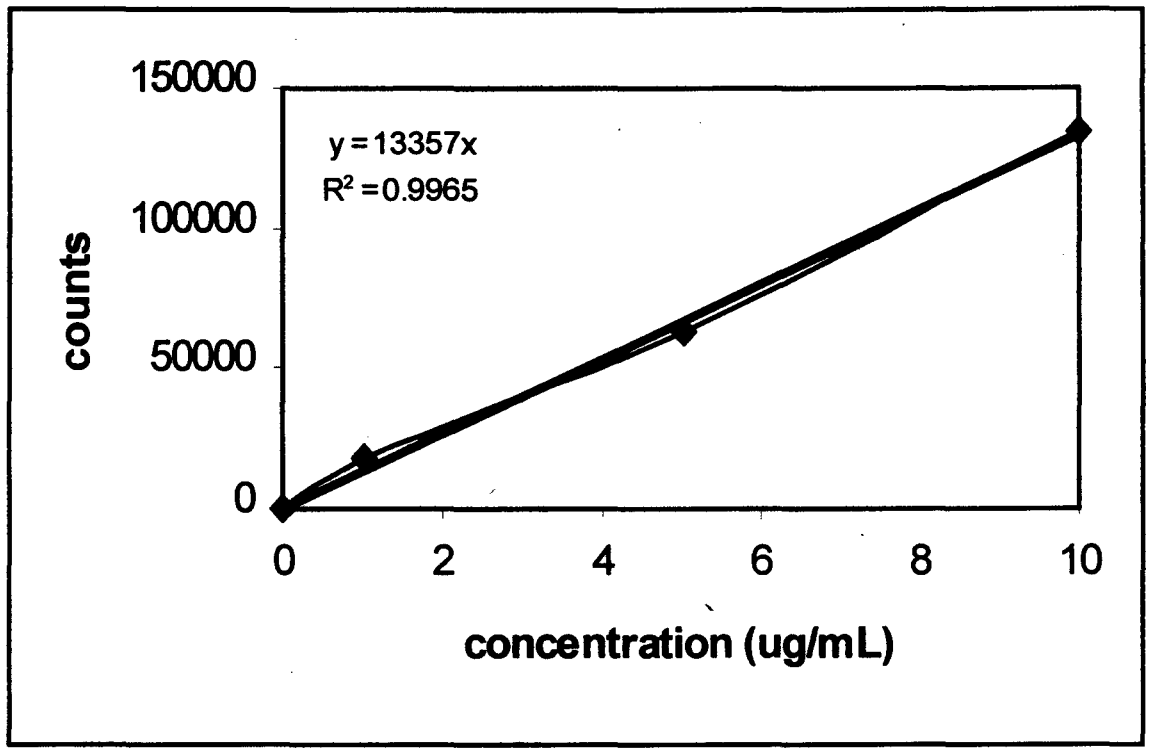

12.4 APPENDIX 4

Shimadzu 265 ultra violet-visible (UV/VIS) spectrometric calibration curves for the metals investigated.

Figure 12.4.1 UV/VIS calibration curve for Ge(IV).

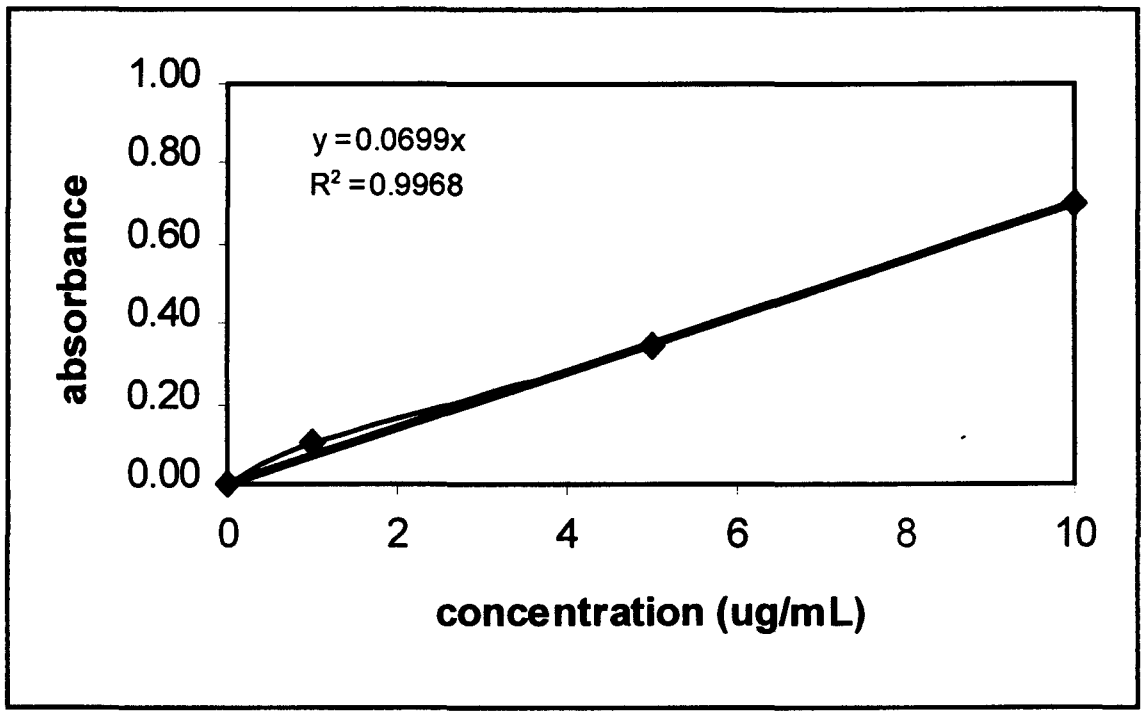

Figure 12.4.2 UV/VIS calibration curve for Zn(II).

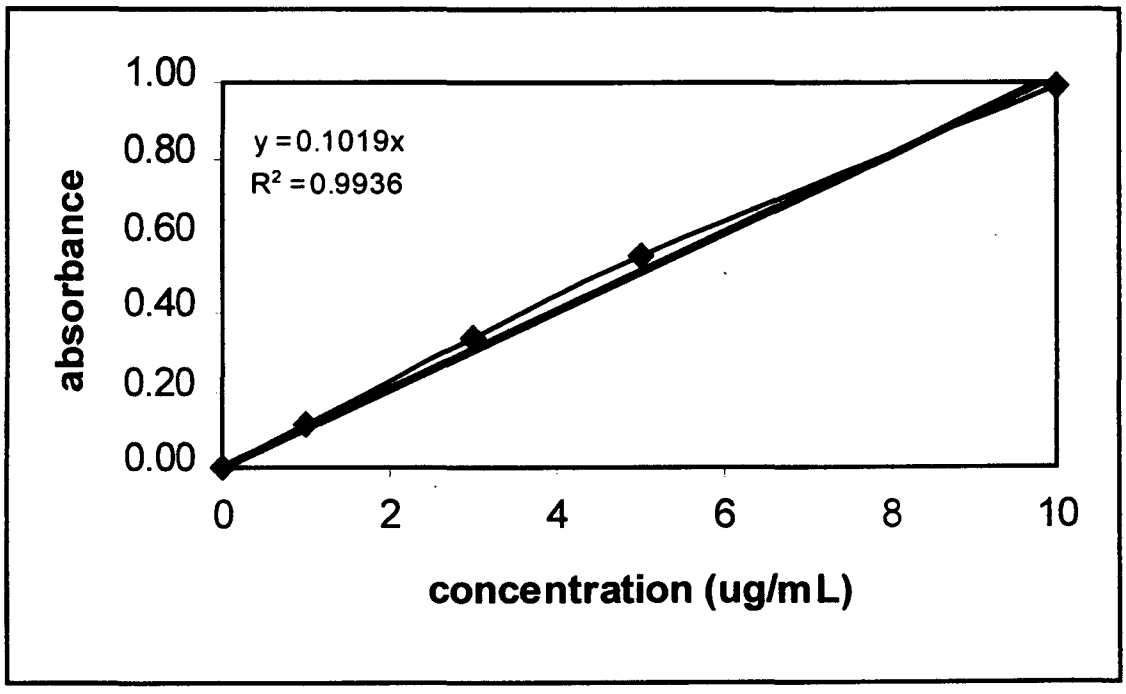

13 BIBLIOGRAPHY

1. Andersen T. and Knutsen A. B., *Acta. Chem. Scand.*, 1962, **16**, 849.
2. Bio-Rad, Guide To Ion Exchange Catologue, 1996.
3. Bjornstad T. and Holtebekk T., *University of Oslo Report,* **OUP-83-1**, 1983.
4. Bonardi M. and Birattari C., *J. Radioanal. Chem.*, 1983, **76**, 311.
5. British Pharmacopoeia (1993), Volume II (Effective date 1 December 1993). London: HMSO, p. 1224.
6. Brits R.J.N. and Strelow F.W.E., *Appl. Radiat. Isot.*, 1990, **41**, 6.
7. Brown L. C., *Int. J. Appl. Radiat. Isot.*, 1971, **22**, 710.
8. Casarett L.J. and Doull J., *Toxicology*, 1975, Macmillan Publishers, New York.
9. Chattopadhyay S., Das M.K., Sarkar B.R. and Ramamoorthy N., 1998, *Appl. Radiat. Isot.*, **49**, 899.
10. Cogman M. and Gilly L., *J. Nucl. Phys.*, 1965, **73**, 122.
11. Corte de F., Winkel van den P., Specke A. and Hoste J., *Anal. Chim. Acta.*, 1968, **42**, 67.
12. Danielsson L., *Acta. Chem. Scand.*, 1965, **19**, 670.
13. Faris J.P. and Buchanan R.F., *Anal. Chem.*, 1964, **36**, 1157.
14. Faris J.P., *Anal. Chem.*, 1960, **32**, 520.
15. Fries J. and Getrost H., *Organic reagents for trace elements*, 1977, E. Merck, Darmstadt.
16. Fritz J.S. and Kaminski E.E., *Talanta*, 1971, **18**, 541.
17. Fritz J.S. and Retting T.A., *Anal. Chem.*, 1962, **34**, 1562.
18. Fritz J.S. and Story J.N., *Anal. Chem.*, 1974, **46**, 825.

19. Garrison W.M. and Hamilton J.G., 1951, *Chem. Revs.*, **49**, 237.

20. Gleuckauf E. and Kitt G. P., *Proc. Roy. Soc.*, 1955, **A228**, 332.

21. Grant P.M., Miller D.A., Gilmore J.S. and O'Brien H.A. Jr., *Int. J. Appl. Rad. Isot.*, 1982, **33**, 415.

22. Grant P.M., O'Brien H.A. Jr., Bayhurst B.P., Gilmore J.S., Prestwood J., Whipple R.E. and Wanek P.M., *J. Labelled Comp. Radiopharm.*, 1979, **16**, 212.

23. Green M.A. and Welch M.J., *Med. Biol.*, 1989, **16**, 5.

24. Grutter A., *Int. J. Appl. Rad. Isot.*, 1982, **33**, 725.

25. Hall G.R., *J. Chem. Soc.*, 1963, **1**, 5205.

26. Helus F. and Maier - Borst W., *J. Labelled Compd. Radiopharm.*, 1973, **19**, 1423.

27. Higashi T., Nahayama Y. and Murata A., *J. Nucl. Med.*, 1972, **13**, 196.

28. Horiguchi T., Kumahora H. and Yoshizawa Y., *Int. J. Appl. Rad. Isot.*, 1983, **34**, 1531.

29. Hupf H.B. and Beaver J.E. , *Int. J. Appl. Radiat. Isot.*, 1970, **21**, 75.

30. Ichikawa F., Urona S. and Imai H., *Bull. Chem. Soc. Japan*, 1961, **34**, 952.

31. Klakl E. and Korkisch J., *Talanta*, 1969, **16**, 1177.

32. Kopecky P. and Mudrova B., *Int. J. Appl. Rad. Isot.*, 1975, **26**, 323.

33. Kopecky P., *Appl. Radiat. Isot.*, 1990, **41**, 606.

34. Korkisch J. and Ahluwahla S.S., *Talanta*, 1967, **14**, 155.

35. Korkisch J. and Klaki J., *Talanta*, 1969, **16**, 377.

36. Kraus K.A. and Nelson F., *ASTM, Spec. Tech. Publ.*, 1958, **195**, 27.

37. Kraus K.A. and Nelson F., *Proc. Inter. Conf.*, 1956, **7**, 113.

38. Kraus K.A., Nelson F. and Rush R.M., *J. Am. Chem. Soc.*, 1960, **82**, 339.

39. Kraus K.A., Nelson F. and Smith G.W., *J. Am. Chem. Soc.*, 1959, **58**, 11.

40. Kuroda R., Ishida K. and Kiriyama T., *Anal. Chem.*, 1968, **40**, 1502.

41. Kuroda R., Oguma K., Kono N. and Takashashi Y., *Anal. Chim. Acta.*, 1972, **62**, 343.

42. Levin V. I., Malin A. B. and Marigina A. B., *Radiokhimyia,* 1972, **14**, 462.

43. Marsh S.F., Alarid J.E., Hammond C.F., McLeod M.J., Roensch F.R. and Rein J.E., Los Alomos Scientific Laboratory Report LA-7084, UC-4, 1978, p. 15.

44. Mayer S. W. and Thompkins E.R., *J. Am. Chem. Soc.*, 1947, **69**, 2866.

45. Morrison G.H. and Freiser H., *Solvent extraction in analytical chemistry*, 1957, John Wiley & Sons, Inc.,NY.

46. Neirinckx R.D. and Merwe M.J., *J. Radiochem. Radioanal. Letts.*, 1971, **7**, 31.

47. Nelson F. and Kraus K., *J.Chrom.*, 1979, **178**, 163.

48. Nelson F. and Michelson D., *J. Chrom.*, 1966, **25**, 414.

49. Nelson F., Maurase T. and Kraus K., *J. Chrom.*, 1964, **13**, 503.

50. Nelson F., Rush R. M. and Kraus K.A., *J. Am. Chem. Soc.*, 1960, **82**, 339.

51. Nortier F.M., Mills S.J. and Steyn G.F., *Appl. Radiat. Isot.*, 1991, **42**, 353.

52. Novgorodov A.F., Zelinski A.F., Sobecka M., Ageev V.A., Kolaczkowski A.G. and Belov A.G., *Radiokhimiya*, 1988, **30**, 672.

53. Perkin Elmer ICP 400, *Instruction and procedure manual*, 1990.

54. Pillay K.K.S., *J. Radioanal. Chem.*, 1986, **97**, 134.

55. Polkowska-Motrenko H. and Dybezynski R., *Chem. Anal.*, 1977, **22**, 1021.

56. Polkowska-Motrenko H. and Dybezynski R., *J. Chrom.*, 1974, **88**, 387.

57. Reiman W and Walton H.F., *Ion exchange in analytical chemistry*, 1970, 1st ed., Pergamon Press, NY.

58. Samuelson O., *Ion exchange in analytical chemistry*, 1963, 3rd ed., John Wily & Sons Inc., NY.

59. Shimadzu UV - VIS 265, *Instruction and procedure manual*, 1992.

60. Skoog D.A. and West D.M., *Fundamentals of analytical chemistry*, 1982, 4th ed., Saunders, Philadelphia.

61. Silvester D.J. and Thakur M.L., *Int. J. Appl. Radiat. Isot.*, 1970, **21**, 630.

62. Smith - Jones P.M., *M.Sc Thesis*, University of Pretoria, 1986.

63. Smith - Jones P.M. and Strelow F.W.E., *Appl. Radiat. Isot.*, 1986, **37**, 3.

64. Stevens C.J., *M. Dip. Thesis*, Cape Tehnikon, (1992).

65. Steyn J. and Meyer B.R., *Int. J. Appl. Radiat. Isot.*, 1973, **24**, 369.

66. Strelow F.W.E. and Bothma C.J.C., *Anal. Chem.*, 1967, **39**, 595.

67. Strelow F.W.E. and Sondorp H., *Talanta*, 1972, **19**, 1113.

68. Strelow F.W.E. and Van Zyl C.R., *Anal. Chim.* Acta., 1968, **41**, 529.

69. Strelow F.W.E., *Anal. Chem.*, 1960, **32**, 1185.

70. Strelow F.W.E., *Anal. Chem.*, 1978, **50**, 1359.

71. Strelow F.W.E., *Anal. Chem.*, 1981, **127**, 63.

72. Strelow F.W.E., *Anal. Chem.*, 1984, **56**, 1053.

73. Strelow F.W.E., Hanekom M.D., Victor A.H. and Eloff C., *Ana.l Chim. Acta.*, 1975, **76**, 377.

74. Strelow F.W.E., Rethemeyer R. and Bothma C.J., *Anal. Chem.*, 1965, **37**, 106.

75. Strelow F.W.E., *Talanta*, 1980, **27**, 727.

76. Strelow F.W.E., Van Zyl C.R. and Bothma C.J.C., *Anal. Chim.* Acta., 1969, **45**, 81.

77. Strelow F.W.E., Victor A.H., Van Zyl C.R. and Eloff C., *Anal. Chem.*, 1971, **43**, 870.

78. Strelow F.W.E., Weinert C.H.S.W. and Eloff C., *Anal. Chem.*, 1972, **44**, 2352.

79. T.N. van der Walt and Strelow F.W.E., *Anal. Chem.*, 1983, **55**, 212.

80. T.N. van der Walt and Coetzee P. P., *S. Afr. J. Chem.*, 1989, **42**, 64.

81. T.N. van der Walt and Coetzee P.P., *S. Afr. J. Chem.*, 1989, **42**, 68.

82. T.N. van der Walt and Fourie P.J., *Appl. Radiat. Isot.*, 1987, **38 (2)**, 158.

83. T.N. van der Walt and Haasbroek F.J., *Synthesis and Applications of Isotopically Labelled Compounds*, 1994, Ed. by Allen and R Voges. John Wiley & Sons Ltd. Proceedings of the 5 th International symposium, Strasbourg, France, 20 - 24 June 1994. Paper **36**, 211-214.

84. T.N. van der Walt and Strelow F.W.E., *S. Afr. J. Chem.*, 1979, **32**, 13.

85. T.N. van der Walt, Haasbroek F.J. and Strelow F.W.E., *S. Afri. J. Chem.*, 1981, **34**, 50.

86. T.N. van der Walt, *M.Sc. Thesis*, Rand Afrikaans University, 1998.

87. T.N. van der Walt, Mayer G.D., Bohmer R.G. and Andersen P., *Radiochimica Acta.*, 1983, **34**, 207.

88. T.N. van der Walt, Strelow F.W.E and Brits R.J.N., *Int. J. Appl. Radiat. Isot.*, 1985, **36 (6)**, 501.

89. T.N. van der Walt, Strelow F.W.E and Haasbroek F.J., *Int. J. Appl. Radiat. Isot.*, 1982, **136**, 429.

90. T.N. van der Walt, Strelow F.W.E and Haasbroek F.J., *Int. J. Appl. Radiat. Isot.*, 1985, **36**, 159.

91. T.N. van der Walt, Strelow F.W.E and Haasbroek F.J., *Talanta*, 1985, **32**, 313.

92. T.N. van der Walt, Strelow F.W.E and Haasbroek, F.J., *Talanta*, 1982, **29**, 583.

93. Taylor D.M. and McCready V.R., *Nuclear Techniques in Diagnostic Medicine*, 1986, Martinus Nijhoff Publishers, Dordrecht.

94. Thakur M.L., *Int. J. Appl. Rad. Isot.*, 1977, **28**, 183.

95. Tosohaas, The Separations Catologue, 1996.

96. The United States Pharmacopoeia (1995), 23rd Revision, Official from 1 January 1995 United States Pharmacopoeial Convention, Inc., Rand McNally, Taunton, MA. p. 698.

97. Vallabhajosula S.R., Harwing J.F. and Wolf W., *J. Nucl. Med. Biol.*, 1981, **8**, 363.

98. Van Rijk P.P., *Nuclear Techniques in Diagnostic Medicine*, 1986, Martinus Nijhoff Publishers, Dordrecht.

99. Varian AA600, *Instruction and procedure manual*, 1989.

100. Varian GTA100, *Instruction and procedure manual*, 1988.

101. Vlatkovic M., Paic G., Kaucic S. and Vekic B., *Int. J. Appl. Rad. Isot.*, 1975, **26**, 377.

102. Vogel A., Textbook of quantitative inorganic analysis, 1983, Longman Press, London.

103. Weinreich R., Chamma D.F.S. and Braghirolli A.M.S., J. *Labelled Compd. Radiopharm.*, 1982, **19**, 1423.

104. Winkel van den P., Corte de F. and Hoste J., *Anal. Chim. Acta.*, 1971, **16**, 849.